Cationic Polymerization of Glycidyl Ethers and Furans: Improved Electron Beam and UV Cured Epoxy Networks

A Thesis

Submitted to the Faculty

of Drexel University

by

Jihean Lee

in partial fulfillment of the

requirements for the degree

of

Doctor of Philosophy

July 2007

© Copyright 2007

Jihean Lee. All Rights Reserved.

DEDICATIONS

To my family

ACKNOWLEDGEMENTS

This thesis is dedicated to my father (Intae), mother (Ae Young), and brother (Young) for their love and support. Throughout my life they have encouraged me to pursuit my goals.

I would like to thank my advisor Dr. Giuseppe Palmese who gave me the opportunity to participate in a new area of research. His guidance has let me achieve more than I ever imagined. I would also like to thank Dr. Mun Choi and Dr. Selcuk Guceri for their guidance thoughout my Ph.D. I would like to express my appreciation to my committee Dr. Antony Loman, Dr. Yossef Elabd, and Dr. Steven Wrenn, and Janis Brown for their suggestions for my research. The assistance I received at University of Dayton Research Institute with Dr. Don Klosterman and Anish Desai allowed me to EB irradiate my samples. Additionally, I would also like to acknowledge my fellow lab mates in the Palmese Research Group especially Jason, Vijay, and John. I would like to express appreciation to Dorothy Porter her administrative help and Dan Luu for his technical assistance. I would like to thank my friends through these years Josh, Che, Sid, Wendolene, Mike, Kris, Angela, Julia, Amy, Felix, Pete, Anish, and Andrew.

I am grateful to several sources that provided funding for me during my graduate research. First, the Airforce R AFOSR under grant F49620-02-1-0360 with Dr. Charles Lee as program monitor. Support for Drexel University through the Dean's Fellowship. Lastly, I received further support from the Koerner family in the form of the Koerner Family Fellowship and guidance on issues in both my career and life.

TABLE OF CONTENTS

LIST OF TABLES..... xi

LIST OF FIGURES.....xiii

ABSTRACT.....xix

Chapter 1: INTRODUCTION 1

1.1. Thermal Curing versus Radiation Curing.....1

1.2. Objective.....2

1.3. Methodology.....2

1.4. Thesis Outline.....4

1.5. References.....5

Chapter 2: BACKGROUND 6

2.1. Epoxies.....6

2.2. Curing of Epoxy Resins.....8

2.3. Thermal Curing.....10

2.4. Radiation Curing.....12

2.5. UV Curing.....13

2.6. Electron beam curing of composites.....15

2.7. References.....20

Chapter 3: EXPERIMENTAL 22

3.1. Experimental apparatus – In situ real time NIR 22

3.2. Near Infrared Spectroscopy (NIR) 23

3.3. Size exclusion chromatography (SEC) 29

3.4. Dynamic Mechanical Analysis (DMA) 29

3.5. Fracture Toughness Testing 29

3.6. Flexural Testing 30

3.7. Short Beam Shear (SBS) Testing 30

3.8. Reference 30

Chapter 4: INFLUENCE OF WATER ON THE KINETICS OF CATIONICALLY PHOTO-INITIATED POLYMERIZATION OF EPOXY GROUPS VIA ULTRA-VIOLET AND ELECTRON BEAM IRRADIATION 31

4.1. Introduction 31

4.2. Experimental 34

4.2.1. Materials 34

4.2.2. Fiber Optic Near IR Spectroscopy 34

4.2.3. Sample Preparation and Irradiation 38

4.3. Results and Discussion 39

4.3.1. Measurement of water concentration 39

4.3.2. Influence of water on PGE cationic polymerization via UV and EB radiation 42

4.3.3. Influence of water on DGEBA cationic polymerization via UV and EB radiation 60

4.4. Influence of water on cured DGEBA properties (T_g and fracture toughness) 68
4.5. Conclusion 71
4.6. References 72
Chapter 5: DARK AND LIGHT RADIATION CURE KINETICS OF EPOXIES VIA UV AND EB 74
5.1. Introduction 74
5.2. Experimental 77
5.2.1. Materials 77
5.2.2. Fiber Optic Near IR Spectroscopy 79
5.2.3. Calorimetry 79
5.2.4. Sample Preparation and Irradiation 80
5.3. Results and discussion 83
5.3.1. Interrupted EB Irradiation 84
5.4. Analysis of Dark Reactions 93
5.5. Reassessment of Previous Calorimetry Experiments 96
5.6. Conclusion 100
5.7. Reference 102
Chapter 6: PROPERTIES OF TRIGLYCIDYL ETHER OF TRISPHENOL-METHANE (TACTIX 742) 103
6.1. Introduction 103
6.2. Materials 103
6.3. Procedure 105

6.3.1. Preparation of DGEBA and Tactix 742 105
6.4. Results 105
6.4.1. Synthesis and Application of Tactix 742 and DGEBA 105
6.5. Conclusion 108
6.6. Reference 108
Chapter 7: IMPROVED EB CURED DGEBA SYSTEMS BY COPOLYMERIZATION WITH NOVEL TETRAHYDROFURAN FUNCTIONAL COMONOMERS 109
7.1. Introduction 109
7.2. Experimental 112
7.2.1. Materials 112
7.3. Procedure 114
7.3.1. Preparation of DGEBA and PGE or CHO Systems 114
7.3.2. Preparation of DGEBA and THF Systems 114
7.3.3. Preparation of DGEBA and Tetrahydro-2-furoic Acid Systems 118
7.3.4. Preparation of DGEBA and Coumaran Systems 123
7.3.5. Preparation of DGEBA and Phthalan Systems 123
7.3.6. Preparation of Tactix 742 and Tetrahydro-2-furoic Acid Systems 125
7.3.7. Composites Processing 125
7.3.8. Sample Irradiation 127
7.4. Results 127
7.4.1. Monofunctional chain extenders 128
7.4.1.1. Chain Extension with Phenyl Glycidyl Ethers (PGE) 128

7.4.1.2. Chain Extension with Cyclohexene Oxide (CHO) 128
7.4.1.3. Chain Extension with Tetrahydrofuran (THF) 131
7.4.2. Difunctional chain extenders 133
7.4.2.1. Synthesis and Application of Chain Extenders by Esterification of DGEBA and Tetrahydro-2-furoic acid 133
7.4.2.2. Synthesis and Application of Chain Extenders by Esterification of DGEBA and Tetrahydro-3-furoic acid 135
7.4.3. Trifunctional chain extenders 137
7.4.3.1. Synthesis and Application of Chain Extenders by Esterification of Trifunctional Epoxies (Tactix 742) with Tetrahydro-2-furoic acid 137
7.4.3.2. Synthesis and Application of Chain Extenders by Esterification of Trifunctional Epoxies (Tactix 742) with Tetrahydro-3-furoic acid 140
7.4.4. Cyclic chain extenders 142
7.4.4.1. Synthesis and Application of Chain Extenders of DGEBA and Coumaran 142
7.4.4.2. Synthesis and Application of Chain Extenders of Epoxies and Phthalan 145
7.4.5. Composite Properties 147
7.5. Conclusions 148
7.6. References 149
Chapter 8: CONCLUSIONS 151

8.1. Summary 151

8.2. Water Reactions 151

8.3. Dark Reactions 152

8.4. Co-monomers for Chain Extension 153

LIST OF TABLES

Table 3.1. Chemical structure of epoxy molecules. 27

Table 4.1. Materials used in the experimental work; PGE as the mono-functional epoxy, DGEBA as the di-functional epoxy, and CD1012 as the photoinitiator. 35

Table 4.2. Mechanical and thermal properties of DGEBA composites curved via EB are obtained through DMA analysis and SENB fracture toughness measurements. G_{1C} values increase with the presence of water and peaks at 0.5 wt% water. T_gs decrease with increase of water concentration. 67

Table 5.1. Materials used in the experimental work. 78

Table 5.2. The kinetic constants for deactivation and its corresponding half-life show there may be long half lives of these active centers..... 95

Table 6.1. The chemical structures of the materials used in this experimental work. 104

Table 7.1. The chemical structures of the materials used in this experimental work. 113

Table 7.2. Calculation of the amount of THF placed into the epoxy system and the actual amount that reacted. 115

Table 7.3. DMA results of the co-polymerization of DGEBA and PGE as the chain extender. 129

Table 7.4. DMA results of the co-polymerization of DGEBA and CHO as the chain extender. 130

Table 7.5. DMA results of the co-polymerization of DGEBA and THF as the chain extender. 132

Table 7.6. Fracture toughness and T_g values for neat DGEBA and GP3 modified DGEBA. 134

Table 7.7. Fracture toughness and T_g values for neat DGEBA and GP2 modified DGEBA 136

Table 7.8. Mechanical properties of DGEBA modified using GP5 at various concentrations. 139

Table 7.9. Mechanical properties of DGEBA modified using GP4 at various concentrations. 141

Table 7.10. Mechanical properties of DGEBA modified using JL1 at various concentrations. 143

Table 7.11. Mechanical properties of DGEBA modified using JL2 at various concentrations. 144

Table 7.12. Material properties of modified DGEBA systems with THF functional monomers, such as SBS strength and flexural strength and modulus. 146

LIST OF FIGURES

Figure 1.1. Proposed methodology for the rational design of improved EB cured epoxies. 3

Figure 2.1. Gillham's time-temperature-transformation (TTT) cure diagram, where liquid, gelled rubber, gelled glass, and ungelled glass are four states of matter. These regions are delineated by a plot of the times to gelation and vitrification during isothermal cure vs. temperature [9-10]..... 9

Figure 2.2. Summary of the different radiation types and their characteristic properties. 14

Figure 2.3. Schematic of electron beam facility at University of Dayton Research Institute: A) overall layout of UDRI EB facility, B) vault interior schematic, C) interior of EB vault, showing scan horn and cart, D) control area of EB facility, showing vault exterior (background), computer monitor and vault camera (foreground, left), computer control rack (foreground, center), and power interface module which contains the system's pulse forming network (foreground, right)..... 16

Figure 2.4. Formation of active species from EB to initiate cationic polymerization. 18

Figure 3.1. This picture is the first generation apparatus made by Mascioni to obtain his NIR measurements. The sample holder is made from two glass slides held together by 3M double sided tape with a resin well cut in the middle [1]..... 24

Figure 3.2. This picture is the second generation setup used to gather spectra for the cure process. This system is a closed system, using sealed tubes, to prevent the samples from absorbing impurities such as moisture during the cure process. All resin placed in the tube can be observed from the top to ensure that it is all being exposed fully to the radiation. 25

Figure 3.3. IR absorption spectrum for PGE (top) and Epon 825 (bottom) before (—) and after (—) curing..... 28

Figure 4.1. NIR spectra of water (1908 nm) and epoxy (2209 nm) peaks decreasing over time during cure and increase of hydroxyl (1426 nm) peak. 37

Figure 4.2. Calibration curve (solid line) is the water concentration in PGE (A) and DGEBA (B) to the water absorbance peak height. The data also show the saturation concentration for water at 60°C. 41

Figure 4.3. Comparison of PGE cure behavior for various concentrations of water cured via UV or EB [UV (A) with 0.67pph initiator at 50°C where ◆ no water, ■ 0.34 wt % water, ▲ 0.73 wt% water, and ● 0.89wt% water; and EB (B) with 1pph initiator at 50°C where ◆ no water and ■ 0.78wt% water]. An increase of water shows a longer delay in epoxy conversion at the beginning followed by an acceleration where conversion is reached at a shorter time. 44

Figure 4.4. Representative plot for the consumption of water and formation of hydroxyls during EB curing processes (epoxy ●, water □, and hydroxyls ◇). This sample contains 0.78 wt% water..... 45

Figure 4.5. Temporal profiles for epoxy and water conversion for the limiting cases of water for UV (A) (epoxy conversion containing 0.13 wt% water ◆ and 0.89 wt% water ●; water conversion containing 0.13 wt% water ◇ and 0.89 wt% ○) and EB (B) (epoxy conversion containing 0.19 wt% water ■ and 0.78 wt% water ●; water conversion containing 0.19 wt% water □ and 0.78 wt% water ○) induced polymerization. The delay can be observed in the epoxy conversion while the water is being consumed in the reaction. When the water has been consumed, there is an acceleration of epoxy conversion. 47

Figure 4.6. Schematic of the activated monomer-monomer reaction. 49

Figure 4.7. Cationic epoxy and water chemical reactions summarized by Equation 4.4. 51

Figure 4.8. Differential balance equations to describe the kinetics given in previous equations. 53

Figure 4.9. Model of epoxy conversion over time where $k_i = 0.001\ s^{-1}$, $k_a = 200\ L\ mol^{-1}s^{-1}$, $k_1 = 2.5\ s^{-1}$, $k_2 = 20.4\ L\ mol^{-1}s^{-1}$, $k_4 = 20.4\ L\ mol^{-1}s^{-1}$, $k_5 = 200\ s^{-1}$ and k_3 is assumed to be fast ($k_3 = 200\ s^{-1}$). No delays were observed with increase of water (— 0.25 wt% water, – – 0.5 wt% water, - - 0.75 wt% water, — 1 wt% water, and - – 1.5 wt% water). 56

Figure 4.10. Model of epoxy conversion over time where $k_i = 0.001\ s^{-1}$,$k_a = 200\ L\ mol^{-1}s^{-1}$, $k_1 = 2.5\ s^{-1}$, $k_2 = 20.4\ L\ mol^{-1}s^{-1}$, $k_4 = 20.4\ L\ mol^{-1}s^{-1}$, $k_5 = 200\ s^{-1}$ and rate of reaction of k_3 is varied to observe the delays in initial epoxy conversion. Slower the rate of reaction k_3 the more pronounced the delay where water concentration was held constant 1wt% where — $k_3 = 0.1\ s^{-1}$, — $k_3 = 0.5\ s^{-1}$, – – $k_3 = 1\ s^{-1}$, – – $k_3 = 5\ s^{-1}$, - - $k_3 = 10\ s^{-1}$. Note that when $k_3 \geq 10\ s^{-1}$ the epoxy conversion does not increase over time. 57

Figure 4.11. Implementing the rates of reaction into the model to show the epoxy and water conversion and the formation of hydroxyls, which correspond with the experimental data. 58

Figure 4.12. The model shows the delay of epoxy conversion with increase of water where $k_i = 0.001\ s^{-1}$,$k_a = 200\ L\ mol^{-1}s^{-1}$, $k_1 = 2.5\ s^{-1}$, $k_2 = 20.4\ L\ mol^{-1}s^{-1}$, $k_4 = 20.4\ L\ mol^{-1}s^{-1}$, $k_5 = 200\ s^{-1}$ and $k_3 = 1\ s^{-1}$, where the conversion is reached at shorter times (— 0 wt% water, - - 0.25 wt% water, - – 0.5 wt% water, — 1.5 wt% water. 59

Figure 4.13. Comparison of DGEBA cure kinetics with various water concentration (UV (A) at 0.67pph initiator at 60°C-0.014 wt% water ◆, 0.265 wt% water ■, 0.701 wt% water ▲, and 0.947 wt% water; ●and EB (B) at 1pph initiator at 60°C-0.12 wt% water ◆ and 0.86 wt% water ■).. 62

Figure 4.14. Temporal profiles for epoxy (closed symbols) and water (open symbols) conversion for high and low initial water concentration for UV (A) where epoxy conversion 0.014 wt% water ◆ and 0.947 wt% water ●; water conversion 0.014 wt% water ◇ and 0.947 wt% water ○ and EB (B) -induced polymerization where epoxy conversion 0.12 wt% water ◆ and 0.86 wt% water ■ and 0.12 wt% water ◇0.86 wt% water □. Similar delays can be observed in the DGEBA data as seen in PGE as the epoxy is being consumed. The final conversion is greater with increase of water concentration. 64

Figure 4.15. Influence of initial water concentration on the final epoxy conversion for isothermal UV cure at 60°C highlighting the significant effect of water on polymer structure formed. 66

Figure 4.16. Second run DMA (ramped to 250°C twice) testing of EB cured DGEBA with and without water following post cure where - - storage modulus of 1.0 wt% water, - - storage modulus of DGEBA, — loss modulus 1.0 wt% water, — loss modulus of DGEBA. 69

Figure 4.17. T_g of DGEBA at 1 pph photo-initiator with varying wt% of water in the system EB with a total dosage of 54 kGy. Increase of water concentration causes a decrease in the final T_g. 70

Figure 5.1. DMA of DGEBA depicting the influence of step irradiation on material behavior, where the single peak line (—) represents continuous irradiation and the double peak line (—) represents discontinuous irradiation. 76

Figure 5.2. Schematic of the EB calorimeter (not to scale) [1]. 81

Figure 5.3. PGE with 1pph photo-initiator concentration at 50°C with varying EB exposure times: 500s EB exposure (◆), 250sEB exposure (■), 200s EB exposure (▲), 150s EB exposure (●), 100s exposure (◇). 85

Figure 5.4. 500 s experimental data (◆) fitted to the Mascioni model (—) for fully cured continuous irradiated EB materials. 87

Figure 5.5. Deviation from theoretical model, for 200s EB exposure: data (◆), theoretical model (—) accounting for the EB exposure time, and Mascioni model (—) for continuous irradiation. 89

Figure 5.6. Model to fit experimental data using Equations 5.7 and 5.8: 100 s (◇),150 s (●), 200 s(▲), 250 s(■), and 500 s(◆) from top to bottom respectively. 92

Figure 5.7. Natural log of the rate of polymerization divided by monomer concentration versus time used to obtain active center deactivation rate: 250 s (■), 200 s (▲), 150 s (●), and 100 s (◇). 95

Figure 5.8. Measured temperature of the specimen (—) and calculated dose (◆) during a multi-step irradiation [1]. 97

Figure 5.9. Measured (◆) and predicted (—) cure rates during a multi-step irradiation – single active center assumed (Masconi model) [1]. 98

Figure 5.10. Measured (▲) and predicted (—) cure rates during a multi-step irradiation – dual active center [1]. 99

Figure 6.1. Various ratios of Tactix 742 and DGEBA were made and cured via EB and tested for fracture toughness (◆) and T_g (▲). With increasing amounts of Tactix 742 fracture toughness decreases, the glass transition temperature increases. 106

Figure 6.2. Various ratios of Tactix 742 and DGEBA were made and cured via EB and tested for strength (▲), modulus (•). With increasing amounts of Tactix 742 strength decreases, and modulus increases. 107

Figure 7.1. Schematic representation of a highly crosslinked network (A) and homogeneously modified by copolymerization with a chain extender (B). . 110

Figure 7.2. The theoretical % of THF (gray) versus the actual % of THF (black) was reacted into the epoxy system. 116

Figure 7.3. GPC of 0wt% to 90 wt% of THF in PGE cured via UV light, where pure PGE (—), 10 wt% THF (- - -), 30 wt% THF (····), 50 wt% THF (·· ——), 70 wt% THF (· · ·), and 90 wt% THF (——). 117

Figure 7.4. Proposed ring opening reaction of DGEBA and THF resulting in the insertion of a flexible chain..... 117

Figure 7.5. The chain extender was synthesized using an esterfication reaction of tetrahydro-2-furoic acid and PGE with AMC-2 catalyst. 119

Figure 7.6. GPC of 20 wt% THF2PGE in PGE cured via UV light were taken at various cure times to show the reaction progression where uncured PGE (—), cured PGE (- - -), uncured THF2PGE (– –), 2 min (· · ·), 4 min (·· – –), 6 min (——). 119

Figure 7.7. GPC of 0wt% to 90 wt% of THF2PGE in PGE cured via UV light where uncured THF2PGE (—), cured PGE (—), 10 wt% (- —), 30 wt% (— —), 50 wt% (· · ·), 70 wt% (- - -), 90wt % (·· ——). 120

Figure 7.8. The chain extender was synthesized using an esterification of tetrahydro-2-furoic acid and DGEBA using AMC-2 catalyst (GP3)..... 122

Figure 7.9. The chain extender was synthesized using an esterification of tetrahydro-2-furoic acid and DGEBA using AMC-2 catalyst (GP2)..... 122

Figure 7.10. Ring opening reaction of DGEBA and Coumaran (JL1). 124

Figure 7.11. Ring opening reaction of DGEBA and Phthalan (JL2). 124

Figure 7.12. GPC of 0wt% to 90 wt% of phthalan in PGE cured via UV light where uncured PGE (—), cured PGE (···– –), uncured phthalan (– —), cured phthalan (— —), 50 wt% phthalan (· · ·), 90wt % phthalan (- -). 124

Figure 7.13. The chain extender was synthesized using an esterification of tetrahydro-2-furoic acid and Tactix 742 with AMC-2 catalyst to produce chain extender (GP5)..... 126

Figure 7.14. The chain extender was synthesized using an esterification of tetrahydro-3-furoic acid and Tactix 742 with AMC-2 catalyst to produce chain extender (GP4)..... 126

Figure 7.15. DMA (2nd run) of DGEBA with PGE as a chain extender, where 1 wt% PGE storage modulus (—),1 wt% PGE loss modulus (···– –), 5 wt% PGE storage modulus (· – · –), and 5 wt% PGE loss modulus (- - -), and 10 wt% PGE storage modulus (····),10 wt% PGE loss modulus (– —) are shown. 129

Figure 7.16. DMA (2nd run) of DGEBA with CHO as a chain extender, where 1 wt% CHO storage modulus (—),1 wt% CHO loss modulus (···– –), 5 wt% CHO storage modulus (· – · –), and 5 wt% CHO loss modulus (- - -), and 10 wt% CHO storage modulus (····),10 wt% CHO loss modulus (– —) are shown. 130

Figure 7.17. DMA (2nd run) of DGEBA with THF as a chain extender, where 1 wt% THF storage modulus (—),1 wt% THF loss modulus (··– –), 5 wt% THF storage modulus (· – · –), and 5 wt% THF loss modulus (- - -), and 10 wt% THF storage modulus (····),10 wt% THF loss modulus (– —) are shown. 132

Figure 7.18. DMA (2nd run) of DGEBA with GP3 as a chain extender, where 20 wt% GP3 storage modulus (—), 20 wt% GP3 loss modulus (– –), 35% wt % GP3 storage modulus (····), and 35% wt % GP3 loss modulus (– —) are shown.. 134

Figure 7.19. DMA (2nd run) of DGEBA with GP2 as a chain extender, where 20 wt% GP2 storage modulus (—), 20 wt% GP2 loss modulus (– –), 35% wt % GP2 storage modulus (····), and 35% wt % GP2 loss modulus (– —) are shown. 136

Figure 7.20. DMA (2nd run) of DGEBA with GP5 as a chain extender, where 1 wt% GP5 storage modulus (—),1 wt% GP5 loss modulus (··– –), 5 wt% GP5 storage modulus (· – · –), and 5 wt% GP5 loss modulus (- - -), and 10 wt% GP5 storage modulus (····),10 wt% GP5 loss modulus (– —) are shown. 139

Figure 7.21. DMA (2nd run) of DGEBA with GP4 as a chain extender, where 1 wt% GP4 storage modulus (—),1 wt% GP4 loss modulus (··– –), 5 wt% GP4 storage modulus (· – · –), and 5 wt% GP4 loss modulus (- - -), and 10 wt% GP4 storage modulus (····),10 wt% GP4 loss modulus (– —) are shown. 141

Figure 7.22. DMA (2nd run) of DGEBA with JL1 as a chain extender, where 1 wt% JL1 storage modulus (—),1 wt% JL1 loss modulus (··– –), 5 wt% JL1 storage modulus (· – · –), and 5 wt% JL1 loss modulus (- - -), and 10 wt% JL1 storage modulus (····),10 wt% JL1 loss modulus (– ─) are shown..... 143

Figure 7.23. DMA (2nd run) of DGEBA with JL2 as a chain extender, where 1 wt% JL2 storage modulus (—),1 wt% JL2 loss modulus (··– –), 5 wt% JL2 storage modulus (· – · –), and 5 wt% JL2 loss modulus (- - -), and 10 wt% JL2 storage modulus (····),10 wt% JL2 loss modulus (– ─) are shown..... 144

Figure 7.24. Improving the fracture toughness while maintaining a high T_g, where neat DGEBA (▬), water (●), THF (□), GP2 (◆), GP3 (▲), GP4 (Δ), GP5 (○), JL1 (◇), JL2 (■), JL3 (x). 146

ABSTRACT

Cationic Polymerization of Glycidyl Ethers and Furans: Improved Electron Beam and UV Cured Epoxy Networks

Jihean Lee

Giuseppe R. Palmese, Ph.D.

Curing composites using electron-beam radiation (EB) offers significant advantages over traditional thermal curing but is limited by poor mechanical characteristics of the resulting polymers and their composites. Commercially, EB has advantages over thermal processing, for a number of reasons. Among these are rapid curing times, reduced energy requirements, curing at lower temperature, reduced shrinkage and residual stresses, the ability to co-cure dissimilar materials, and long shelf life as well as reduced volatile organic compounds (VOC) emissions. These characteristics allow for the manufacture of complex composite structures using low cost tooling and staged operations. However, composites made from such polymer systems suffer from low compressive strength, poor interlaminar shear strength, and low fracture toughness when compared to incumbent thermally cured systems. Thus, while possessing great processing benefits, EB cured polymers' poor mechanical performance prevents them from being adopted.

The objective of this work is to develop a fundamental understanding of the physical and chemical processes underlying EB and ultra-violet (UV) polymerization of epoxy systems that will enable the design of improved systems. Specific goals include (i)

obtaining a detailed understanding of the influence of process parameters, particularly water concentration and discontinuous application of EB dose on polymerization behavior, (ii) developing an understanding of relationships among cure process variables with network structure/morphology and properties, and (iii) designing new systems with improved properties based in part on the understanding developed in i and ii.

EB and UV curing processes were monitored *in-situ* using near infrared (NIR) fiber optic spectroscopy. Based on such data, a detailed kinetic model was developed that elucidates the influence of water on EB induced polymerization of glycidyl ethers. Moreover, the influence of initial water concentration on final polymer behavioral characteristics were assessed quantifying the potentially deleterious effects of not controlling humidity during EB processing.

Previous studies of epoxy cure behavior have been conducted under continuous irradiation. The processing of parts via EB generally occurs in a step-wise fashion. The transient behavior upon stopping irradiation, "dark reaction," was examined and revealed that while pronounced initial reductions in reaction rates occur, active centers responsible for polymerization persist for many thousands of hours. Therefore for practical purposes this is a living polymerization. It was found that traditional deactivation models do not capture the observed behavior suggesting that the combination of diffusion limitations and chain transfer reactions need to be considered as a possible explanation.

A novel class of comonomers for improving the fracture toughness of EB and UV cured epoxy systems was discovered and studied. These monomers are based on the five-member furan ring that was shown to ring open and copolymerize with glycidyl ethers. By using tetrahydrofuran, a string of four methylene units is inserted in the

network providing chain extension and greatly increased fracture toughness. Multifunctional monomers based on this chemistry were developed that increase the fracture toughness of the base epoxy resin five fold while maintaining the glass transition temperature. This is a remarkable achievement because it is an enabling technology that solves the major deficiency of EB and UV cured epoxies.

CHAPTER 1: INTRODUCTION

Polymers can generally be divided into two main families: thermosets and thermoplastics. Thermoplastics are linear or branched macromolecules that can be made to flow upon heating. Thermosets are crosslinked polymers possessing a three-dimensional network structure. This structure is formed by the reaction of multifunctional monomers generally induced by heating. Thermosetting materials, like epoxies, are useful because they do not flow or melt upon heating. Yet the crosslink structure results in brittle systems generally used below their glass transition temperature. Moreover, processing conditions are known to affect the final properties of thermosets and the process-structure-property relationship must be well understood for such systems in order to exploit the high performance characteristics of these systems.

1.1. Thermal Curing versus Radiation Curing

Generally, high performance epoxies require high temperatures during thermal curing. This results in a product with excellent chemical and heat resistance, high adhesive strength, low shrinkage, good impact resistance, high strength and hardness, and high electrical insulation. Most importantly, the kinetics of this process are well known. Radiation curing by electron beam (EB) offers advantages over thermal curing. These advantages include greater energy efficiency, shorter curing time, lower energy requirements, lower temperatures which result in reduced residual stresses, reduced material shrinkage, the ability to co-cure dissimilar materials, reduced VOC emissions, and a longer shelf life [1-3]. Despite these benefits the epoxy system materials cured by radiation have poor mechanical properties. Moreover, the cure processes and their relation to processing parameters such as temperature, time, dose and dose rate are not

understood.

1.2. Objective

The objective of this work is to develop a fundamental understanding of the physical and chemical processes underlying EB polymerization of epoxy systems that will enable the design of improved systems. Specific goals include (i) obtaining a detailed understanding of the influence of process parameters, particularly water concentration and discontinuous application of dose, on polymerization behavior; (ii) developing an understanding of relationships among cure process variables and network structure, morphology, and properties; and (iii) designing new systems with improved properties based in part on the understanding developed in i and ii.

1.3. Methodology

The approach followed for designing improved EB cured epoxies is summarized schematically in Figure 1.1. This methodology allows a logical progression in understanding the underlying process of EB curing of epoxies. A number of control variables must be considered that can influence the properties of the cured epoxy resin. These include traditional process variables such as time and temperature and ones specific to EB curing like dose and dose rate. Additionally, material variables such as photoinitiator concentration, use of co-monomers and the presence of impurities such as water must be considered. The first step is to investigate how these variables affect the curing processes. Second, a link between these chemical and physical processes and network formation needs to be established. Finally, the link is made to mechanical properties so that a loop is formed that can be used to design improved materials.

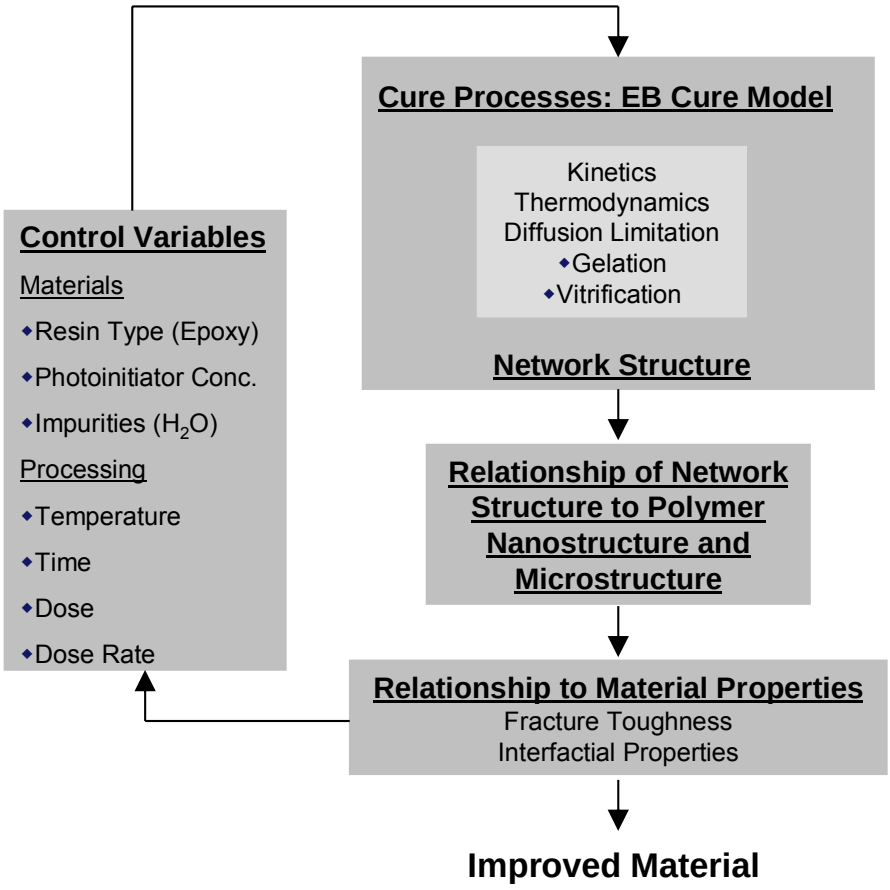

Figure 1.1. Proposed methodology for the rational design of improved EB cured epoxies.

1.4. Thesis Outline

Three main topics are discussed in this work. These are listed below in the order in which they will be presented.

1. An investigation of the influence of water on the polymerization kinetics of glycidyl ethers induced by UV and EB irradiation.
2. A a study of epoxy cure behavior following periods of UV and EB irradiation (dark reactions).
3. The design of Improved EB cured diglycidyl ether bisphenol A (DGEBA) systems by copolymerization with novel tetrahydrofuran functional comonomers.

In Chapter 2 background is discussed regarding the polymerization of epoxy systems. The importance of understanding thermal curing is discussed in this chapter. There are other curing techniques that must be considered to show why the method of curing was chosen for this work. Chapter 3 describes the experimental techniques developed in this study, which were used to monitor the reactions of interest, material characterization techniques, and the principal materials used. Chapter 4 reports the results of the investigation into the influence of water on the polymerization kinetics of glycidyl ethers induced by UV and EB irradiation This includes the development of a kinetic model as well as a discussion of the influence of water on the resulting network structure and material properties. In previous work, the In Chapter 5 the effects of discontinuous irradiation are discussed. In previous studies dark reactions had not been considered. Chapters 6 and 7 summarize work conducted to tailor material properties via the incorporation of comonomers. Chapter 6 presents results of experiments using a trifunctional epoxy to improve T_g without decreasing other properties. Chapter 7 describes the use of tetrahydrofuran functional monomers as chain extenders to

improve fracture toughness. Chapter 8 is a summary of the main achievements of this project.

1.5. References

1. Dake KD. Adhesives Age, 12, 12 (2002).

2. Sands JM, Fink BK, McKnight SH, Newton CH, Gillespie JW, Palmese GR. Clean Products and Processes, 2, 228-235 (2001).

3. Kulshreshtha A, Vasile C. Handbook of Polymer Blends and Composites, 1, Chapter 11 (2002).

CHAPTER 2: BACKGROUND

2.1. Epoxies

In the early 1900s, Prileschajew, a Russian chemist, discovered that olefins reacted with peroxybenzoic acid to form epoxides. However, Schlack is known as the inventor of epoxy resins in 1934. His patent details the preparation of high molecular weight polyamines by reacting amines with epoxide compounds, produced by the reaction of epiclorohydrin and bisphenol-A [1]. Epoxy resins were commercialized in 1946 by Ciba Specialty Chemicals. The chemistry of epoxies and the range of commercially available variations allow cured polymers to be produced with a very broad range of properties.

Thermosetting epoxy products are used for paints and surface coatings, molded and reinforced plastics, electronic components, adhesives, spray foams, and dental cements. As a coating, epoxy is used as a primer to improve adhesion of paints to metal surfaces and to prevent corrosion. Adhesives that are used for high strength bonding needed in the construction of airplanes, automobiles, and bicycles are often epoxy based. These adhesives can be used for wood, metal, glass, stone, and plastic products. Composites can also be produced with epoxies which produce stronger and more temperature resistant parts than polyester resins and vinyl ester resins. For example, circuit boards can be bonded together into a composite by an epoxy resin. Also, fiber reinforced composites can be produced for parts used in aerospace, automotive, and recreation industries.

There is a wide range of epoxy formulations. Epoxies can polymerize by two methods. One is step-growth polymerization, where epoxy reacts with amines,

anhydrides, or other hardeners in a stepwise manner as shown in Equation 2.1.

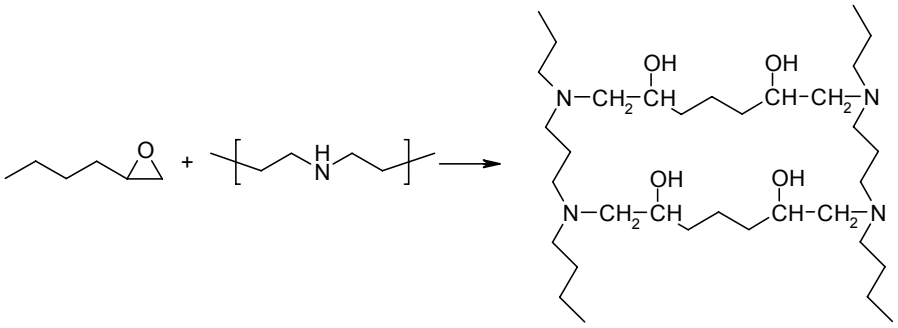

[2.1]

The other is chain-growth polymerization, where monomer molecules add on to a growing polymer chain one at a time. A chain initiator can be used to make a reactive active center where new monomer adds on the growing polymer chain Thus epoxies can homopolymerize as shown in Equation 2.2.

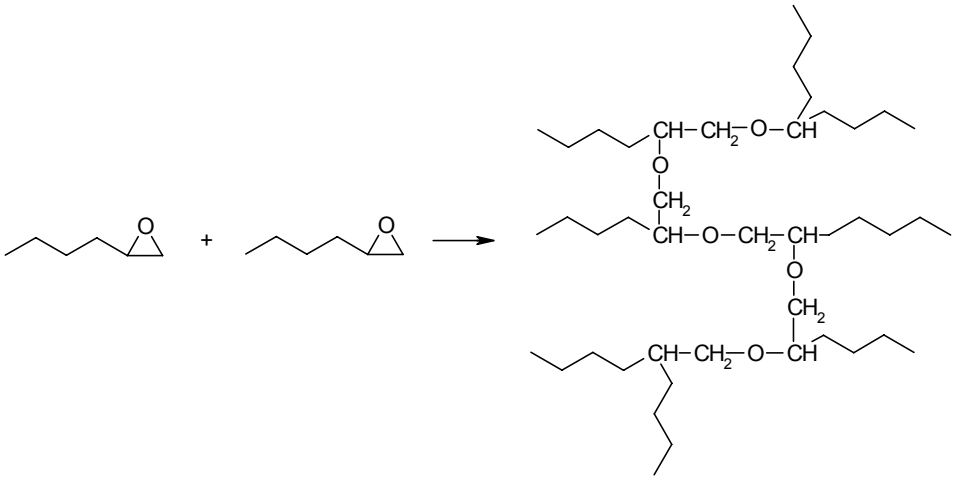

[2.2]

Anionic polymerization of epoxies can be initiated by alkoxides, hydroxides, metal oxides, or organometallic species as shown in Equation 2.3.

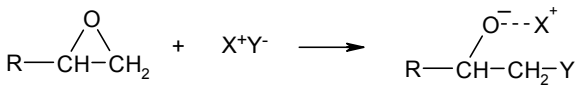

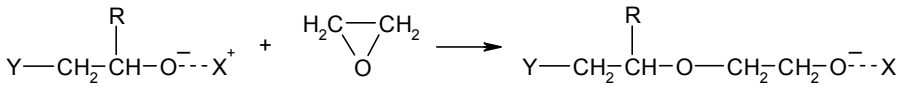

[2.3]

Cationic polymerization of epoxies can be initiated by Lewis acids and protonic reagents and will be discussed in detail in section 2.3. Epoxies can be cured at various temperatures and times. The properties can be modified by changing the processing conditions. They are generally known for their excellent adhesion, chemical and heat resistance, good mechanical properties, and good electrical insulating properties.

2.2. Curing of Epoxy Resins

In order to understand the curing process of thermosets, Gillham monitored the entire cure process from liquid to solid by using the torsional braid analysis (TBA) technique. The isothermal curing of an epoxy/amine system gave an understanding of the gelation and vitrification that occur as transitions in development of the network structure. Gillham developed a state diagram to represent the cure process; Figure 2.1 shows a time-temperature-transition (TTT) cure diagram.

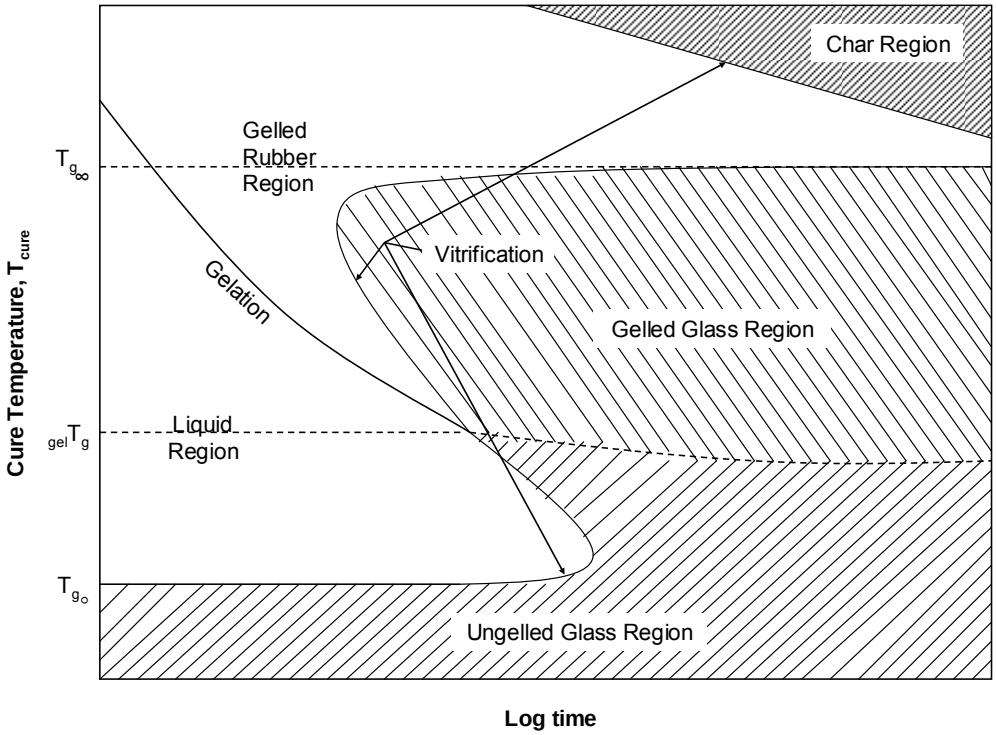

Figure 2.1. Gillham's time-temperature-transformation (TTT) cure diagram, where liquid, gelled rubber, gelled glass, and ungelled glass are four states of matter. These regions are delineated by a plot of the times to gelation and vitrification during isothermal cure vs. temperature [9-10].

Gelation is defined as the formation of an infinite molecular network and gives long range elastic behavior in the macroscopic fluid. Vitrification is defined as transformation from a liquid or rubbery state to a glassy state as a result of an increase in molecular weight. When T_g rises to the cure temperature (T_{cure}), vitrification occurs. The material is considered glassy when $T_{cure}<T_g$, whereas it is liquid or rubbery when $T_{cure}>T_g$. In the vitrified state, the rate of cure is drastically decreased, since diffusion will control the reaction rather than the intrinsic chemical kinetics. However it is possible to continue curing by heating the partly cured material above its T_g. During isothermal cure above the ultimate glass transition temperature ($T_{g\infty}$) of the polymer, only gelation will occur [9-10]. Although this diagram was developed for thermally induced step growth epoxy polymerization, similar phenomena are encountered in cationic chain polymerization of epoxies. Only cationic polymerization of glycidyl ethers will be considered in this work.

2.3. Thermal Curing

Many authors have investigated the thermally induced cationic polymerization of epoxies by employing BF_3-amine complexes as initiators [1-7]. BF_3-amine catalysts activate an epoxy monomer by forming an oxonium active center and a primary amine as shown in Equation 2.4.

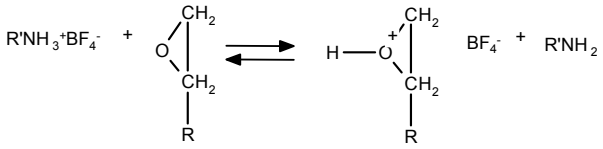

(2.4)

These protonated epoxy molecules can then react with other epoxy monomers and proceed in cationic chain propagation by the activated chain end (ACE) or activated monomer (AM) mechanisms.

In the ACE mechanism, tertiary oxonium ions ($M_{n+1}H^+$) are formed and the chain

propagates by repeated addition of monomer molecules as shown in Equation 2.5.

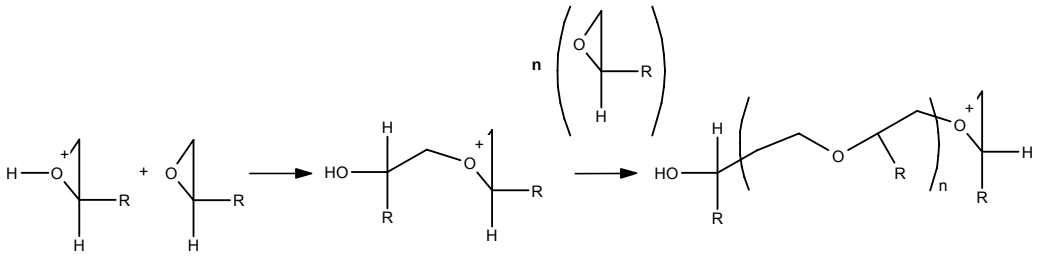

(2.5)

MH^+ **M** **$HOMM^+$** **$HOM_{n+1}M^+$**

The AM mechanism is given by Equation 2.6. As the oxiranium ring opens, hydroxyl groups are formed, and with a high formation of active centers, more hydroxyl ions will form. Reaction with these hydroxyl containing species followed a transfer of charge with a monomer to generate the activated monomer (MH^+), which is again added to a hydroxyl containing species. Thus this path becomes more important as the hydroxyl concentration increases with increasing initiation [1-3, 8].

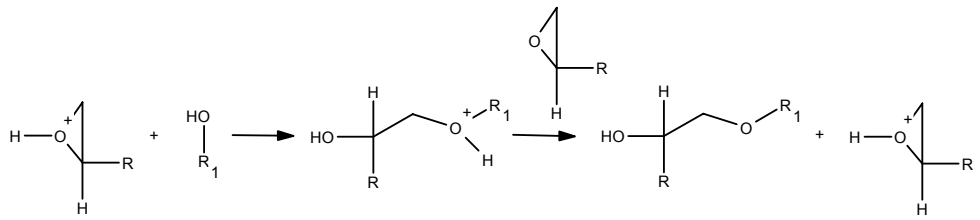

(2.6)

MH^+ **R_1OH** **$HOMOR_1^+$** **$HOMOR_1$** **MH^+**

Another reaction in addition to those mentioned above is a chain transfer reaction where an activated chain reacts with a hydroxyl group, specifically that of water shown in Equation 2.7.

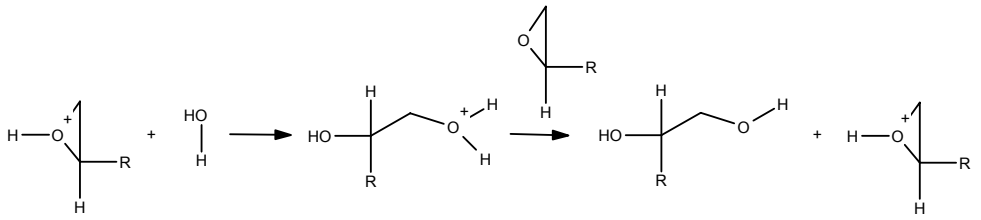

(2.7)

MH^+ HOH $MHHOH^+$ MHOH MH^+ HOM_nOH

2.4. Radiation Curing

Exposing polymeric precursor materials to high energy radiation sources in order to initiate polymerization or cross-linking of resin has been developed in the last 50 years. The growing interest in radiation curable resins is due to the broad range of advantages these materials have over traditional thermally cured polymers. Radiation curing requires shorter times, reduces emissions of toxic volatile components, and cures at low temperatures thus reducing energy consumption and costs. There are different types of radiation that are applicable to different situations. The forms of radiation that have been investigated in the past as a viable initiation source for ionic and/or free radical polymerizations are summarized in Figure 2.2. Radiowaves and microwaves, low energy radiation, are unable to initiate polymerization but are used as a source of thermal energy. Infrared are also used as a heating source. At medium energy, visible light can initiate photo-polymerization with the addition of photo-initiator. Ultra-violet (UV) light is used in coating industries, but has limited application in the composite area due to poor penetration depth. At higher energy there is electron beam (EB) that can initiate polymerization without using initiators, in some cases, and is efficient for curing thick composites. Lastly X-rays and γ-rays are high energy sources that can be used to cure materials. Practically, UV and EB radiation are widely used to cure materials. If the penetration depth is relatively small, UV radiation can be used to cure materials. High

energies, EB radiation can cure thick composite suitable for many applications [1]. Epoxies cured by EB do not require an amine hardener but rather react through cationic chain polymerization induced by the combination of radiation and a photoinitiator.

2.5. UV Curing

Ultra-violet (UV) curing technology was explored in the early 1940s as an alternative to thermal curing of polymeric materials. UV curing uses electromagnetic radiation energy in the form of photons to induce chemical change in monomers and form polymer networks. These methods were explored to eliminate non-reactive solvents and reduce drying process for coatings and inks. UV light generates reactive species, free radicals or ions, with small amounts of a photoinitiator. There are two classes of UV curable resin. One is radical polymerization, is often used to initiate acrylates or unsaturated polyesters by homolytic photocleavage of aromatic ketones. The other is cationic epoxy or vinyl ether polymerization that initiate active species by photolysis of arylonium salts to form protonic acids [15, 24-26].

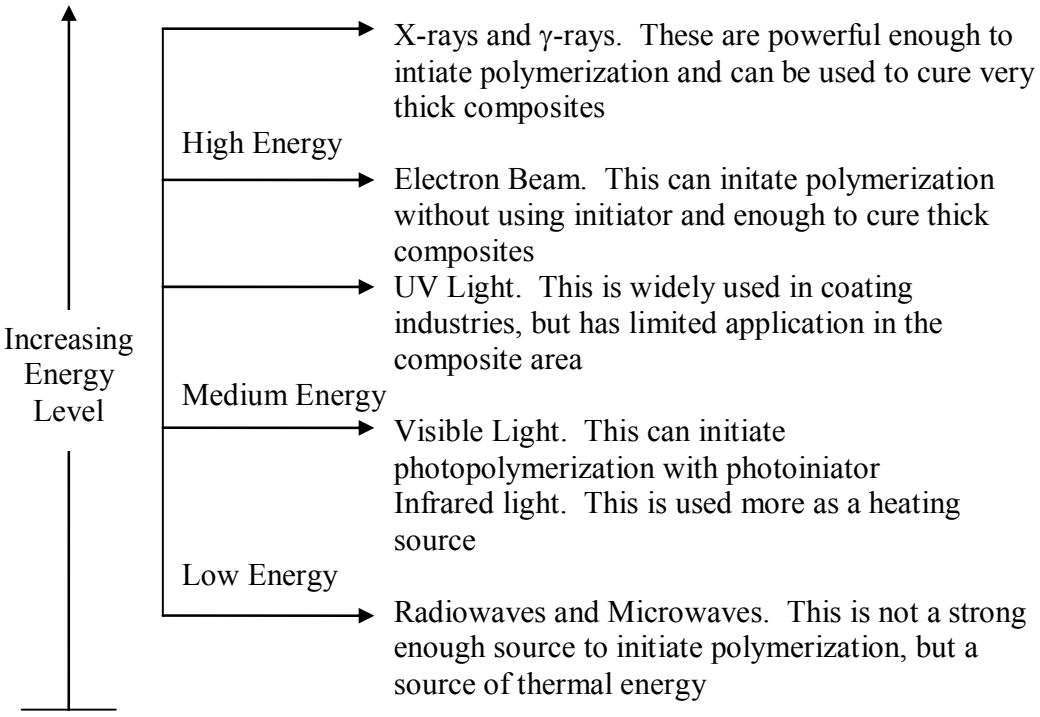

Figure 2.2. Summary of the different radiation types and their characteristic properties.

2.6. Electron beam curing of composites

Electron beams are able to penetrate thicker systems than UV light. A schematic of the EB facility used in Dayton, Ohio is shown in Figure 2.3. The depth of penetration of the electron beam is dependent on the beam energy and the density and geometry of the irradiated material. The higher the electron energy the deeper the penetration will be. The processing rate or throughput is directly proportional to the power of the accelerator.

EB curing can reduce fabrication and assembly costs and increase design freedoms. EB process allows large integrated structures to be bonded and cured at low temperature without the use of autoclaves. Using EB for curing can overcome the disadvantages of heat curing processes such as limited throughouput, liberation of low molecular weigh volatiles that cause voids or pollution, and residual stresses upon cooling. In 1994, a Cooperative Research and Development Agreement (CRADA) was established for the advancement in electron beam curing of Polymer Matrix Composites (PMCs) technology. The goal of the CRADA program was to develop and optimize resin systems and PMCs to meet the performance of thermally cured composites. Over the years further development of environmentally friendly processes and EB curable cationic resin systems were developed.

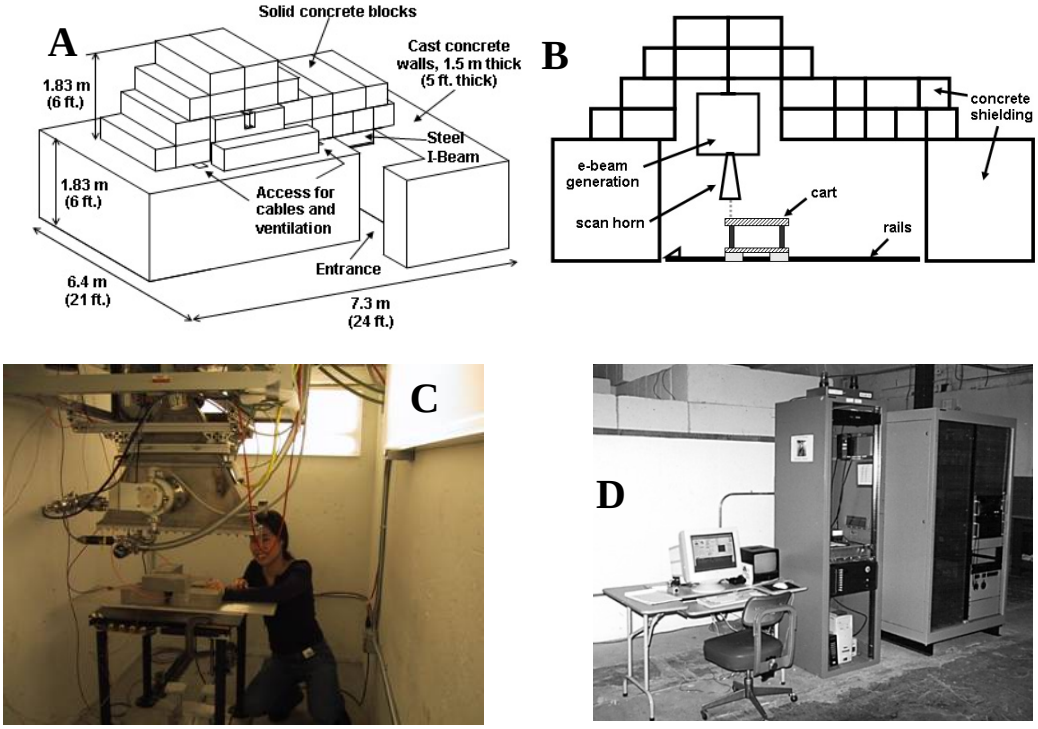

Figure 2.3. Schematic of electron beam facility at University of Dayton Research Institute: A) overall layout of UDRI EB facility, B) vault interior schematic, C) interior of EB vault, showing scan horn and cart, D) control area of EB facility, showing vault exterior (background), computer monitor and vault camera (foreground, left), computer control rack (foreground, center), and power interface module which contains the system's pulse forming network (foreground, right).

To obtain a fundamental understanding of the cationic polymerization of radiation-induced cationic cure of epoxies, a basis can be provided by the thermally cured systems. UV- and EB-induced polymerization should follow the same ACE and AM mechanism after the active centers are formed. However the initiation of active centers differs. For UV, Crivello et al. have studied the effect of onium salts that undergo photolysis where a powerful Bronsted acid is released as a multi-step mechanism shown in Equation 2.8 corresponds to the steps in Figure 2.4 [21-23].

$$
\begin{aligned}
&\xrightarrow{h\nu} \\
&Ar_2I^+X^- \rightarrow [Ar_2I^+X^-]^* \\
&Ar_2I^{+*} + Ar^* \rightarrow X^- \\
&Ar_2I^{+*} + SH \rightarrow ArI^+H + S^* \\
&ArI^+H \rightarrow ArS + H^+
\end{aligned}
\qquad (2.8)
$$

A super acid is produced from UV photo-initiation, such that the H^+ ion reacts with the epoxy group of the monomer and produces an active species, MH^+, similar to the thermal system. With EB, Crivello et al. found through tests on cyclohexene oxide with photo-initiator that two kinds of cationic species are formed. EB-induced initiation causes radical species to form from the irradiation that reacts with an epoxy monomer. This complex then rearranges to form a stable resonance structure of a carbon centered radical. This can be reduced by the photo-initiator where the cation can directly attack the epoxy or polymerize with the protonic acid formed if there is a trace amount of water forming another cationic active center as shown in Equation 2.9 [23].

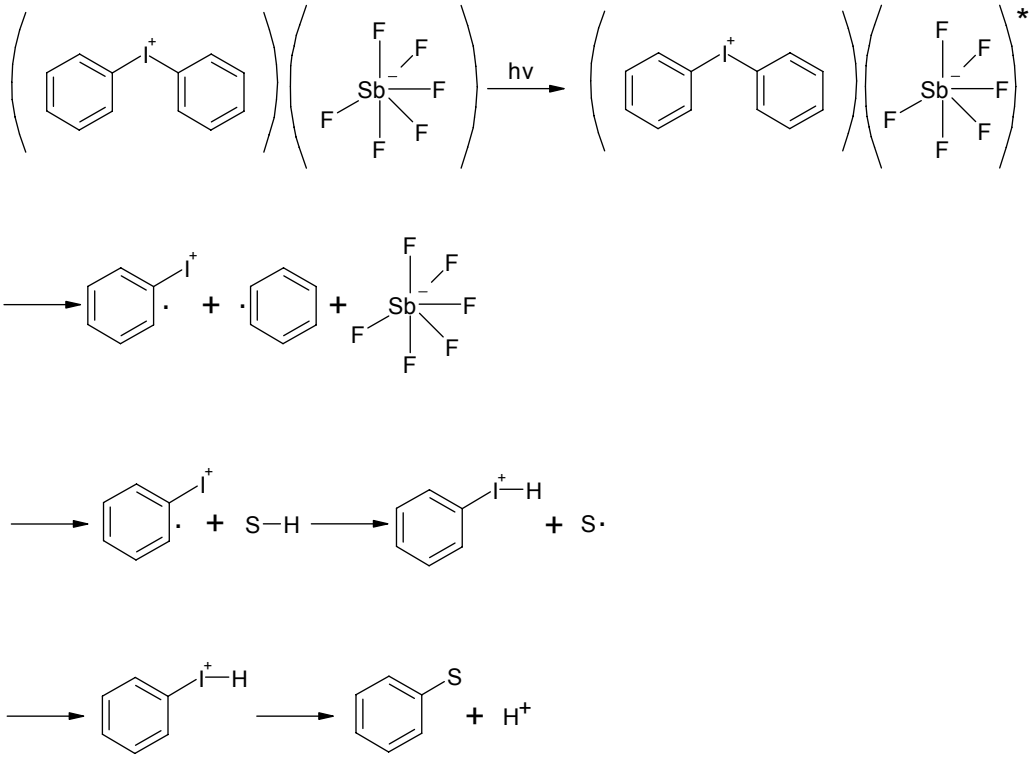

Figure 2.4. Formation of active species from EB to initiate cationic polymerization.

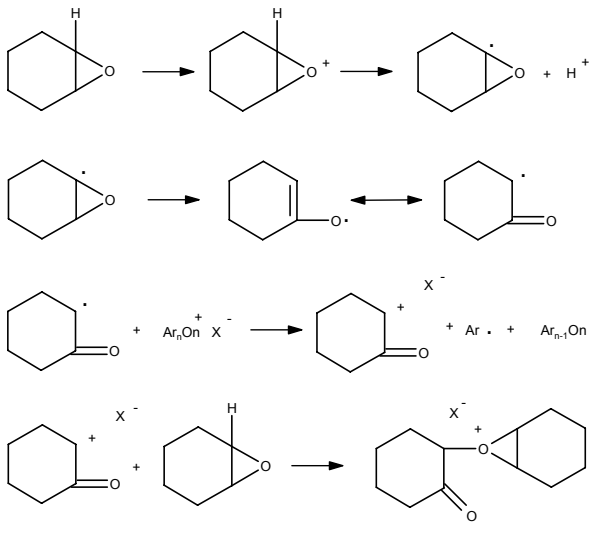

(2.9)

In this investigation, the concern is placed on the existence, rather than the type, of active centers that are formed. Thus the propagation mechanism for cationic polymerization will be consumed universally for thermal, UV, and EB. Cationic polymerization of heterocyclic monomers can be initiated using protonic acids, Lewis acids/protons, iodine, and photo-initators [15, 16]. New photo-initators for UV induced polymerization were discovered by Crivello.

The mechanism of chain growth involves nucleophilic attack of the oxygen of an incoming monomer onto a carbon atom in the α -position with respect to the oxonium site whereby the cycle opens and the site is reformed on the attacking unit [19]. In some cases cationic polymerizations can be considered 'living'. In such cases the reaction mechanism involves only initiation and propagation steps. However, the active sites can be deactivated by addition of adequate nucleophiles, such as, amines.

Cationic polymerization can be commercially advantageous. Unlike radical polymerization, cationic polymerization is oxygen insensitive, can operate at low temperatures efficiently and can be used with a wide range of monomer systems including epoxides, vinyl ethers, and oxetanes [20]. In recent years, novel class of

epoxide and vinyl ether monomers have been investigated that display outstanding reactivities. The resulting polymers also possessed excellent adhesion, chemical resistance and mechanical properties. Cationic photopolymerization is applied practically in a variety of areas, including photoresists, stereolithography, holography and highly sensitive cationic coatings and adhesives [21-22].

2.7. References

1. Chabanne P, Tighzert L, Pascault J. J Appl Polym Sci, 53, 769 (1994).
2. Chabanne P, Tighzert L, Pascault J. J Appl Polym Sci, 53, 787 (1994).
3. Chabanne P, Tighzert L, Pascault J, Bonnetot B. J Appl Polym Sci, 53, 685 (1994).
4. Bouillon N, Pascault J, Tighzert L. Macromol Chem, 191, 1403 (1990).
5. Bouillon N, Pascault J, Tighzert L. Makromol Chem, 191, 1417 (1990).
6. Bouillon N, Pascault J, Tighzert L. Makromol Chem, 191, 1435 (1990).
7. Lunak S, Krejcar E. Die Angew Makol Chem, 10, 109 (1970).
8. Palmese GR, Ghosh NN, McKnight SH. SAMPE Int Symp, 45, 1874 (2000).
9. Enns JB, Gillham JK. J Appl Polym Sci, 28, 2567 (1983).
10. Manzione LT, Gillham JK. J Appl Polym Sci, 26, 889 (1981).
11. Crivello JV. Nucl Instr and Meth in Phys Res B, 151, 8-21 (1999).
12. Lecamp L, Lebaudy P, Yourssef B, Bunel C. Polymer, 42, 8541-8547 (2001).
13. Burdick JA, Peterson AJ, Anseth KS. Biomaterials, 22, 1779-1786 (2001).
14. Udagawa A, Yamamoto Y, Inoue Y, Chujo R. Polym J, 23, 1081 (1991).
15. Decker C, Bianchi C, Decker D, Morel F. Prog in Org Coatings, 42, 253-266 (2001).

16. Schrof W, Beck E, Koniger R, Reich W, Schwalm R. Prog of Org Coatings, 35, 197-204 (1999).

17. Palmese GR, Ghosh NN, McKnight SH. SAMPE Int Symp, 45,1874 (2000).

18. Hallpap P, Stadermann D, Bolke M, Heublein G. Acta Polym, 39, 350 (1988).

19. Hallpap P, Stadermann D, Bolke M, Heublein G. Acta Poly, 39, 211 (1988).

20. Crivello JV, Lam J. J Polym Sci: Polym Chem, 17, 977-999 (1979)

21. Crivello JV, Lockhart TP, Lee JL. J Polym Sci: Polym Chem, 21, 97-109 (1983).

22. Odian G. Principles of Polymerization, (1991).

23. Lazauskaite R, Grazulevicius JV. Poly for Adv Tech, 16, 571 (2005).

24. Decker C. J Polym Sci: Polym Chem, 30, 913 (1992).

25. Decker C. Prog in Polym Sci, 21, 593 (1996).

26. Decker C. Pigment and Resin Tech, 30, 278 (2001).

CHAPTER 3: EXPERIMENTAL

This chapter describes the basic experimental setup used in our kinetic studies as well as other testing methods employed throughout this investigation. Section 3.1 describes the development of the apparatus design for intrinsic NIR monitoring. Section 3.2 describes real time infrared spectroscopy (RT-NIR) and how it is used to analyze the kinetics of chemical reactions. Sections 3.3, 3.4, 3.5, 3.6 describe methods for dynamic mechanical analysis (DMA), fracture toughness testing, flexural testing, and short beam shear testing respectively.

3.1. Experimental apparatus – In situ real time NIR

This study was built upon the experimental setup developed by Mascioni [1]. The experimental apparatus consists of a NIR spectrometer from Control Development Incorporated (CDI-South Bend, IN, USA), a radiation source (UV or EB), and a custom sample chamber and holder, shown in Figure 3.1 equipped with cartridge heaters and temperature controller. The chamber was designed to align the NIR light through the center of the sample to obtain the spectra. Above the sample a hole is positioned in the sample holder for the UV or EB radiation source. The sample holder was fashioned from an aluminum block so that heating elements could be added to control the temperature of the reaction. The resin well was made by two glass slides with double sided tape from 3M with a well cut into the tape to place the resin in an open system [1]. However, in later work, it was found that an open environment could result in altered cure behavior. The second generation of the apparatus was developed to eliminate potential problems that could occur in an open environment. It incorporated a closed system to prevent impurities like water from affecting cure behavior. A schematic and picture of this set-up

is given in Figure 3.2.

Instead of using open glass slide holders, samples were placed in sealed glass tubes (1.6 mm ID, and 3.0 mm OD). This prevented introduction of impurities, including water, from the environment during cure. The glass tubes were filled such that all the epoxy would be exposed to the UV or EB radiation, since any unexposed resin would cause a change in the cure process. The rest of the design includes NIR spectrometer, heating, and radiation sources were same as to the first generation design.

3.2. Near Infrared Spectroscopy (NIR)

In previous work by Mascioni, the NIR system purchased from CDI had a spectral range of 1160 to 2250 nm with a resolution of 4 nm. In this study, the maximum spectral collection rate was found to be one per 0.134 s. We used low-hydroxyl silica fiber optic cables from Thorlabs Inc. (Newton, NJ, USA) to minimize attenuation of transmitted light in the NIR region. The design of the fibers was as follows: numerical aperture of 0.22, a nominal diameter of the silica core of 200 μm, a primary fluorine-doped silica cladding with a 20 μm thickness, a coating with a 10 μm thickness, and an external buffer with a 70 μm thickness, which were the same parameters as that used by Mascioni.

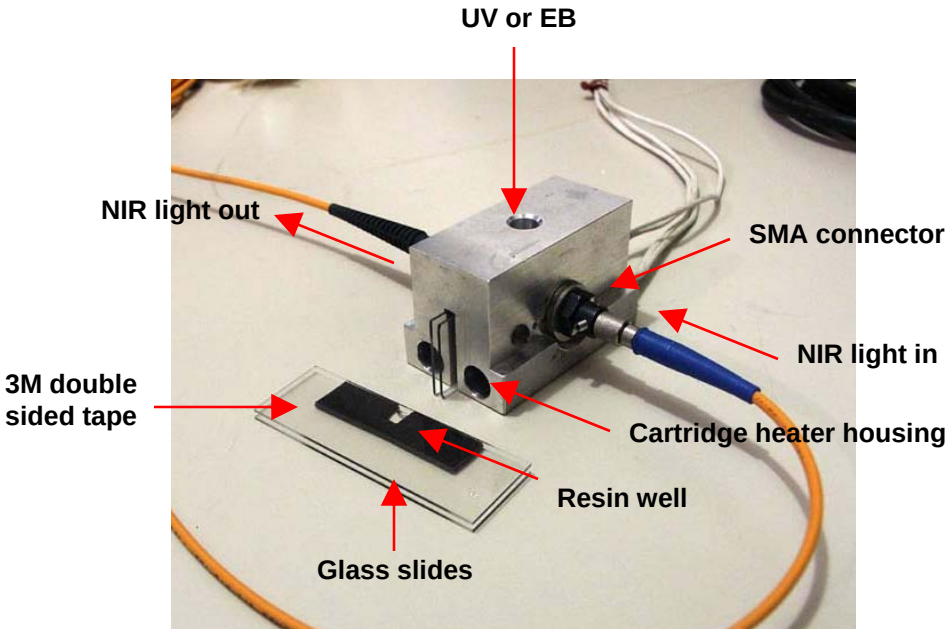

Figure 3.1. This picture is the first generation apparatus made by Mascioni to obtain his NIR measurements. The sample holder is made from two glass slides held together by 3M double sided tape with a resin well cut in the middle [1].

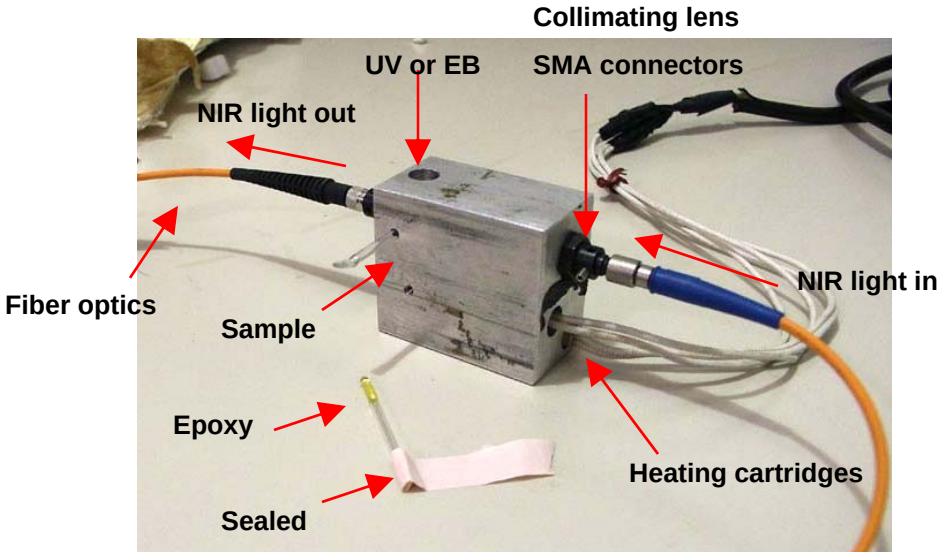

Figure 3.2. This picture is the second generation setup used to gather spectra for the cure process. This system is a closed system, using sealed tubes, to prevent the samples from absorbing impurities such as moisture during the cure process. All resin placed in the tube can be observed from the top to ensure that it is all being exposed fully to the radiation.

The light used in the fiber optic cables was produced by a white light source transmitted through an optical link that collimated the light that passed through the sample, which was then collected by a focusing lens that passes the light to the spectrometer [1]. When using the system with EB, the entire sample holder except for the radiation hole on top and fiber optics were then covered with lead bricks to protect the system from the harsh radiation. Only the radiation hole on top of the aluminum sample holder was exposed. This design allowed the collection of spectra in harsh conditions without exposing the fiber optics to high EB radiation doses, which discolor the optics over time and eventually distort the spectra. The CDI system was used to gather NIR absorption spectra. The structure and the characteristic spectra of "dry" phenyl glycidyl ether (PGE) and diglycidyl ether bisphenol A (DGEBA) before and after cure are shown in Table 3.1 and Figure 3.3 respectively. The major peaks monitored included 1623 and 2209 nm for the epoxy ring, 2143 nm for the aromatic ring, for water at 1908 nm, and 1436 nm for $^{-}$OH.

Table 3.1. Chemical structure of epoxy molecules.

Material	Chemical Structure
Phenyl glycidyl ether (PGE) from Aldrich Chemical Company, Inc. USA	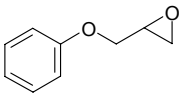
Diglycidyl ether of bisphenol A (DGEBA). EPON 825 from Miller-Stephenson (n=0.0228)	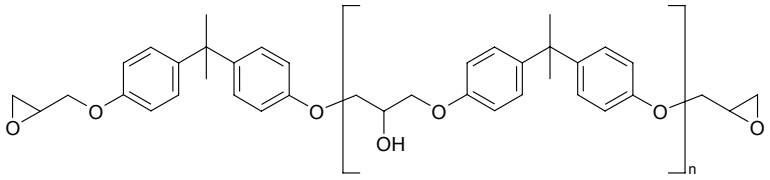

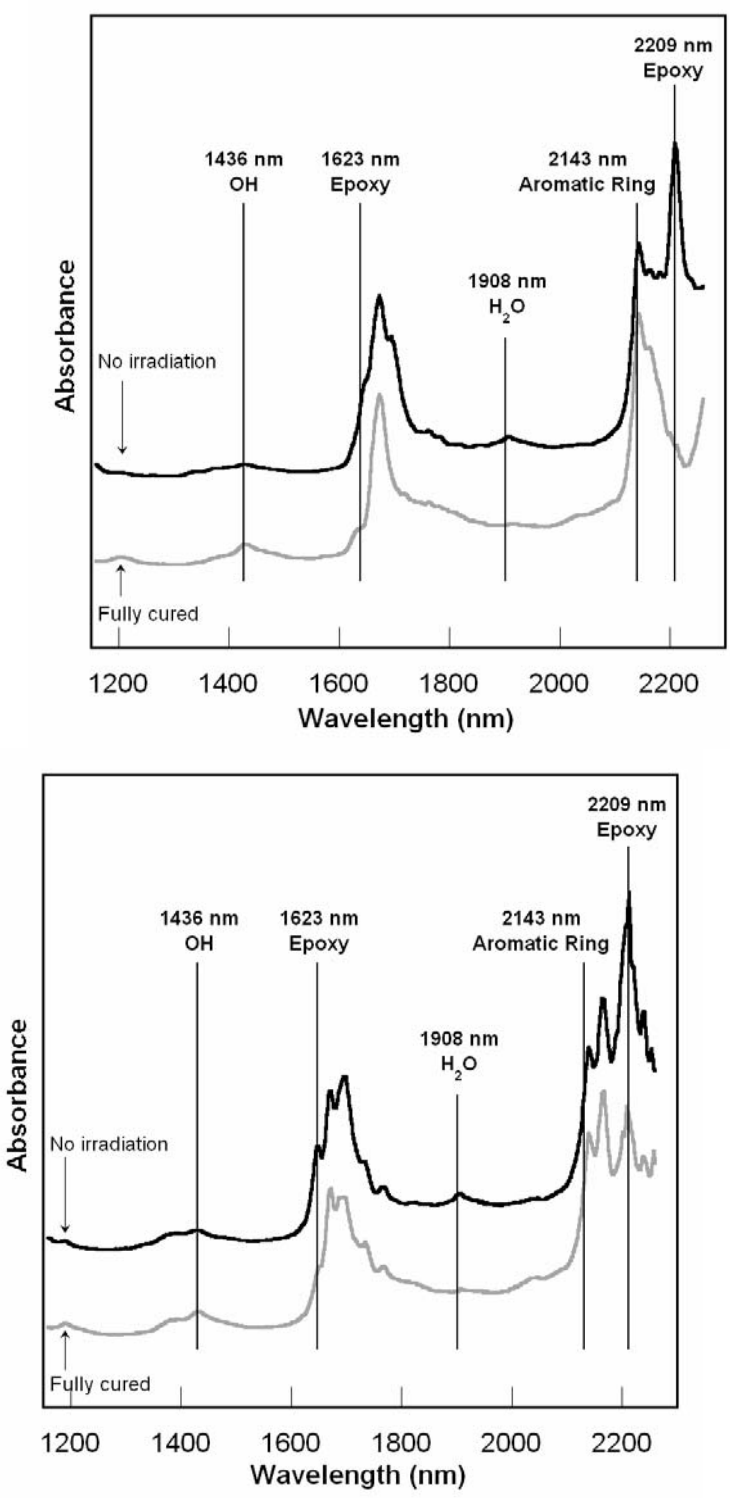

Figure 3.3. IR absorption spectrum for PGE (top) and Epon 825 (bottom) before (—) and after (—) curing.

3.3. Size exclusion chromatography (SEC)

Size exclusion chromatography (SEC) was run on the linear polymers PGE and new synthesized comonomers. Molecules in solution must be linear, branched, or globular so crosslinked systems cannot be tested with this method. A Waters 515 GPC pump was used with two 30 cm long, 7.5 mm diameter, and 5.0 μm styrene-divinyl benzene columns in series. The columns were equilibrated and run at 30°C using tetrahydrofuran (THF) (Aldrich, Milwaukee, WI) as the elution solvent at a flow rate of 1.0 mL/min. The column effluent was monitored by two detectors operating at 30°C a Waters 2410 refractive index detector and a Waters 2487 dual absorbance detector operating at 270 and 254 nm (absorbed by phenyl rings). Samples were prepared by dissolving a 1 mg sample of the material in 1 mL of THF. Since species of high molecular weight do not diffuse as easily into the packing, they elute first, while species of lower molecular weight elute later [3].

3.4. Dynamic Mechanical Analysis (DMA)

A TA Instruments DMA 2980 dynamic mechanical analysis (DMA) was used to evaluate the loss and storage moduli as a function of temperature from 30°C to 250°C and the T_g of each DGEBA system was measured. Temperature scans with a frequency of oscillation of 1 Hz and amplitude of 15 μm were performed at a rate of 2°C/min. Typical sample dimensions were 18 mm in length, 13 mm in width, and 2 mm in thickness. The T_g was taken as the temperature corresponding to the peak of the loss modulus curve.

3.5. Fracture Toughness Testing

Three-point single-edge notch bend (SENB) specimens were used for fracture

toughness measurements. ASTM 5045-93 specifies sample dimensions of 2.00 × 0.50 × 0.25 in. to assure plain strain conditions. A notch was made that was half the sample thickness and a sharp razor blade was used to initiate a crack at the base of the notches. The samples were tested using an Instron 8872 in flexural mode at a crosshead speed of 0.05 in./min. All tests were performed at ambient conditions. When tests were completed, the fracture surfaces of the specimens were examined for signs of plastic deformation. If plastic deformation was apparent, the sample was not included in the reported results.

3.6. Flexural Testing

Three-point flexural testing in accordance with ASTM D 790-03 was used to evaluate the flexural strength and modulus of the materials. Sample sizes and crosshead speed varied dependent on the thickness of the material.

3.7. Short Beam Shear (SBS) Testing

Interlaminar shear strength testing was conducted on the composites in accordance with ASTM D 2344/D 2344M. The samples were tested using a crosshead speed of 0.05 in./min. where the force of breakage was recorded to calculate the shear strength.

3.8. Reference

1. Mascioni M. Real Time In-Situ Spectroscopic Characterization and Modeling of Radiation Induced Cationic Polymerizations of Glycidyl Ethers, Master Thesis, (2002).
2. Jancovicova V. J of Photochem and Photobio A: Chem, 136, 195-202 (2002).
3. Garcia A, Bonen M, Ramirez-Vick J, Sadaka M. Biosep Process Sci. Malden: Blackwell Sci, 181–183 (1999).

CHAPTER 4: INFLUENCE OF WATER ON THE KINETICS OF CATIONICALLY PHOTO-INITIATED POLYMERIZATION OF EPOXY GROUPS VIA ULTRA-VIOLET AND ELECTRON BEAM IRRADIATION

4.1. Introduction

There has been a growing interest in radiation curing of resins and composites due to processing advantages over thermal curing. However, epoxy based composites cured this way suffer from low compressive strength, poor interlaminar shear strength, and low fracture toughness [1-11]. Furthermore, many aspects of the cure processes, including chemical kinetics and the influence of processing conditions and impurities, such as water, on behavioral kinetics are not fully understood. We have found that the presence of water significantly alters the UV and EB cure behavior of such epoxies by initially retarding the rate of polymerization and accelerating the rate relative to that of "dry" systems in latter stages of the reaction [12-13].

The purpose of this investigation is to gain further understanding of the influence of water on phenyl glycidyl ether (PGE) and diglycidyl ether of bisphenol A (DGEBA) polymerization. UV- and EB-induced polymerization are assumed to follow the same ACE and AM mechanism after the active centers are formed as described for thermal curing in Chapter 2. However, the formation of active centers may differ substantially in these cases. Crivello et al. have studied initiation of epoxy polymerization with UV light using onium salts that undergo photolysis to form a powerful Bronsted acid through a multi-step mechanism. Thus, a super acid is produced from UV photo-initiation, such that the H^+ ion reacts with the epoxy group of the monomer and produces an active species, MH^+, similar to that observed using BF_3-amine complexes for thermally induced

reaction. For EB induced polymerization, Crivello et al. examined the cationic reaction of cyclohexene oxide using similar onium salts as initiators. Initiation using EB was found to be significantly more complex as a result of the generation of epoxy based free radicals that reduce the onium salt to form the initiating cation that can react with an epoxy moiety to form an oxonium active center. This mechanism results in polymer not containing a hydroxyl functional end group. Alternatively Crivello et al. suggest that that direct reduction of the onium salt by solvated electrons to form protonic acids could also initiate polymerization. This mechanism is analogous to thermally induced as well as UV photopolymerizations and would result in hydroxyl terminated polymers [21-25]. However, similar studies were not reported for glycidyl ethers and it is not clear that the radical mechanism suggested by Crivello et al. would play the same role for glycidyl ethers [26] since the pertinent radical would be a less stable secondary carbon radical compared to the tertiary radical formed for cyclohexyl epoxy. In this investigation, the emphasis is the propagation steps for cationic polymerization that should be independent of the initiation mechanism whether thermal, UV, or EB.

A number of researchers have observed changes in reaction kinetics and final material characteristics of cationically cured epoxies resulting from the presence of water. There are numerous and sometimes contradictory observations. Past studies has shown that chain transfer agents are known to induce a latency period in BF_3^- initiated cationic cure of epoxies. Chabanne's et al. study of the influence of water on cationic polymerization via thermal curing resulted in the observation of a decrease in PGE conversion with increasing water concentration and that the rate of epoxy polymerization slowed down. Chabanne concluded this was due to water acting as a transfer agent and

completion of the AM and ACE mechanisms in PGE polymerization. Importantly a latency period during the beginning of the reaction was not observed [14-16]. In the study of the influence of water on epoxy polymerization via UV cure, Crivello observed that the addition of OH containing groups to cycloaliphatic diepoxides resulted in an increase in the rate of polymerization [24]. Hartwig et al. made similar observations for cycloaliphatic diepoxides and with an increase of humidity, the rate of polymerization increased. However, DGEBA epoxy systems reactivity decreased with the increase of humidity. Hartwig concluded that the decrease in reactivity for DGEBA was due to the formation of a stable five member intermediate. [28-29]. Our preliminary study with UV- and EB- induced polymerization of glycidyl ethers has shown that the presence of water caused an initial retardation in the polymerization of epoxies followed by a sharp acceleration, and in the case of DGEBA, higher degrees of conversion for a given isothermal cure temperature. The results suggest that care must be taken to control the water content in cationically cured epoxy systems. This is a relatively simple proposition for liquid molding applications where containers can be sealed and purged, however it is more problematic for pre-preg applications where pre-pregs are subjected to moist environments during the various stages of composite manufacture. In recent studies, Riberio et al. found that the resin glass transition temperatures are considerably lower than the thermally epoxies [30]. In our preliminary work, similar results were observed. The objective of this work is to gain a fundamental understanding of the influence of water on the kinetics of EB and UV induced polymerization of glycidyl ethers and the relation to thermomechanical properties. A fiber optic based spectroscopic technique was used to monitor epoxy and water concentration *in situ* for EB and UV-induced

polymerization of DGEBA and its monfunctional analog PGE. The results elucidate the influence of water on the kinetics of epoxy cationic polymerization and resulting changes in material behavior.

4.2. Experimental

4.2.1. Materials

Diglycidyl ether of bisphenol A (DGEBA) (Miller-Stephenson Epon-825) and phenyl glycidyl ether (PGE) (Aldrich Chemical Company) were used with diphenyl iodonium hexafluoroantimonate (CD1012) photo-initiator obtained from Applied Poleramic Inc. (Benica, CA). The chemical structures of these compounds are shown in Table 4.1. Epon-825 DGEBA has molecular weight of 354 g/mol. PGE is the mono-functional analog of DGEBA with a molecular weight of 150.17 g/mol. Reactants were dried using 4Å molecular sieves (Aldrich Chemical Company, Inc) to obtain "dry" epoxy. The sieves were dried at 120°C for 12 hours prior to use. Such drying limits water concentration to below 0.1% in the reactants.

Known quantities of de-ionized water were added to the "dry" epoxy to vary initial "wet" epoxy water concentrations. Mixtures of de-ionized water with DGEBA or PGE were used to evaluate the influence of water on epoxy cure behavior. A NIR spectroscopic technique was used to obtain quantitative measurements of water concentration throughout the reaction.

4.2.2. Fiber Optic Near IR Spectroscopy

The spectral analysis performed in this work was based on a near infrared spectroscopy technique discussed in Chapter 3 [27-28].

Table 4.1. Materials used in the experimental work; PGE as the mono-functional epoxy, DGEBA as the di-functional epoxy, and CD1012 as the photoinitiator.

Material	Chemical Structure
Phenyl glycidyl ether (PGE) from Aldrich Chemical Company, Inc. USA	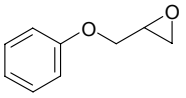
Diglycidyl ether of bisphenol A (DGEBA). EPON 825 from Miller-Stephenson (n=0.0228)	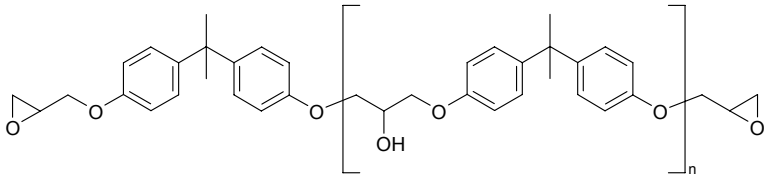
Diphenyl iodonium hexafluoroantimonate CD1012	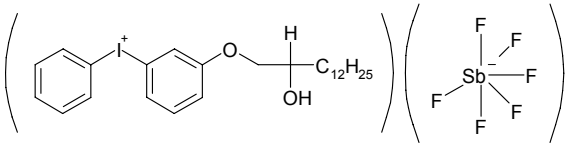

The experimental apparatus consists of a NIR spectrometer from Control Development Incorporated (South Bend, IN, USA), a heating and cooling temperature control, a radiation source (UV or EB), and a custom sample chamber and holder. The sample holder was fashioned from an aluminum block and was designed to align input and output radiation sources (UV, EB, IR), and to accommodate heating elements for temperature control. Samples were placed in sealed glass tubes (1.6 mm ID, and 3.0 mm OD) to prevent water absorption from the environment during cure [29]. The spectrometer possesses a spectral range of 1160 to 2250 nm with a resolution of 4 nm with a maximum spectral collection rate of one per 0.134 s. In order to ensure minimal attenuation of transmitted light, low-hydroxyl silica fiber optic cables were used (Thorlabs Inc., Newton, NJ, USA). The fibers have a numerical aperture of 0.22, a nominal diameter of the silica core of 200 μm, a primary fluorine-doped silica cladding with a 20 μm thickness, a coating with a 10 μm thickness, and an external buffer with a 70 μm thickness. The infrared probe light was produced by a white light source transmitted through an optical link that collimated the light. The collimated beam passed through the sample and was subsequently collected by a focusing lens that passes the light to the spectrometer through the fiber optic. The advantage of this design was that measurements of radiation-induced cure could be performed without exposing the spectrometer to harsh radiation environments. Characteristic peaks of epoxy, hydroxyl, and water were monitored as shown in Figure 4.1, where the formation of hydroxyl moieties and the depletion of water and epoxy are evident. The major peaks monitored via the NIR are epoxy at 1623 and 2209 nm, aromatic ring at 2143 nm, water at 1908 nm, and OH peak at 1436 nm.

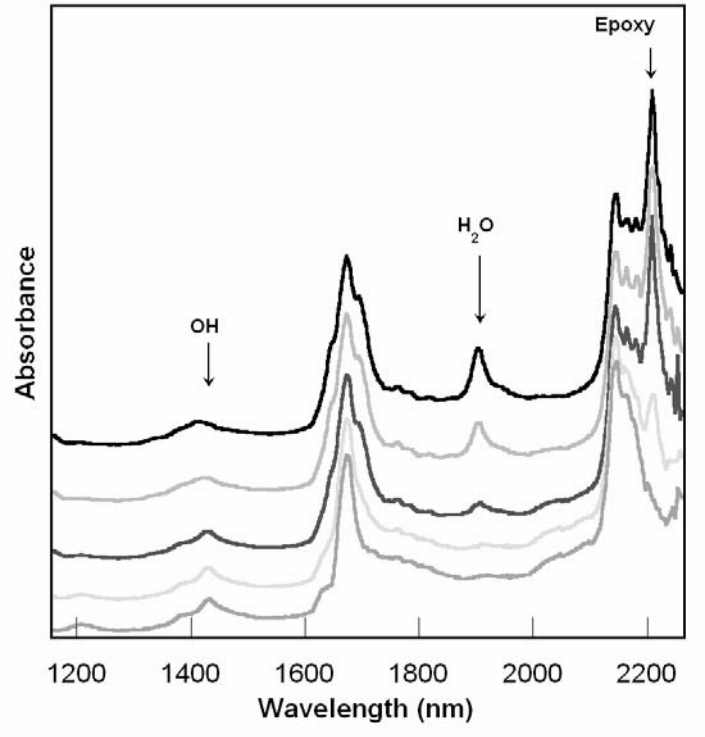

Figure 4.1. NIR spectra of water (1908 nm) and epoxy (2209 nm) peaks decreasing over time during cure and increase of hydroxyl (1426 nm) peak.

4.2.3. Sample Preparation and Irradiation

The photo-initiator was dissolved in the epoxy resin before the addition of de-ionized water. After water was added, samples were mixed and allowed to equilibrate at 60 °C in sealed containers. The photo-initiator concentration was 0.67 pph for UV experiments and 1.00 pph EB experiments. Samples were prepared with water concentrations ranging from 0.132 wt% to 0.889 wt% for PGE and 0.014 wt% to 1.0 wt% for DGEBA based experiments as measured using the NIR technique described later. After approximately 30 minutes at 60°C the mixtures appeared clear. The mixtures of water with PGE or DGEBA were placed in glass tubes (1.6 mm ID, and 3.0 mm OD) and then hermetically sealed. The samples were inserted into an aluminum block equipped with cartridge heaters, where isothermal cure experiments were conducted at 50°C for PGE and 60°C for DGEBA.

UV experiments were conducted using a Novacure™ (EFOS Inc., Mississauga, ON, CANADA) UV light source. It consists of three main components: an ultraviolet lamp, a set of quartz fiber light guides, and a UV-bandpass filter. The light source was equipped with a high pressure 100 Watt mercury vapor short arc lamp. Experiments were conducted using a light intensity of 32 mW/cm^2.

EB cure experiments were performed at the University of Dayton Research Institute Laboratory for Research on Electron Beam Curing of Composites. The EB machine is a 3 MeV EB accelerator specifically designed for irradiating samples in a controlled manner. The samples were cured for 500s at 5.5 kGy/min for the kinetics study of PGE and DGEBA [34-35].

EB curing was also conducted to make resin plaques using DGEBA for

mechanical property testing. DGEBA containing 1 pph photoinitiator was mixed with water to produce samples containing approximately 0%, 0.25%, 0.5%, 0.75%, and 1.0 wt% water. Polymerization was carried out in 15 passes at 3.6 kGy/pass for a total dose of 54 kGy. To control the reaction exotherm, the 2 mm thick samples were placed on an aluminum plate and chilled by ice water. The resin plaques were then subjected to a 2-hour thermal post-cure at 130°C.

4.3. Results and Discussion

This section addresses the influence of water on the cure kinetics and performance of glycidyl ethers based systems. The first part of this investigation involves the *in-situ* quantitative assessment of water concentration using a NIR technique. The second part of this work focuses on evaluating the reaction kinetics of epoxy with water for mono- and di-functional reactants. The final part addresses the influence of initial water concentration on the mechanical properties of the cured DGEBA resin.

4.3.1. Measurement of water concentration

A spectroscopic technique was developed to quantitatively assess the influence of water on the cationic polymerization of epoxies. Water shows a strong and distinct absorbance in the NIR spectrum at a wavelength of 1908 nm. In order to quantify the water concentration in the epoxy, calibration curves were constructed. "Wet" PGE and DGEBA samples were prepared as described in the experimental section without using photoinitiator. Subsequently the mixtures were placed in hermetically sealed glass tubes and spectra were taken. In previous studies, the peak height at 1908 nm for a fixed geometry was found to vary linearly with water concentration [12].

In this work the water peak height at 1908 nm was normalized by the epoxy peak height

at 2209 nm to obtain a calibration plot independent of path length. Plots of the normalized water peak versus the weight fraction of water added are given in Figure 4.2 for PGE (A) and DGEBA (B). The dashed line shows the linear relationship expected based on the Beer-Lambert Law. The data also show that a significant peak for water is present for the "dry" epoxy, indicating that the water content for the "dry" epoxies is not zero. The true water concentration can be obtained by shifting the dashed line so that it passes through the origin. This shift is shown in Figure 4.2 by the solid line, which represents an absolute calibration curve relating relative water peak height to weight fraction of water in PGE (A) and DBEGA (B). The equations for these lines are given by Equation 4.1 for PGE and Equation 4.2 for DGEBA:

$$Abs_{1908nm}/Abs_{2209nm} = 40.1(x_{water}) \pm 0.0166 \qquad (4.1)$$

$$Abs_{1908nm}/Abs_{2209nm} = 39.5(x_{water}) \pm 0.00532 \qquad (4.2)$$

This analysis suggests that the "dry" samples used to prepare the "wet" samples actually contained 0.25 wt% water. Moreover a saturation limit of 1.3 wt% for PGE and 1.0 wt% for DGEBA is observed for the temperatures evaluated. It should be noted that if proper care is taken to maintain the samples under a water-free environment after drying, the water content of the epoxy resin can be kept well below 0.1 wt%. However, once the resin is removed from the molecular sieves and comes into contact with moisture in the environment, significant levels of water can be transferred to the sample in a short period of time.

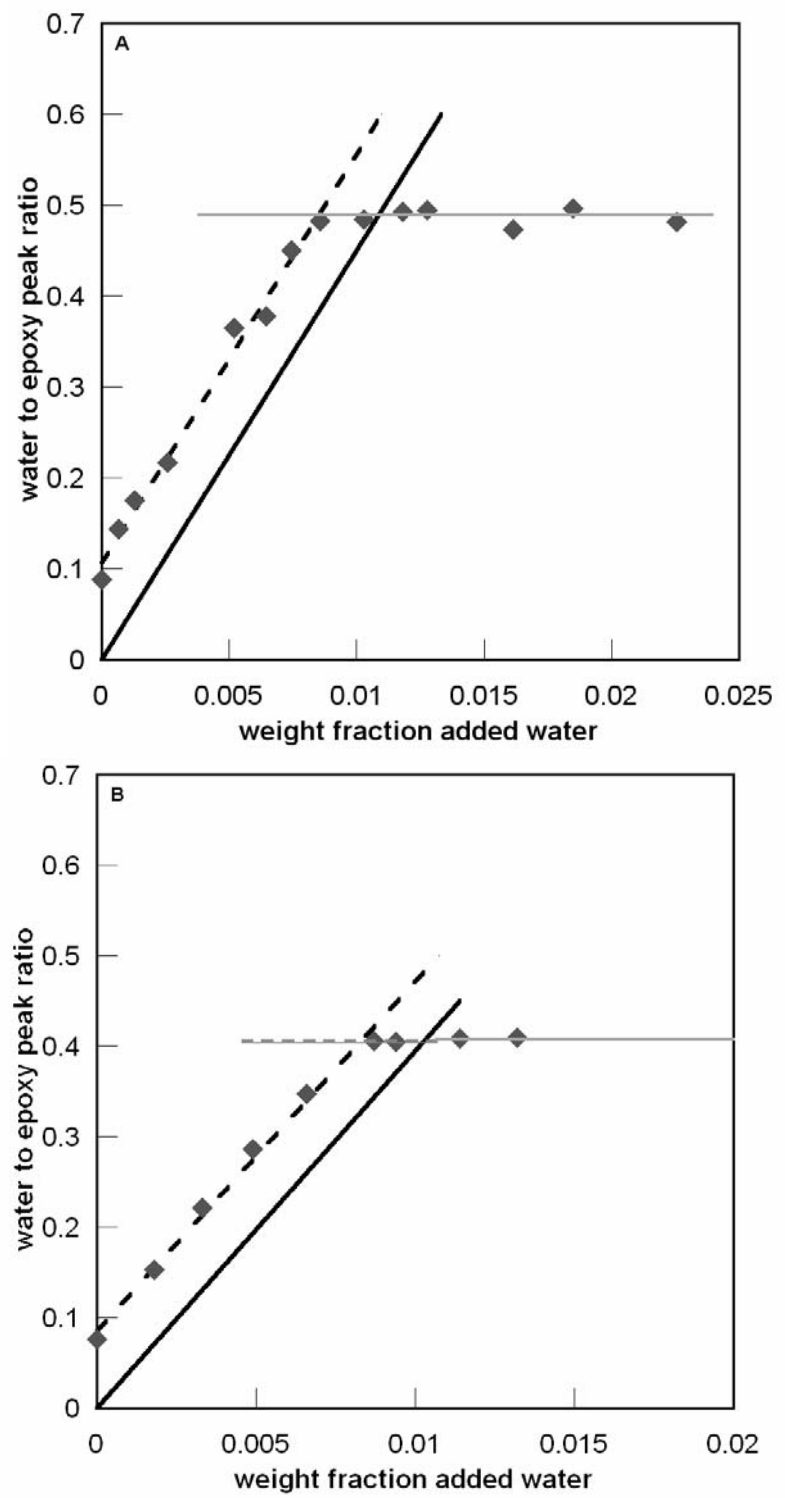

Figure 4.2. Calibration curve (solid line) is the water concentration in PGE (A) and DGEBA (B) to the water absorbance peak height. The data also show the saturation concentration for water at 60°C.

4.3.2. Influence of water on PGE cationic polymerization via UV and EB radiation

The initial water concentration in PGE was measured using calibration curve A in Figure 4.2 and showed initial water concentration values ranging from 0.18 wt% to 0.78 wt% for the samples cured by EB and from 0.13 wt% to 0.89 wt% for UV cured samples. The PGE samples were cured by UV and EB as described in the experimental section. The resulting spectra were analyzed by measuring water and epoxy peak heights as a function of time and assuming a linear dependence of peak heights with concentration. Epoxy peak heights were normalized by the initial peak height and the resulting values are dimensionless concentration. Representative plots of PGE epoxy concentration as a function of time for a number of initial water concentrations are given in Figure 4.3 for UV and EB studies.

These plots show that the addition of water greatly influences the chemical kinetics of polymerization. The presence of water leads to an initial retardation of epoxy conversion that is followed by an accelerated rate of epoxy conversion relative to that of dry systems. Figure 4.4 shows the consumption of water ((peak height at 1908 nm)/(initial peak height at 1908 nm)) and the formation of hydroxyl groups ((peak height at 1436 nm)–(initial peak height at 1436 nm)) for a representative experiment indicating an inverse relationship between water consumption and hydroxyl group formation. Figure 4.5 shows water and epoxy conversion data for “dry” and “wet” systems reacted under UV and EB irradiation. These plots show the temporal variation of water concentration where it is clear that the retardation in epoxy conversion occurs while the water is being consumed. When most of the water has been consumed, there is an apparent acceleration in epoxy reaction.

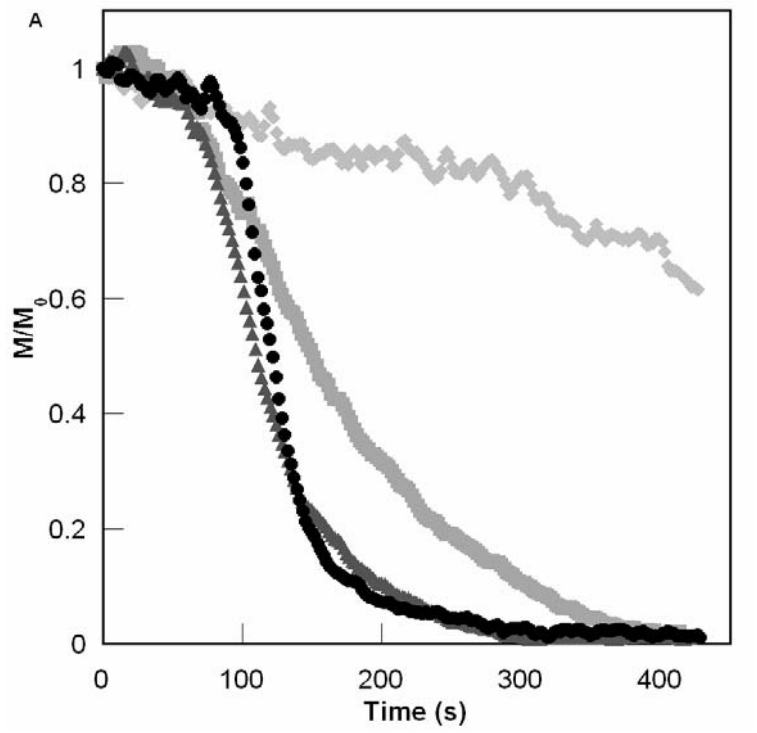
A
1
0.8
0.6
0.4
0.2
0
M/M0
0
100
200
300
400
Time (s)

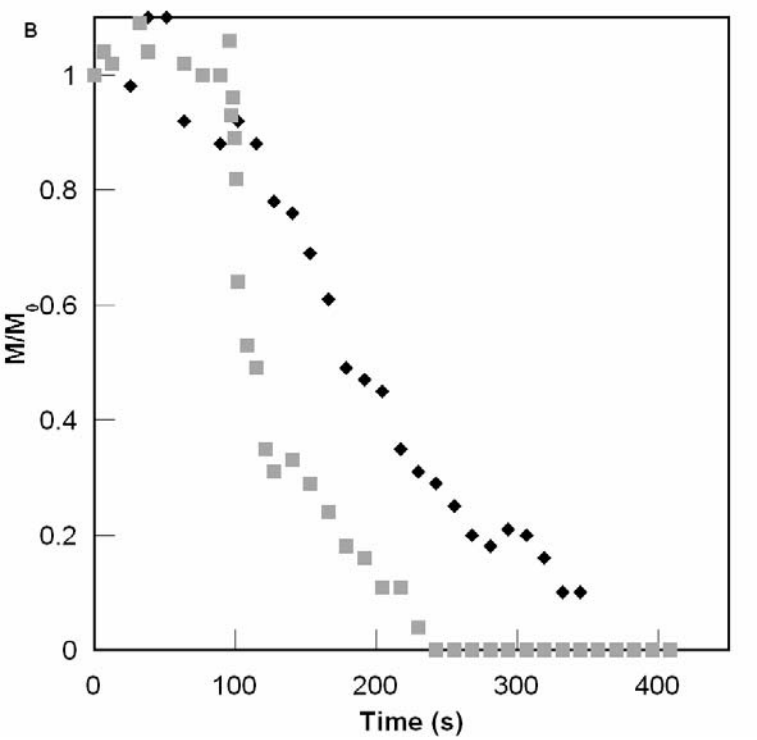
B
1
0.8
0.6
0.4
0.2
0
M/M0
0
100
200
300
400
Time (s)

Figure 4.3. Comparison of PGE cure behavior for various concentrations of water cured via UV or EB [UV (A) with 0.67pph initiator at 50°C where ◆ no water, ■ 0.34 wt % water, ▲ 0.73 wt% water, and ● 0.89wt% water; and EB (B) with 1pph initiator at 50°C where ◆ no water and ■ 0.78wt% water]. An increase of water shows a longer delay in epoxy conversion at the beginning followed by an acceleration where conversion is reached at a shorter time.

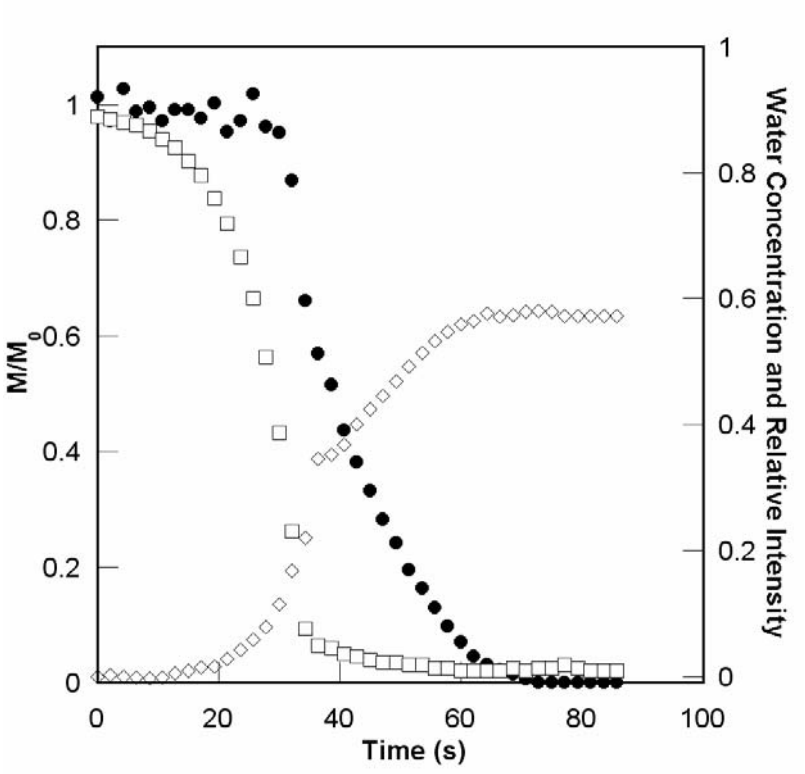

Figure 4.4. Representative plot for the consumption of water and formation of hydroxyls during EB curing processes (epoxy ●, water □, and hydroxyls ◇). This sample contains 0.78 wt% water.

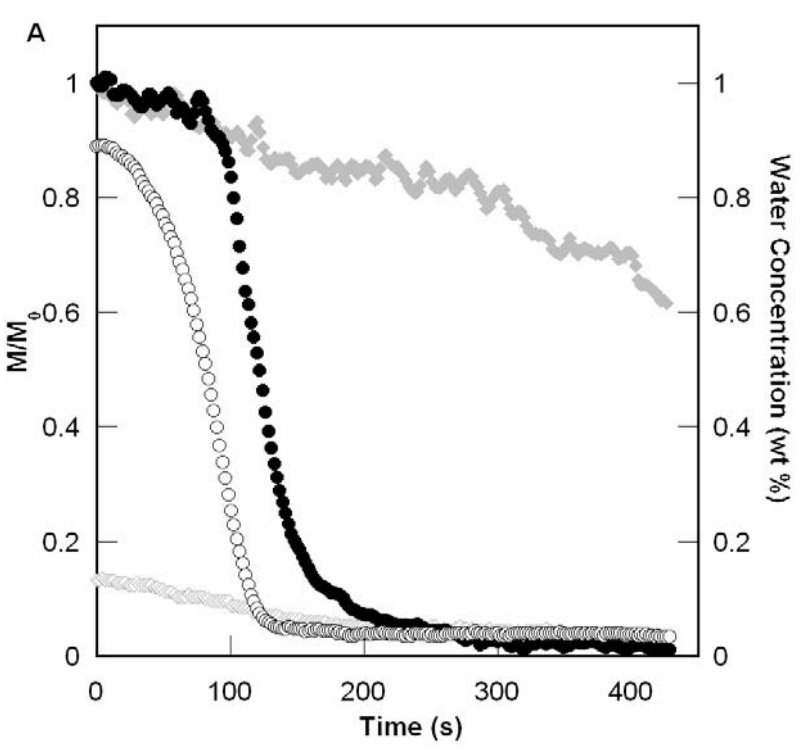
A
M/M∞
Water Concentration (wt %)
Time (s)
0
0.2
0.4
0.6
0.8
1
0
100
200
300
400

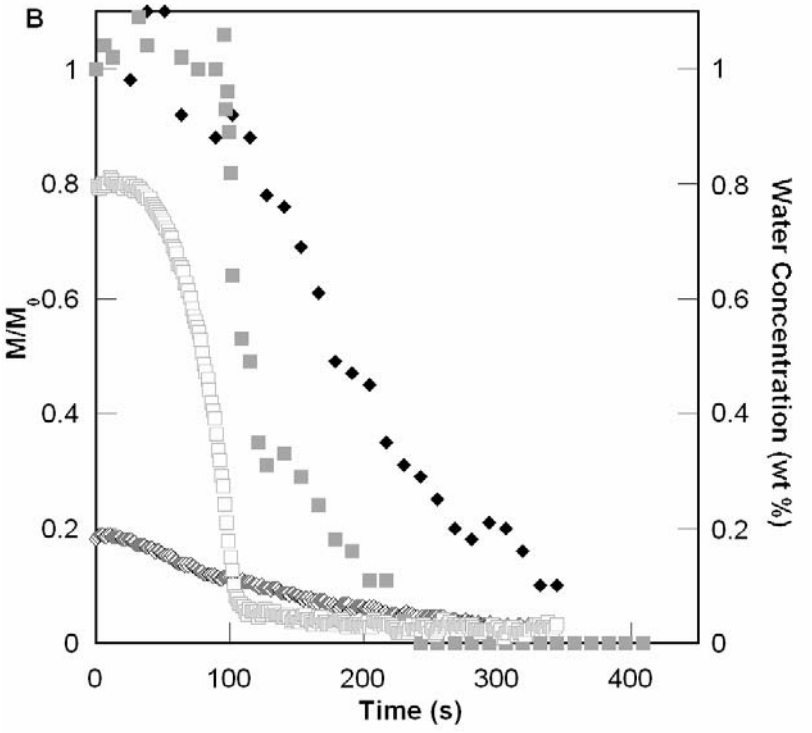
B
M/M∞
Water Concentration (wt %)
Time (s)
0
0.2
0.4
0.6
0.8
1
0
100
200
300
400

Figure 4.5. Temporal profiles for epoxy and water conversion for the limiting cases of water for UV (A) (epoxy conversion containing 0.13 wt% water ◆ and 0.89 wt% water ●; water conversion containing 0.13 wt% water ◇ and 0.89 wt% ○) and EB (B) (epoxy conversion containing 0.19 wt% water ■ and 0.78 wt% water ●; water conversion containing 0.19 wt% water □ and 0.78 wt% water ○) induced polymerization. The delay can be observed in the epoxy conversion while the water is being consumed in the reaction. When the water has been consumed, there is an acceleration of epoxy conversion.

One possible condensed set of reactions describing the initiation and propagation of epoxy polymerization using photo-initiators is given by Equation 4.3. Equation 4.4(a) describes the generation of the super acid, (b) is the reaction of the super acid with the monomer to form the activated monomer. Equation 4.3(c) represents the activated monomer-to-monomer reaction, where the AM reaction is given by Equation 4.3(b) and Figure 4.6. With the assumptions that (i) termination does not occur, (ii) diffusion limitations are not important, (iii) that there is a negligible concentration of hydroxyl groups present either initially or as the photo-initiator is consumed, and (iv) reactivity is independent of size of the polymer chain, this set of equations has been used successfully to describe the reaction of "dry" mono-functional glycidyl ethers such as PGE under continuous EB and UV irradiation [12, 27-28].

$$
\begin{aligned}
&C \xrightarrow{k_i} H^+X^- && \text{(a)} \\
&H^+ + M \xrightarrow{k_a} MH^+ && \text{(b)} \\
&MH^+ + M \xrightarrow{k_1} HOMM^+ && \text{(c)}
\end{aligned}
\qquad (4.3)
$$

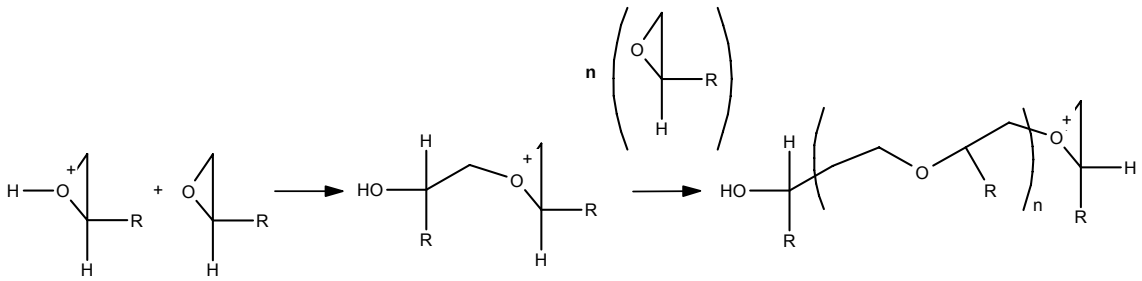

Figure 4.6. Schematic of the activated monomer-monomer reaction.

However, the results given in Figure 4.7 show that epoxy reaction changes dramatically with the addition of water. The qualitative influence of water can be understood by the set of reactions given in Equation 4.4 based on the explicit chemical expressions given by equation 4.4(b) and 4.4(c) using the shorthand notation. These represent the reaction of water with the initial activated monomer species (4.4(a)) and the formation of a new alcohol moiety with the regeneration of an activated monomer (4.4(b)) followed by the reaction of active species with such alcohols (4.4(c) and 4.4(d)). In writing these reactions it is assumed that the concentration of hydroxyl groups formed from photo-initiation is negligible. This is a valid simplification in that the concentration of hydroxyl groups formed from the water reaction is much greater than that obtained by possible initiation via direct reduction of the onium photo-initiator since the molar concentration of photo-initiator is much lower than the molar concentration of water investigated in this study. The ROH represents alcohol formed from the water reactions.

$$
\begin{aligned}
&MH^+ + HOH \xrightarrow{k_2} HOMOH^+ && (a)\\
&HOMOH^+ + M \xrightarrow{k_3} HOMOH + MH^+ && (b)\\
&MH^+ + ROH \xrightarrow{k_4} HOMOR^+ && (c)\\
&HOMOR^+ + M \xrightarrow{k_5} HOMOR + MH^+ && (d)
\end{aligned}
\qquad (4.4)
$$

ROH represents the hydroxyl groups formed for the water reaction (MHOH) and other hydroxyl containing polymers. The explicit chemical reactions summarized by Equation 4.4 are given Figure 4.7.

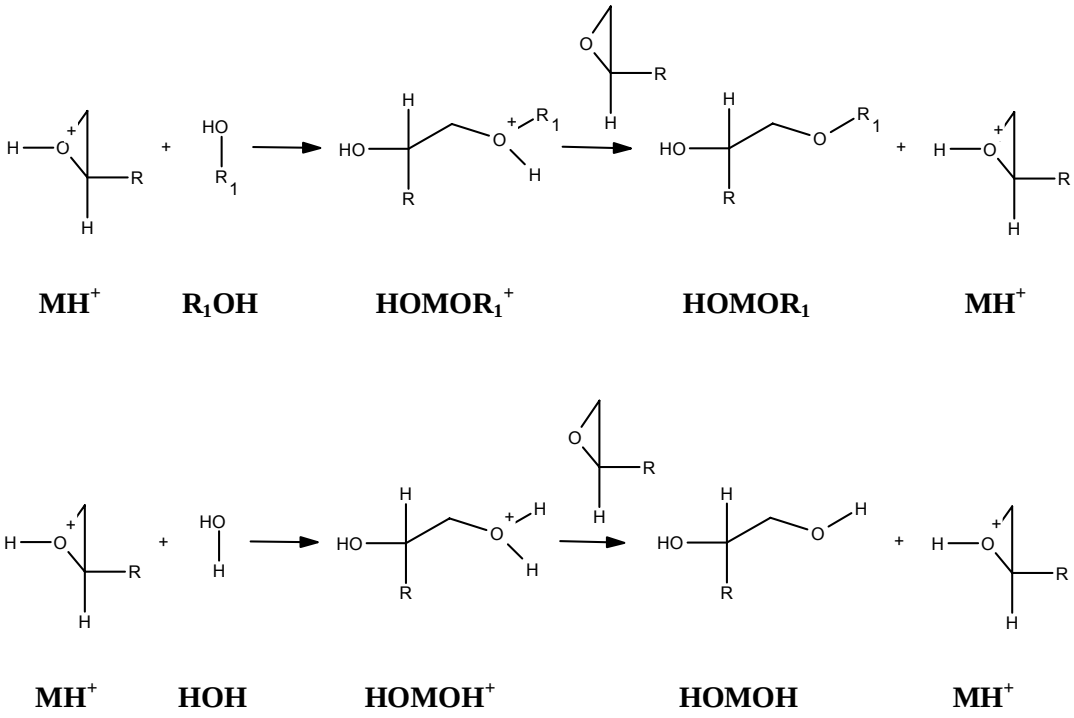

Figure 4.7. Cationic epoxy and water chemical reactions summarized by Equation 4.4.

The experimental results show that the initial reaction of water is fast and appears to retard the reaction of epoxy. This would be possible if the reaction 4.4(a) proceeded much more rapidly than 4.4(b). However, this by itself would not explain the eventual acceleration of the epoxy reaction. Hartwig et al. have attributed the slower initial conversion of the epoxy to the formation of a stable resonance structure. It was argued that the subsequent release of the proton to initiate the next chain (4.4(b)) is hindered by a stable five-member ring system [28-29]. Equation 4.5 shows the reaction of an activated PGE molecule with water to form this stable five member ring that could cause retardation by potentially "sequestering" propagating active centers.

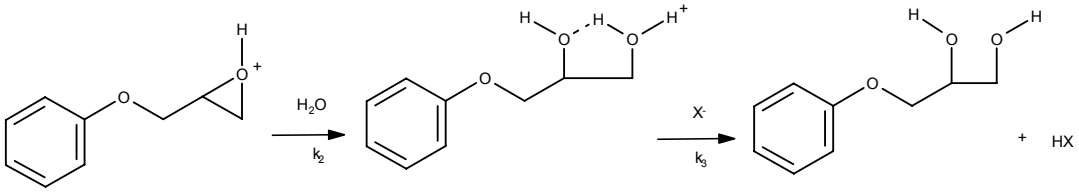

(4.5)

Although reaction 4.4(b) may be slow compared to 4.4(a), once the water is consumed not only will reaction 4.4(b) become important, but also reactions 4.4(c) and 4.4(d) of the alcohols generated from 4.4(b) with activated monomers. It is known that the reaction of such alcohols with active centers is faster than the reaction of epoxies with the active center [11, 36]. Hence, the continued generation of active centers through photo-initiation and the release of "sequestered" active centers with the concomitant formation of alcohols would result in an accelerated rate of epoxy conversion. Differential balance equations from the equations 4.3 (a-c) and 4.4 (a-d) to describe the kinetics of the process were derived and are given in Figure 4.8.

$$C(t) = C_0 \cdot \exp[-k_i \cdot t]$$

$$\frac{d[H^+]}{dt} = -k_a \cdot [M] \cdot [H^+] + k_i \cdot [C]$$

$$\frac{d[MH^+]}{dt} = k_a \cdot [M] \cdot [H^+] - k_2 \cdot [HOH] \cdot [MH^+] + k_3 \cdot [M] \cdot [HOMOH^+] - k_4 \cdot [ROH] \cdot [MH^+] + k_5 \cdot [M] \cdot [HOMOR^+]$$

$$\frac{d[M]}{dt} = -k_a \cdot [M] \cdot [H^+] - k_1 \cdot [M] \cdot [MH^+] - k_3 \cdot [M] \cdot [HOMOH^+] - k_5 \cdot [M] \cdot [HOMOR^+]$$

$$\frac{d[HOH]}{dt} = -k_2 \cdot [HOH] \cdot [MH^+]$$

$$\frac{d[ROH]}{dt} = k_3 \cdot [M] \cdot [HOMOH^+] - k_4 \cdot [ROH] \cdot [MH^+] + k_5 \cdot [HOMOR^+] \cdot [M]$$

$$\frac{d[HOMOH^+]}{dt} = k_2 \cdot [HOH] \cdot [MH^+] - k_3 \cdot [M] \cdot [HOMOH^+]$$

$$\frac{d[HOMOR^+]}{dt} = k_4 \cdot [ROH] \cdot [MH^+] - k_5 \cdot [M] \cdot [HOMOR^+]$$

Figure 4.8. Differential balance equations to describe the kinetics given in previous equations.

From these differential equations, the rate of reaction of epoxy, hydroxyl moiety, and water can be determined provided knowledge of the rate constants. To test the reasoning presented in the preceding paragraph the differential equations resulting from Equations 4.3 and 4.4 were solved numerically and a parametric study was conducted to evaluate the importance of the relative values of the reaction rate constants. Previously obtained values of k_1 and k_a were used (note that $k_i > k_a$) [31-32]. The water reaction data at short times was used to determine that k_2 is eight times greater than k_1 [33]. The rate of reaction of the activated monomer with an aliphatic alcohol has been found to be much greater than that with another monomer so that $k_4 > k_1$. Moreover it was assume $k_5 >> k_4$ making the k_4 the rate limiting step in the set of equations 4.4(c) and 4.4(d) [11, 14-16, 36]. Thus the following was assumed that $k_5 >> k_2 \geq k_4 > k_1$. However the relative rate of reaction of 4.4(b) to 4.4 (a) (k_3 to k_2) is unknown. First it was assumed analogously that in the alcohol reactions 4.4(c) and 4.4(d) $k_3 >> k_2$. Values of the rate constants were selected to satisfy these observations and were used as a basis of a parametric analysis designed to probe the qualitative behavior of the set of equations given above. In particular the influence of the value of k_3 on the conversion of epoxy for varied water concentration was examined. The following values of reaction rate constants were fixed in the calculations: $k_i = 0.001\ s^{-1}$, $k_a = 200\ L\ mol^{-1}s^{-1}$, $k_1 = 2.5\ s^{-1}$, $k_2 = 20.4\ L\ mol^{-1}s^{-1}$, $k_4 = 20.4\ L\ mol^{-1}s^{-1}$, $k_5 = 200\ s^{-1}$. Additionally, The initial concentration (t = 0 s) were: [M] = 7.31 mol/L, [ROH] = 0, $[C]_0 = 0.0145$ mol/L, and the concentration of all other species was set to 0.

Plots of epoxy concentration as a function of time are given in Figure 4.9 for a number of initial water concentrations ranging from 0 to 1 wt% using $k_3 = 200\ s^{-1}$. This

value was chosen based on the assumption that the regeneration step (4.4(b)) would behave similarly to the regeneration step 4.4(d) for the alcohol reaction. The plots show a clear increase in the overall rate of epoxy conversion as initial water concentration is increased. However the model fails to show the initial retardation observed in experimental data with the chosen rates of reaction.

Reanalyzing the model with Hartwig's suggestion that a stable ring structure may be formed is shown in Equation 4.5, a slower rate of reaction of k_3 were modeled. The retardation period was more apparent as k_3 decreased as shown in Figure 4.10.

Lastly, implementing the rates of reaction such that $k_5 >> k_2 \geq k_4 > k_1 > k_3$ into the equations given above, various water concentration were modeled. The increase of water concentration resulted in a longer retardation period followed by acceleration where epoxy conversion is reached at a shorter time as shown in Figure 4.11.

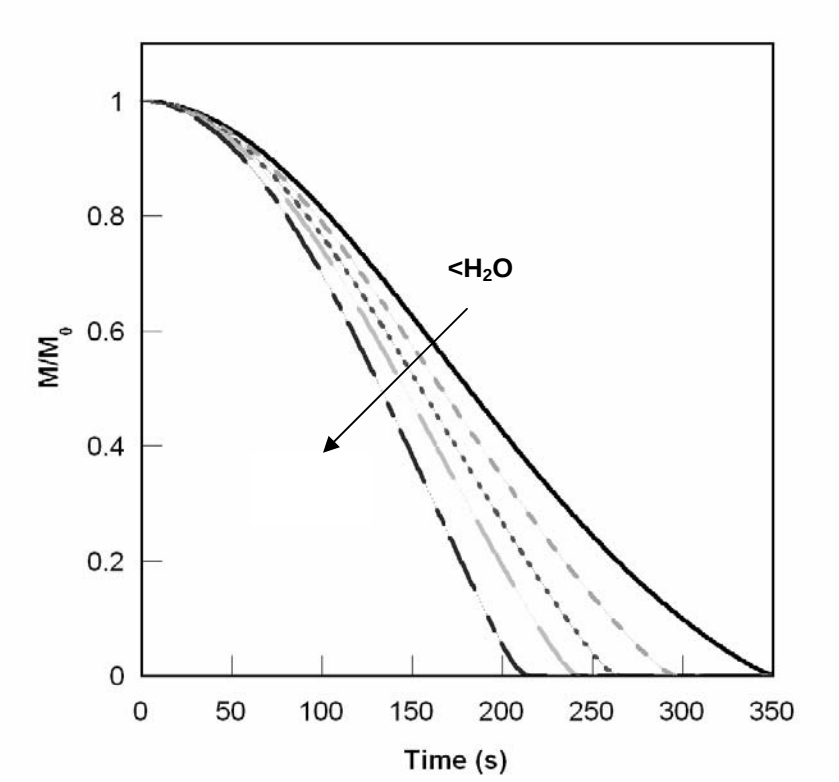

Figure 4.9. Model of epoxy conversion over time where k_i = 0.001 s^{-1},k_a = 200 L $mol^{-1}s^{-1}$, k_1 = 2.5 s^{-1}, k_2 = 20.4 L $mol^{-1}s^{-1}$, k_4 = 20.4 L $mol^{-1}s^{-1}$, k_5 = 200 s^{-1} and k_3 is assumed to be fast (k_3 = 200 s^{-1}). No delays were observed with increase of water (— 0.25 wt% water, – – 0.5 wt% water, - - 0.75 wt% water, — 1 wt% water, and - – 1.5 wt% water).

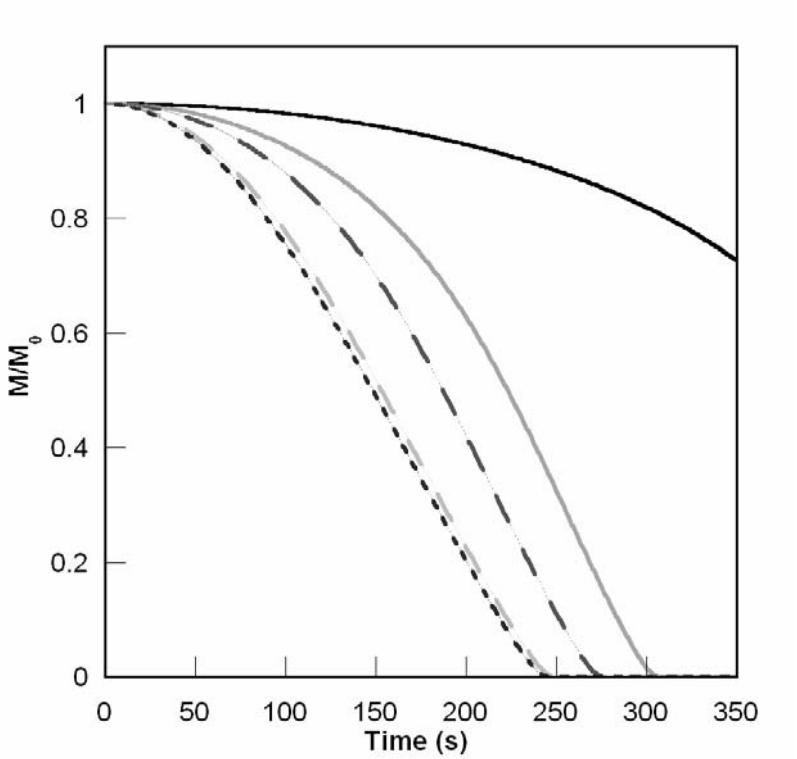

Figure 4.10. Model of epoxy conversion over time where $k_i = 0.001\ s^{-1}$, $k_a = 200\ L\ mol^{-1}\ s^{-1}$, $k_1 = 2.5\ s^{-1}$, $k_2 = 20.4\ L\ mol^{-1}s^{-1}$, $k_4 = 20.4\ L\ mol^{-1}s^{-1}$, $k_5 = 200\ s^{-1}$ and rate of reaction of k_3 is varied to observe the delays in initial epoxy conversion. Slower the rate of reaction k_3 the more pronounced the delay where water concentration was held constant 1wt% where — $k_3 = 0.1\ s^{-1}$, — $k_3 = 0.5\ s^{-1}$, – – $k_3 = 1\ s^{-1}$, – – $k_3 = 5\ s^{-1}$, - - $k_3 = 10\ s^{-1}$. Note that when $k_3 \geq 10\ s^{-1}$ the epoxy conversion does not increase over time.

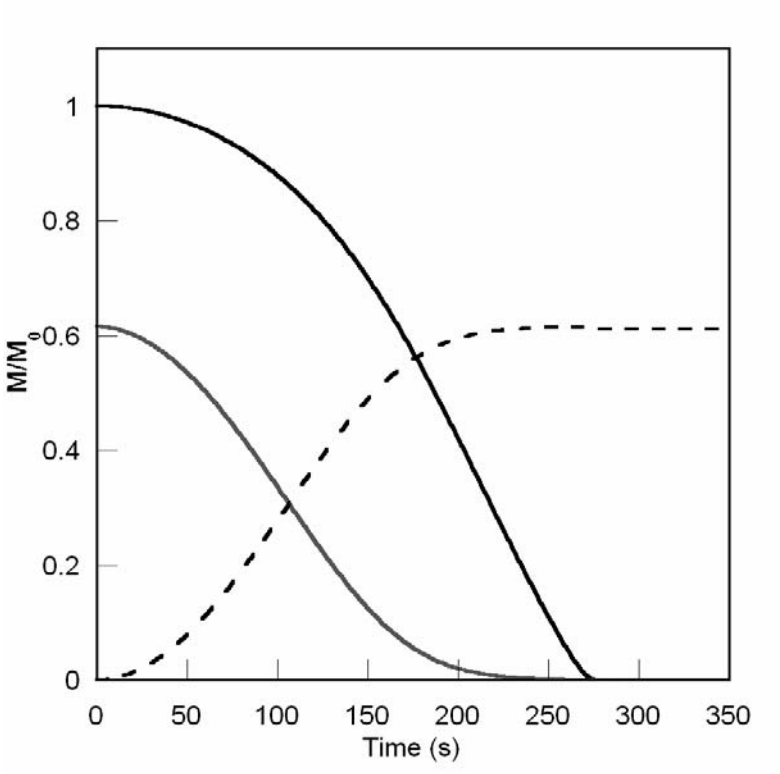

Figure 4.11. Implementing the rates of reaction into the model to show the epoxy and water conversion and the formation of hydroxyls, which correspond with the experimental data.

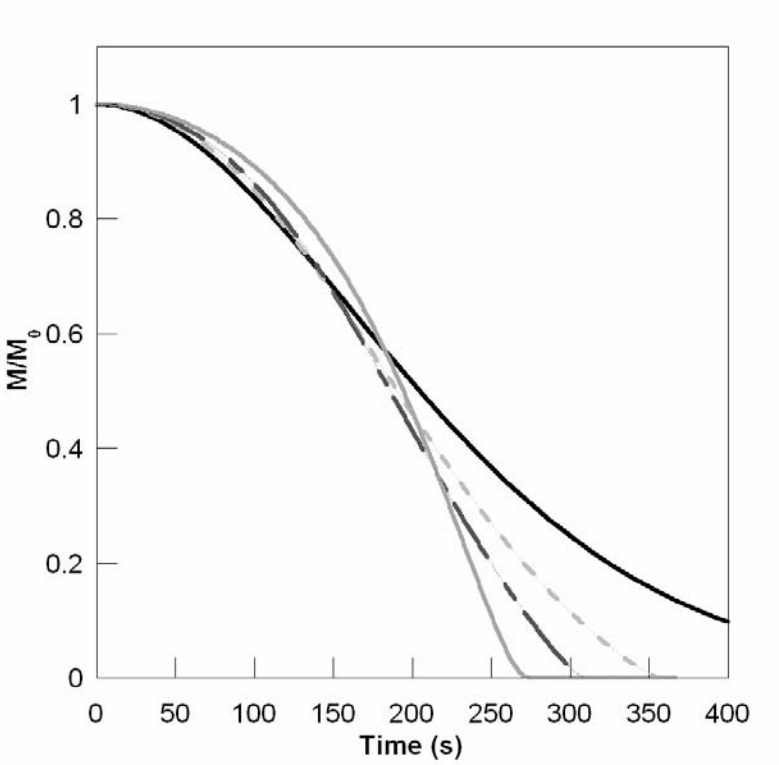

Figure 4.12. The model shows the delay of epoxy conversion with increase of water where $k_i = 0.001\ s^{-1}$, $k_a = 200\ L\ mol^{-1}s^{-1}$, $k_1 = 2.5\ s^{-1}$, $k_2 = 20.4\ L\ mol^{-1}s^{-1}$, $k_4 = 20.4\ L\ mol^{-1}s^{-1}$, $k_5 = 200\ s^{-1}$ and $k_3 = 1\ s^{-1}$, where the conversion is reached at shorter times (— 0 wt% water, - - 0.25 wt% water, - – 0.5 wt% water, — 1.5 wt% water.

The epoxy conversion can be modeled by implementing the rates of reactions given above, which captures the retardation and acceleration observed in the experimental data shown in Figure 4.12.

4.3.3. Influence of water on DGEBA cationic polymerization via UV and EB radiation

Investigations were also conducted on the influence of water on the polymerization of the di-functional epoxy, DGEBA, as described in the experimental section. Water concentrations for UV experiments ranged from 0.014 wt% to 0.994 wt% and from 0.13 wt % to 0.86 wt % for EB trials.

DGEBA experiments similarly to the PGE results, a 90-100 second retardation period is observed before significant reaction occurs for the "wet" system, while the nearly dry material exhibits significantly greater reaction rates from the start. While the initial reaction of DGEBA parallels results for PGE, DGEBA never reaches complete conversion at the isothermal cure temperature due to vitrification. However, with increasing initial water concentration, higher degrees of epoxy conversion were observed. Figure 4.13 shows the results for water concentrations of 0.014 wt% to 0.994 wt% water for UV experiments 0.13 wt % to 0.86 wt % for EB experiments. In all cases, the concentration of water upon completion of the reaction is close to 0 (0.03 wt% or less). EB-irradiation experiments of DGEBA showed the same results as the UV cured systems.

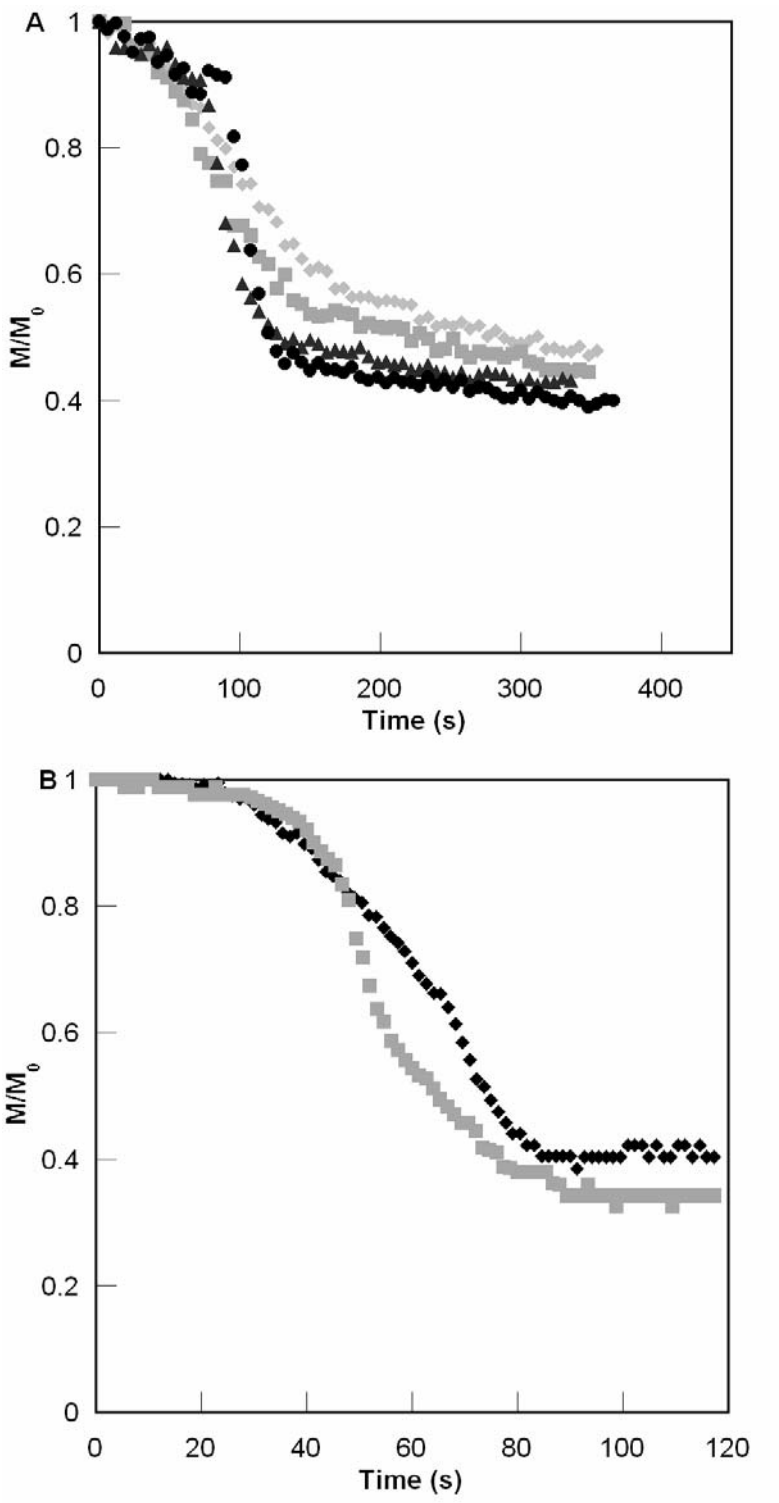
A
B
M/M0
Time (s)
0
0.2
0.4
0.6
0.8
1
0
100
200
300
400
20
40
60
80
120

Figure 4.13. Comparison of DGEBA cure kinetics with various water concentration (UV (A) at 0.67pph initiator at 60°C-0.014 wt% water ◆, 0.265 wt% water ■, 0.701 wt% water ▲, and 0.947 wt% water; ●and EB (B) at 1pph initiator at 60°C-0.12 wt% water ◆ and 0.86 wt% water ■).

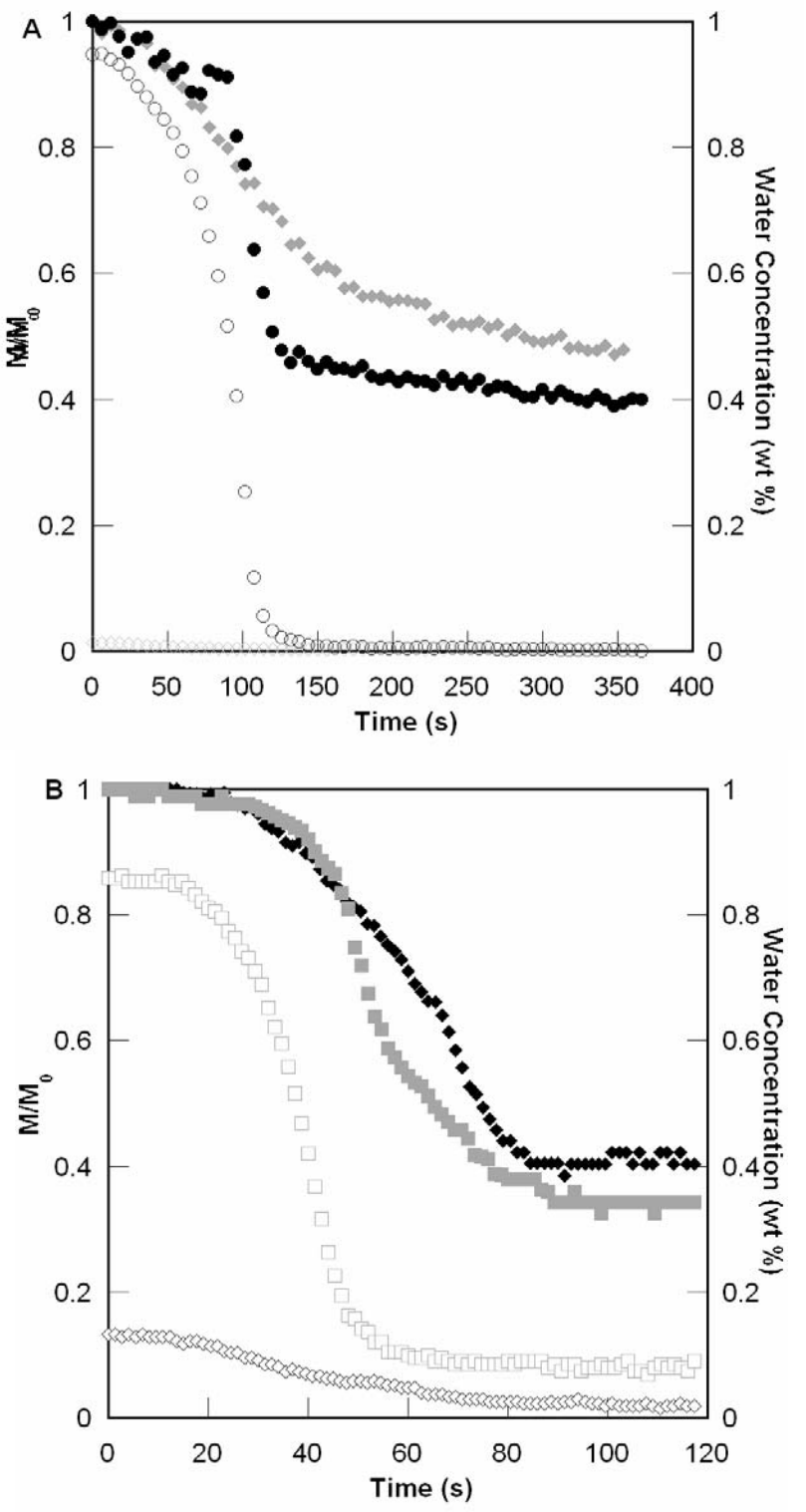
A
B
M/M0
Water Concentration (wt %)
Time (s)
0
0.2
0.4
0.6
0.8
1
0
50
100
150
200
250
300
350
400
0
20
40
60
80
100
120

Figure 4.14. Temporal profiles for epoxy (closed symbols) and water (open symbols) conversion for high and low initial water concentration for UV (A) where epoxy conversion 0.014 wt% water ◆ and 0.947 wt% water ●; water conversion 0.014 wt% water ◇ and 0.947 wt% water ○ and EB (B) -induced polymerization where epoxy conversion 0.12 wt% water ◆ and 0.86 wt% water ■ and 0.12 wt% water ◇ 0.86 wt% water □. Similar delays can be observed in the DGEBA data as seen in PGE as the epoxy is being consumed. The final conversion is greater with increase of water concentration.

Another point of discussion is the influence of water on the final conversion of epoxy for a given isothermal temperature of cure. Figure 4.14 shows the relationship between initial water content and final extent of epoxy conversion during isothermal cure at 60°C for our series of UV experiments. The final extent of reaction was significantly influenced by the presence of water. There is a general increase in final conversion as water content is increased with values ranging from 50 to 60% as initial water content approaches 1.0%. The reactions were allowed to proceed to cessation because the temperature was held constant. Thus the conversion values shown in Figure 4.15 represent extents of reaction at vitrification for isothermal cure. This means that the T_g of all these systems was 60°C yet their composition is very different. One possibility is that water in the system plasticizes the network so that molecular mobility is significantly enhanced allowing higher conversion for the given cure temperature. However, the experimental data shows that water is completely consumed prior to vitrification. Therefore this behavior is due to the water co-polymerizing into the network resulting in a less cross-linked system that requires greater DGEBA conversion to attain the same T_g. It is clear that not only does the presence of water alter processing behavior, but also the structure of the polymer being formed. It is likely also that this will significantly influence the behavioral characteristics of the polymer and its composites as discussed in the following sections.

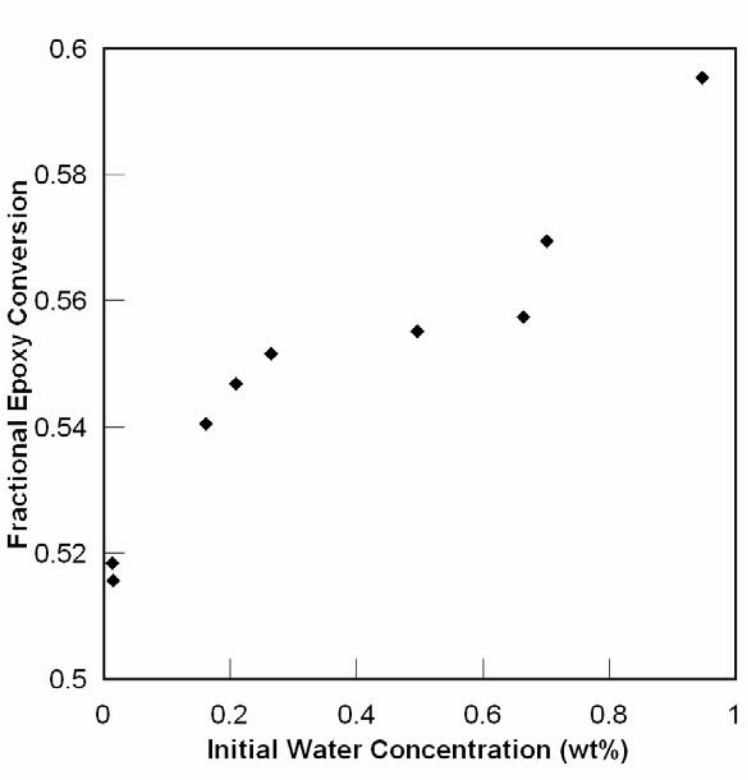

Figure 4.15. Influence of initial water concentration on the final epoxy conversion for isothermal UV cure at 60°C highlighting the significant effect of water on polymer structure formed.

Table 4.2. Mechanical and thermal properties of DGEBA composites curved via EB are obtained through DMA analysis and SENB fracture toughness measurements. G_{1C} values increase with the presence of water and peaks at 0.5 wt% water. T_gs decrease with increase of water concentration.

Water concentration	**G_{1C} (J/m^2)**	**Storage Modulus E' (GPa)**	**T_g (°C)**
0 wt%	56.0±7.0	2.35	188
0.25 wt%	120±34	2.00	181
0.5 wt%	140±35	2.23	174
0.75 wt%	120±7.0	2.49	170
1.0 wt%	113±35	2.20	168

4.4. Influence of water on cured DGEBA properties (T_g and fracture toughness)

The addition of a solvent can change the inherent matrix toughness and resulting microstructure. The resulting morphology influences the properties and performance of the cured resins. Table 4.2 summarizes the thermal and mechanical properties for the systems investigated in this work.

The water free DGEBA possess low fracture toughness (G_{1c}) of 57 J/m^2, high storage modulus of 2.3 GPa at 30°C, and a high T_g of 188°C. The addition of water has considerably increased the fracture toughness. The addition 1.0 wt% water increases the G_{1c} of DGEBA to 113 J/m^2. The results of the critical strain energy release rate measurements are given in Table 4.2. These results suggest that the decrease of cross-link density resulting from chain transfer reactions with water results in the increase of G_{1c} [37-38]. Although the water addition increases the fracture toughness, there is a decrease of T_g and storage modulus at 30°C. The T_g decreases from 188 °C to 167 °C and modulus decreases from 2.35 GPa to 2.20 GPa with the addition of water. These results combined with the kinetics indicate that the water is a factor that must be considered in the polymerization of epoxies.

Dynamic Mechanical Analysis (DMA) was used to obtain important information concerning the mechanical and thermal properties of these systems. DMA tests were conducted after the plaques were post-cured at 130°C. Figure 4.16 shows representative second run DMA traces for “dry” DGEBA and “wet” DGEBA containing 1.0 wt% water. However, a significant sharpening of the peak is observed that implies a more homogenous network is formed in the presence of water.

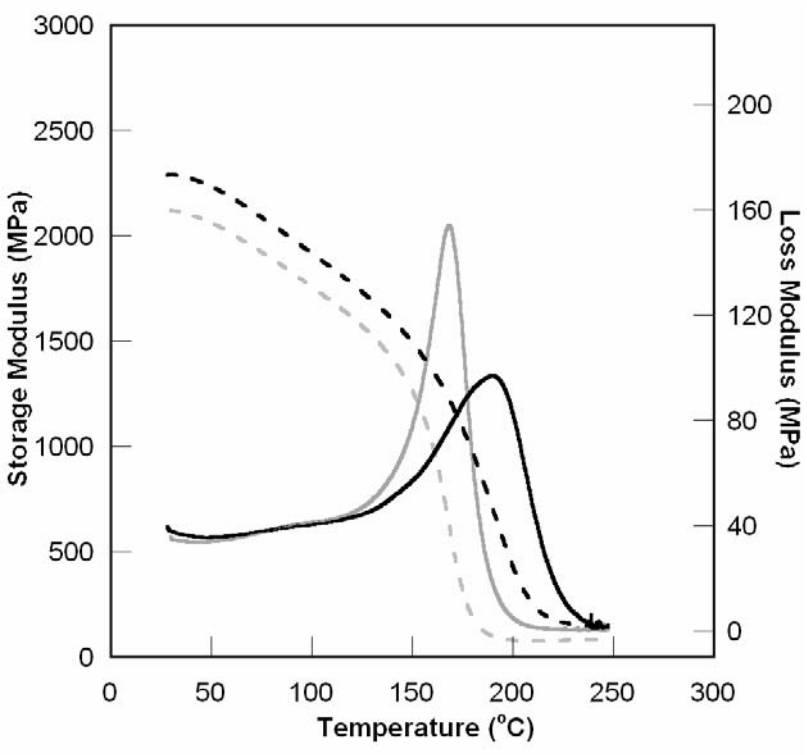

Figure 4.16. Second run DMA (ramped to 250°C twice) testing of EB cured DGEBA with and without water following post cure where - - storage modulus of 1.0 wt% water, - - storage modulus of DGEBA, — loss modulus 1.0 wt% water, — loss modulus of DGEBA.

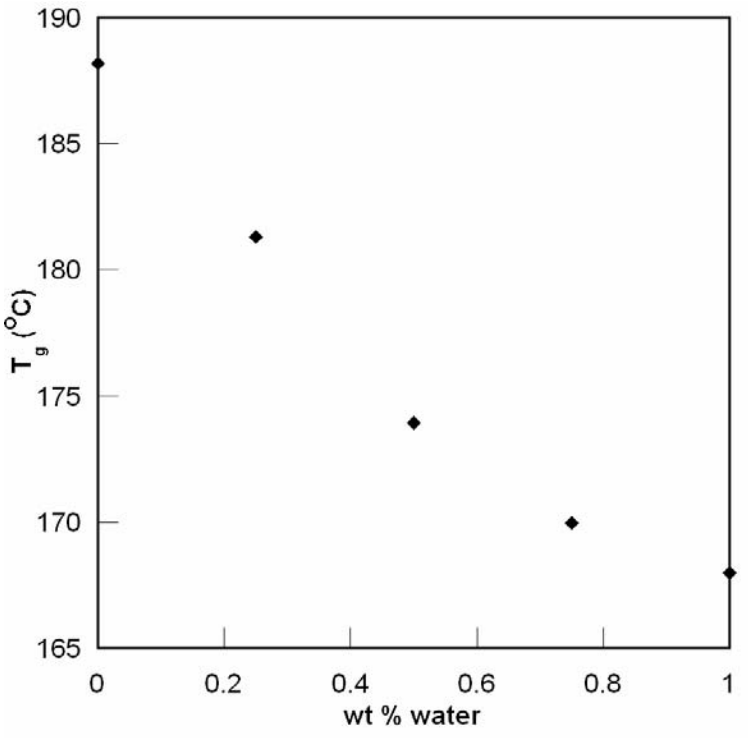

Figure 4.17. T_g of DGEBA at 1 pph photo-initiator with varying wt% of water in the system EB with a total dosage of 54 kGy. Increase of water concentration causes a decrease in the final T_g.

Thus the addition of water alters of the final polymer network structure and reduces T_g with increasing water concentration, where Figure 4.17 shows this behavior over a range of initial water concentration. In light of these results, it is clear that the presence of water alters not only the kinetic behavior as discussed earlier, but also behavioral characteristics of the epoxy materials.

4.5. Conclusion

An *in situ* fiber optic spectroscopic technique was used for quantifying water concentrations in epoxy samples, and data was presented concerning the influence of water on the UV- and EB-induced polymerization behavior of PGE and DGEBA. The presence of water in PGE and DGEBA was observed to significantly alter the cure behavior in important ways. There is a pronounced retardation period followed by an accelerated reaction regime relative to that observed for "dry" systems. A mechanism was proposed to explain this behavior. It is based on the relatively faster reaction of water with an activated monomer to form a relatively stable five member ring system compared to the reaction of epoxy with the activated monomer. The observed acceleration is thought to result from the slow regeneration of active centers and the generation of alcohol moieties from these ring structures as water reacts to completion. A kinetic model was used to test the proposed mechanism and the results were found to be in excellent qualitative agreement with the observed behavior. Because the water is consumed during the polymerization, it must alter the resulting network structure. Water was found to decrease the T_g of the epoxy network significantly and also to substantially increase its fracture toughness.

4.6. References

1. Decker C, Moussa K. J Polym Sci: Part A, 28, 3429 (1990).
2. Benziers D, Capdepuy B. SAMPE Int Symp, 35, 1220 (1990).
3. Saunders CB, Lopata VJ, Kremers W, McDougall TE, Tateishi M, Singh A. SAMPE Int Symp, 38, 1682 (1993).
4. Saunders CB, Lopata VJ, Kremers W, Chung M, Barnard JW. SAMPE Int Symp, 40, 112 (1995).
5. Janke CJ, Havens SJ, Dorsay GF, Lopata VJ. SAMPE Tech Conf, 41, 196 (1996).
6. Janke CJ, Havens SJ, Dorsay GF, Lopata VJ. SAMPE Tech Conf, 28, 901 (1996).
7. Janke CJ, Havens SJ, Lopata VJ, Chung M. SAMPE Tech Conf, 28, 901 (1996).
8. Goodman DL, Brix DL, Palmese GR, Chen A. SAMPE Tech Conf, 41, 207 (1996).
9. Janke CJ, Norris RE, Yarborough K, Havens SJ, Lopata VJ. SAMPE Intl Conf, 42, 477 (1997).
10. Dabestani R, Ivanov I. SAMPE Int Symp, 46, 2075 (2001).
11. Palmese GR, Ghosh NN, McKnight SH. SAMPE Int Symp, 45, 1874 (2000).
12. Palmese GR, Stein G. SAMPE Int Symp, 48 (2003).
13. Lee J, Palmese GR. SAMPE Int Symp, (2005).
14. Chabanne P, Tighzert L, Pascault J. J Appl Polym Sci, 53, 769 (1994).
15. Chabanne P, Tighzert L, Pascault J. J Appl Polym Sci, 53, 787 (1994).
16. Chabanne P, Tighzert L, Pascault J, Bonnetot B. J Appl Polym Sci, 53, 685 (1994).
17. Bouillon N, Pascault J, Tighzert L. Macromol Chem, 191, 1403 (1990).
18. Bouillon N, Pascault J, Tighzert L. Makromol Chem, 191, 1417 (1990).

19. Bouillon N, Pascault J, Tighzert L. Makromol Chem, 191, 1435 (1990).

20. Lunak S, Krejcar E. Die Angew Makol Chem, 10, 109 (1970).

21. Crivello JV, Liu S. J Polym Sci Part A: Poly Chem, 38, 389 (2000).

22. Crivello JV, Fan M, Bi D. J Polym Appl Sci, 44, 9 (1992).

23. Crivello JV, Mingxin F, Daoshen B. J Appl Polym Sci, 44, 9 (1992).

24. Crivello JV. Nucl Instr and Meth B, 151, 8 (1999).

25. Crivello JV. Macromol Symp, 183, 65 (2002).

26. Alessi S, Dispenza C, Spadaro G. Macromol. Symp, 247, v (2007).

27. Decker C, Nguyen T, Viet T, Decker D, Weber-Koehl E. Polymer, 42, 5531 (2001).

28. Hartwig A. Int J of Adhes Adhes, 22, 409 (2002).

29. Hartiwg A, Schneider B, Lühring A. Polymer, 43, 4243 (2002).

30. Riberio R, Morgan RJ, Bonnaud L, Lu J, Sue HJ, Choi J, Lopata V. J Comp Mat, 39, 1433 (2005).

31. Mascioni M, Sands JM, Palmese GR. SAMPE Int Symp, 47, 93 (2002).

32. Mascioni M, Sands JM, Palmese GR. Nucl Instr and Meth B, 208, 353 (2003).

33. Lee J, Johnston A, Palmese GR. SAMPE Int Symp, (2004).

34. Klosterman DA. SAMPE Int Symp, 48, (2003).

35. Goodman DL, Palmese GR. Handbook of Poly Blends and Comp, 1, 459 (2002).

36. Ghosh NN, Palmese GR. Bulletin of Mat Sci, 6, 603 (2005).

37. Palmese GR, McCullough RL. J Appl Polym Sci, 46, 1863 (1992).

38. Lee J, Yee AF. Polymer, 41, 8375 (2000).

CHAPTER 5: DARK AND LIGHT RADIATION CURE KINETICS OF EPOXIES VIA UV AND EB

5.1. Introduction

The focus of this chapter is to understand how irradiation time influences UV and EB induced polymerization of glycidyl ethers. In Chapter 3, a fiber optic based spectroscopic method was described that allows for the determination of *in-situ* kinetics of UV and EB induced polymerization of glycidyl ethers. These investigations were based on monomer systems that were dried using molecular sieves because a major concern for cationic polymerization of glycidyl ethers is the chain transfer reactions that can occur with water as described in the previous chapter. The model presented by Mascioni et al. for the experiments summarized above was based on the assumption that once generated, there is no deactivation of active centers (i.e. they are effectively "immortal") shown in Equation 5.1 [3].

$$\frac{M}{M_o} = \exp\{-k_p \cdot C_o \cdot t + \frac{k_p}{k_i} \cdot C_o \cdot [1 - \exp(-k_i \cdot t)]\} \quad (5.1)$$

Literature supports this contention that the half-life of active centers are far greater than the total irradiation time so that for reactions where polymerization times are much less than deactivation half-lives the decrease in active center concentration can be ignored [4-5]. Thus this model predicts the rate at which cationic polymerization of monofunctional epoxy systems cure under continuous EB irradiation.

The model was found to give very good predictions of cure rates during continuous exposure of epoxy resins to both UV and EB irradiation. However, in practice, EB processing is often not conducted in a continuous fashion, but rather during

a set of irradiation steps separated by variable lengths of irradiation-free periods. Experiments performed by Johnston et al., in which reaction rates during interrupted EB irradiation were measured using calorimetry, it was determined that while the model predicted well many features of the irradiation process, significant unexplainable discrepancies were also apparent [6]. In particular, while the overall trend of cure rate versus dose and temperature (experiments were not isothermal) were well-predicted by the model, unpredicted drops in cure rate were observed immediately after each dose of EB irradiation.

Other EB curing experiments also showed that interrupted irradiation altered the structure of the polymer being formed, as evidenced by the mechanical response of cured polymer specimens. Two samples were cured at a rate of 3.6 kGy/pass for a total dosage of 54 kGy. One sample was cured in a continuous manner. The second sample was cured in a step-wise fashion (radiation on and radiation free periods). Dynamic mechanical testing was performed on both samples and the presence of two T_gs is observed for step-wise irradiation as shown in Figure 5.1. It should be noted that this is not always the case that such distinct peaks are observed.

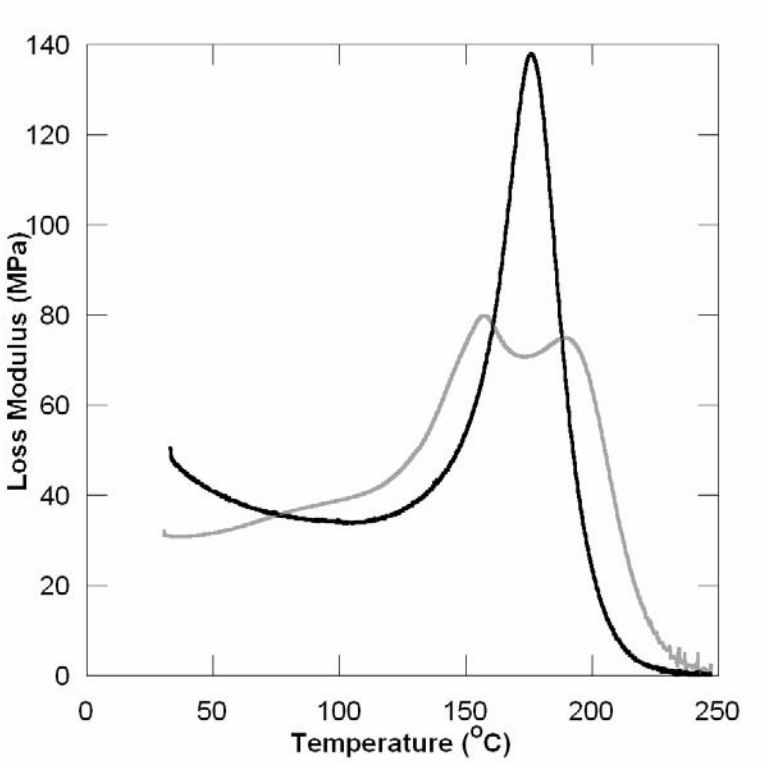

Figure 5.1. DMA of DGEBA depicting the influence of step irradiation on material behavior, where the single peak line (—) represents continuous irradiation and the double peak line (—) represents discontinuous irradiation.

The continuously irradiated sample showed a "typical" result obtained for such curing, showing a single loss modulus peak with T_g of 180°C. The step-irradiation sample resulted in a double peak with T_gs of 160°C and 190°C, which indicates the possible formation of two different network structures and a phase separation of the resin during the cure process. Since pre-preg composites would in practice typically is cured in a step-wise fashion, the formation of several network structures is of concern. In this study we investigate dark reactions (i.e. post-irradiation) using the developed NIR fiber optic technique to evaluate the kinetics of active center deactivation and potential impacts that this might have on typical cure processing of composite materials.

5.2. Experimental

5.2.1. Materials

Two different epoxy resins, Miller-Stephenson Epon-825 and Aldrich Chemical Company phenyl glycidyl ether (PGE) epoxy resin, were cured using Applied Poleramic Inc. CD1012 (diphenyl iodonium hexafluoroantimonate) photo-initiator in this investigation. The chemical structures of these compounds are shown in Table 5.1. Epon-825 is diglycidyl ether of bisphenol A (DGEBA) resin with an average molecular weight of 354 g/mol. PGE is the mono-functional analog of DGEBA with a molecular weight of 150 g/mol. Reactants were dried using 4Å molecular sieves (Aldrich Chemical Company, Inc) to make "dry" epoxy. The sieves were dried at 120°C for 12 hours prior to use. Such drying limits water concentration to below 0.1% in the reactants where previous communications found water to alter cure behavior of epoxies [4, 10]. The ratio of CD1012 photo-initiator to epoxy resin considered is 1 parts per hundred (1pph).

Table 5.1. Materials used in the experimental work.

Material	Chemical Structure
Phenyl glycidyl ether (PGE) from Aldrich Chemical Company, Inc. USA	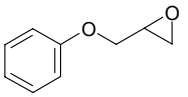
Diglycidyl ether of bisphenol A (DGEBA). EPON 825 from Miller-Stephenson (n=0.0228)	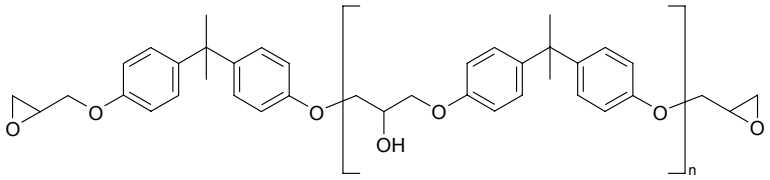
Diphenyl iodonium hexafluoroantimonate CD1012	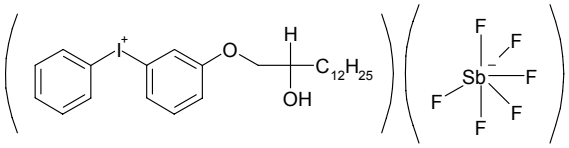

5.2.2. Fiber Optic Near IR Spectroscopy

The spectral analysis performed in this work was based on a near infrared spectroscopy technique described in Chapter 3. Samples were placed in sealed glass tubes (1.6 mm ID, and 3.0 mm OD) to prevent water absorption from the environment prior to and during cure [4]. The advantage of this design is that measurements of radiation-induced cure could be performed without exposing the spectrometer to harsh radiation environments.

5.2.3. Calorimetry

Epoxy cure rate data during irradiation was also collected using an *in-situ* calorimetry-based technique [11, 12]. In the standard design (shown in Figure 5.3), up to eight removable cylindrical blocks of low-density (64 kg/m3) insulating foam (OD = 80 mm) are mounted on a wooden base via small dowels. Within each of the blocks is inserted a 1 mL polypropylene syringe (OD = 6.64 mm, ID = 4.64 mm), filled with either pre-cured or uncured resin. The uncured specimens are used to determine cure rate, while the pre-cured specimens are used as "references" and their temperature rise during irradiation is used to calculate dose rate. Each syringe has embedded in it a 30 gauge K-type thermocouple placed as close as possible to the geometric center of the syringe.

For cure trials, the calorimeter is either passed back-and-forth in front of an accelerator electron beam, or held steady in front of the beam for the entire radiation process (which was done in the experiments described here). Using the back-and-forth process, up to 4 specimens can be tested at once, which allows 4 reference specimens to be used to calculate dose rate with time. For this work, only a single reference specimen and a single curing specimen were tested during each experiment.

Temperatures measured during irradiation by the embedded thermocouples are acquired by a computer-based data acquisition system. A finite-difference based analytical model then uses this data to calculate the energy absorbed by the calorimeter from the impinging electrons and the exothermic energy generated by the reaction of the curing resin. These values are in turn used to determine the EB dose rate and the resin cure rate. Material parameters related to heat transfer were determined in experiments performed with preheated reference samples. These calorimetric experiments were performed by Andrew Johnston in parallel with NIR experiments.

5.2.4. Sample Preparation and Irradiation

The epoxy resin with 1pph CD1012 were mixed together and allowed to equilibrate at 50 °C for NIR experiments. After approximately 30 minutes, when the mixed samples appeared clear such that the initiator has dissolved, the mixture was taken out of the oven. The resin sample is housed in a sealed glass tube inserted into an aluminum block equipped with cartridge heaters for temperature control. These cure experiments were conducted at 50°C.

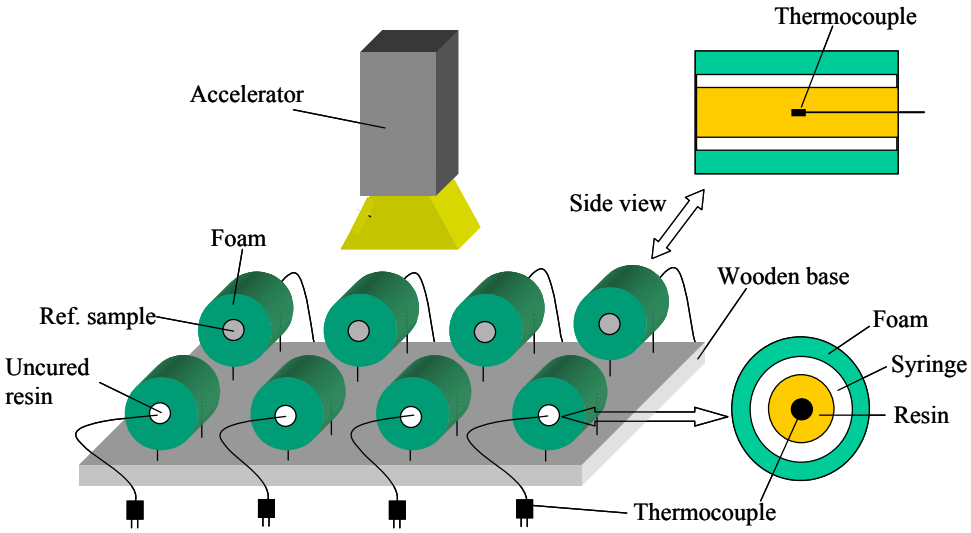

Figure 5.2. Schematic of the EB calorimeter (not to scale) [1].

Samples for calorimetry experiments were prepared in a similar fashion except that 3 pph CD1012 photoinitiator was used (with DGEBA in all cases described here). After mixing and heating, resin samples were drawn into the mentioned 1 mL syringes, which were then sealed, covered with aluminum foil to prevent UV irradiation, then placed into sealed plastic bags to prevent moisture absorption. Immediately prior to cure, the syringes were removed from the sealed bags, unwrapped, and placed into the calorimeter foam blocks. The foam block and specimens were then allowed to come to thermal equilibrium at the starting test temperature, which was measured to be near 20 °C for all tests described herein.

EB cure experiments were performed at the University of Dayton Research Institute Laboratory for Research on Electron Beam Curing of Composites. The EB machine is a 3 MeV EB accelerator specifically designed for irradiating samples in a controlled manner. For NIR experiments, irradiation settings were kept constant as follows: 25 pulses/second, 60% scan width, 150 mA/pulse, and 5.5 kGy/min and different samples were irradiated for 450, 250s, 200s, 150s, and 100s. For the calorimetry experiments, the number of pulses per second was adjusted to deliver irradiation at average dose rates of between 2.4 kGy/min and 24 kGy/min. During each test, radiation was delivered in a series of discrete doses of roughly 1.0 to 2.0 kGy, between which the beam was turned off for various periods of up to 300s. In all cases, temperatures from all embedded calorimeter thermocouples were acquired at intervals of 0.2 s and stored for later processing.

EB cure experiments were also conducted using DGEBA to make resin plaques for mechanical property testing. Dry DGEBA plaques containing 1 pph of photo-initiator were polymerized using either continuous or discontinuous irradiation. In both cases, a total of 54 kGy of irradiation was applied at a rate of 5.5 kGy/min, either in one continuous does or during 15 passes of 3.6 kGy/dose. To control the reaction exotherm, the 2 mm thick samples were placed on an aluminum plate and chilled by ice water keeping all experiments under 10°C. The resin plaques were then subjected to a 2-hour thermal post-cure at 130°C.

5.3. Results and discussion

There is a lack of understanding of the link between processing parameters and the resulting properties of the material formed during cure. Many processes requiring radiation cure of composites are conducted with stepped doses in which the part is subjected to a number of cycles comprised of “radiation on” and “radiation off” segments. This section of the chapter addresses the influence of dose rate, time, and the associated total dose on the cure kinetics and performance of epoxy systems. The first part of this work used the NIR technique to evaluate cure during and after irradiation. The second part of this work focuses on the kinetics after the radiation has been removed to understand the fate of active centers responsible for the polymerization. The third part of this work is to investigate the life time of active centers and the rate of deactivation. The final part of this work reevaluates past calorimetry data.

5.3.1. Interrupted EB Irradiation

A series of PGE samples were prepared using 1pph photo-initiator and placed into the capillary tube as described in the procedure section. Typically a hermetically sealed sample was placed in the sample holder and heated to 50°C. It was found that 2 minutes were sufficient to reach thermal equilibrium; thus samples were held for 2-5 minutes before the start of irradiation. During this time proper alignment of the sample was ensured by maximizing the peak height at 2209 nm corresponding to the oxirane ring. A series of experiments was conducted in which the dose rate was held constant but the time of irradiation was varied between 100 s and 500 s. The dose rate was 5.5 kGy/min and the total dosage thus varied from 9.2 kGy to 45.8 kGy. Spectra were collected every 0.134s for a period of 500s in each experiment thus capturing changes in composition before and after the EB was turned off. The results of these experiments are plotted in Figure 5.3. In these plots epoxy concentration data is plotted every ten seconds and the times when the EB radiation was turned off are noted. These data were obtained by measuring the peak height at 2209 nm for given time and normalizing it by the initial peak height before EB exposure. Previous work demonstrated that this ratio also represents M/M_0, where M is PGE concentration as function of time and M_0 is the initial PGE concentration [11, 12].

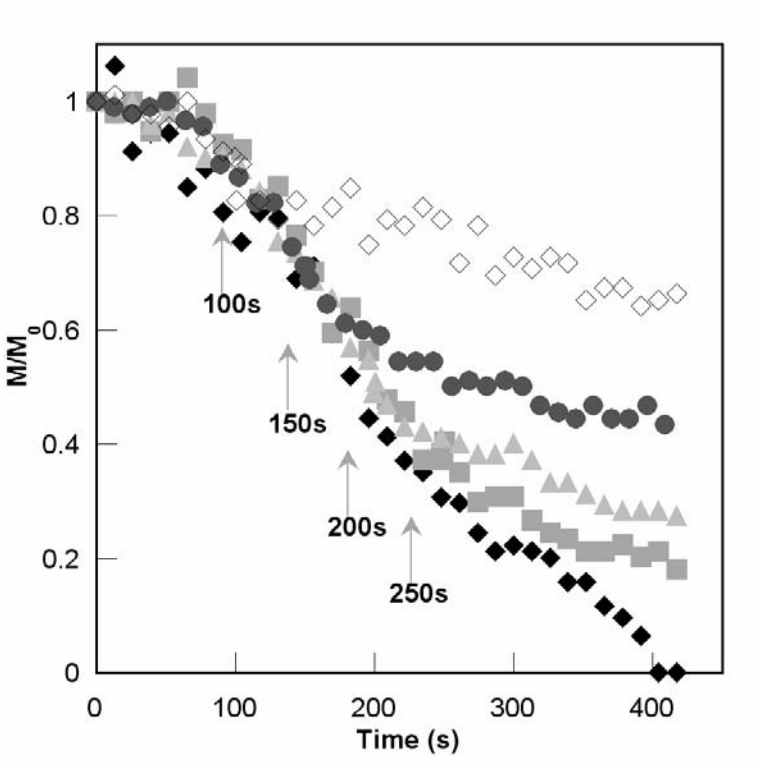

Figure 5.3. PGE with 1pph photo-initiator concentration at 50°C with varying EB exposure times: 500s EB exposure (◆), 250sEB exposure (■), 200s EB exposure (▲), 150s EB exposure (●), 100s exposure (◇).

The radiation exposure times used were 100 s, 150 s, 200 s, and 250 s and 500 s. The sample exposed for 500 s (◆) reached complete conversion. In all cases, the data collected for the other runs matches the 500 s run closely until the time that the EB was turned off. Upon the cessation of EB exposure the rate of change of epoxy concentration decreases significantly in all cases. A decrease in rate would be expected since additional active centers capable of promoting polymerization are no longer being generated. The data collected from the sample irradiated for 500 s reached complete cure and could be analyzed on the basis of the Mascioni Model developed for continuous irradiation. In this model the initiation reaction is assumed to be first order with respect to the concentration of photo-initiator. Since active centers are assumed not to deactivate, the active center concentration is given by Equation 5.2, where C_0 is the initial photo-initiator concentration and k_i is the initiation rate constant that was found to depend linearly on dose rate.

$$I = C_0 \cdot \left(1 - \exp^{-k_i t}\right) \qquad (5.2)$$

In this model the polymerization reaction was represented as a second order rate expression given by Equation 5.3 where M is the concentration of monomers, k_p is rate of polymerization.

$$\frac{dM}{dt} = -k_p \cdot M \cdot I \qquad (5.3)$$

Integration of Equation 5.4 yields the following expression relating dimensionless epoxy concentration to time.

$$\frac{M}{M_0} = \exp\left[-k_p \cdot C_0 \cdot t + \frac{k_p}{k_i} \cdot C_0 \cdot \left(1 - \exp^{-k_i \cdot t}\right)\right] \qquad (5.4)$$

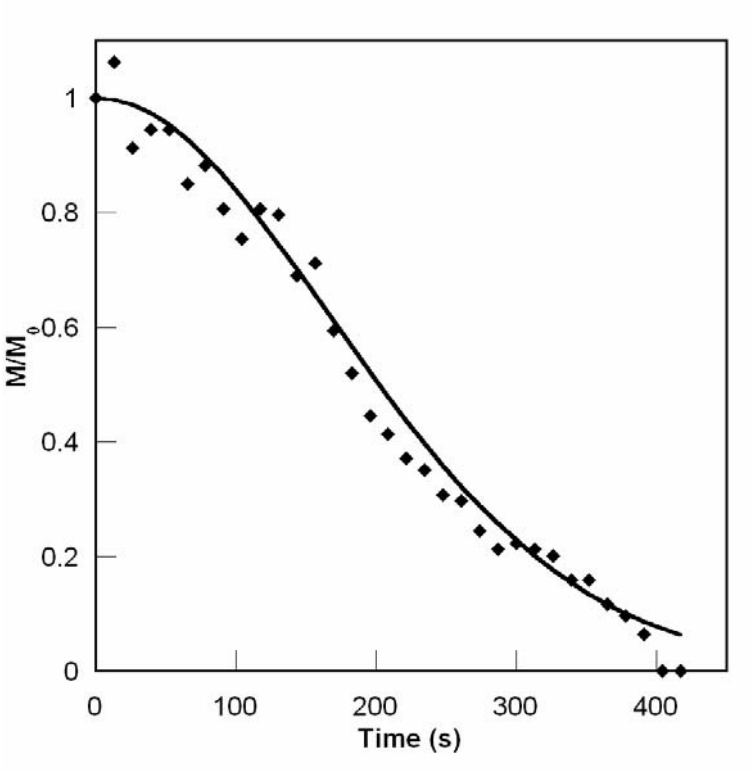

Figure 5.4. 500 s experimental data (◆) fitted to the Mascioni model (—) for fully cured continuous irradiated EB materials.

Fitting this equation to the 500 s data yields the following rate parameters: k_i=0.001s^{-1} and k_p=2.5 mol^{-1}s^{-1}, with a good fit as shown in Figure 5.4. These parameters are very close to the ones obtained by Mascioni et al. for similar polymerization conditions. Attempts were subsequently made to use the model of Mascioni et al. to fit the data from interrupted exposure experiments by removing initiation when irradiation is stopped. Representative results are given in Figure 5.6 for the case of 200 s exposure. In this figure the composition data is plotted with model results for continuous irradiation and the interrupted experiment using the equation given below to compute composition once the EB is switched off at time t_s .

$$\frac{M}{M_{ts}} = \exp\left[-k_p \cdot C_0 \cdot t \cdot \left(1 - \exp^{-k_i \cdot ts}\right)\right] \qquad (5.5)$$

The interrupted EB model results predict a decrease in reaction rate with time, not an immediate drop in reaction rate once the light has been turned off but a much gentler decrease than is actually observed. Clearly, the model is not able to replicate the behavior of interrupted exposure experiments. Specifically, a much sharper decrease in the rate of reaction is observed than can be predicted. More careful inspection of the experimental data shows that the rate of reaction decreases very rapidly as soon as the light is turned off – within a matter of a few seconds. The reaction rates were computed at a time immediately preceding (t-10 s) the interruption of EB exposure and compared with those obtained for a time immediately after exposure (t+10 s). In all but the 100 s exposure experiment a 60% decrease in the reaction rate was observed. The 100 s case showed an 80% decrease.

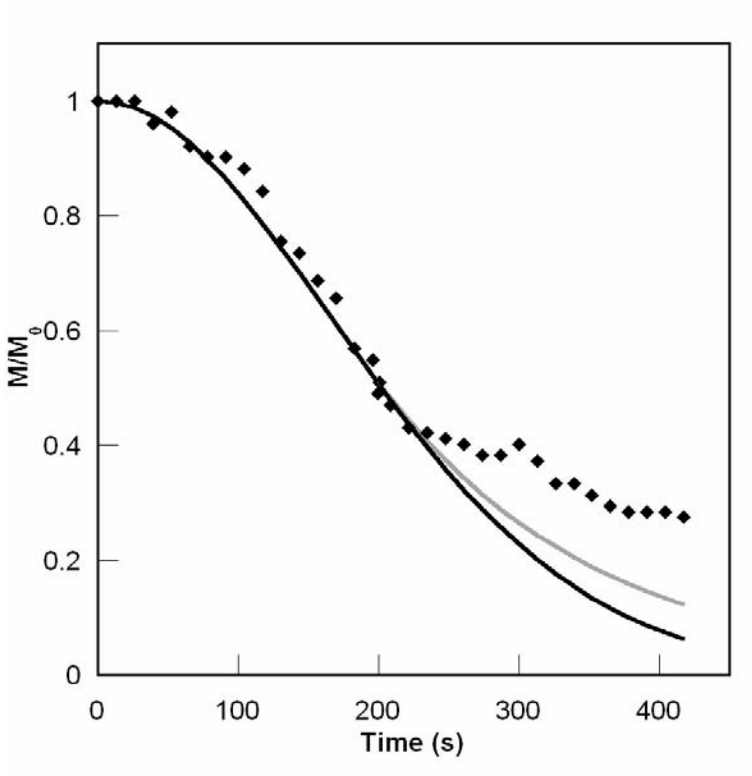

Figure 5.5. Deviation from theoretical model, for 200s EB exposure: data (◆), theoretical model (—) accounting for the EB exposure time, and Mascioni model (—) for continuous irradiation.

The most likely sources for the observed drop in reaction rate are either a sudden decrease in propagating center concentration or a rapid drop in temperature. The potential of temperature effect was examined first. Due to the exothermic nature of this polymerization significant exotherms can occur even with temperature control. This is the case particularly for high dose rates where a change in temperature of up to 10ºC has been observed. The reaction rate constant is strongly dependent on temperature. Using the parameters for k_p obtained by Mascioni et al. for the Arrhenius expression

$$k_p = k_{p0} \cdot \exp(-E/RT) \qquad (5.6)$$

where R is the ideal gas law constant, T is reaction absolute temperature, E is 70.152 kJ/mol, and k_{po} is $2.027 \cdot 10^{11}$ liter/(mol·s) a 60% decrease in k_p would require a decrease in temperature from 62 to 50ºC. It was found by testing the dynamic thermal behavior of the sample holder, however, that to change the temperature inside the capillary by 10ºC from 60 to 50ºC would require 48 s. This time scale is much greater than the time scale associated with the sudden decrease in reaction rate observed after stopping EB exposure. Thus it was concluded that the sharp decrease in reaction rate is not a result of a rapid change in temperature but rather a result of a sharp decrease in the concentration or reactivity of active centers. In the Mascioni model, it was assumed that there was no diffusion limitation for continuous irradiation, but how it effected discontinuous irradiation was unknown.

The experimental results also show that although there is a rapid decrease in the rate of reaction following EB, the rate of reaction does not become 0, rather, a steady decrease of epoxy concentration is observed. In fact all the samples evaluated showed full conversion of epoxy when tested at a later date. A hypothesis that would explain this

behavior is that there are two classes of active centers; one with a short lifetime that therefore exists primarily when the EB is on and another set that is long lived and allows for continued propagation once the EB is turned off. However, the hypothesis of having more than one active center is not supported by initiation studies. A second hypothesis is that unlike the assumptions made in developing the Mascioni model, the reactivity of the active center is dependent on growing polymer molecular weight. During irradiation active centers are being formed that have short attached polymers, with time the active polymer chain grows possibly forming a diffusion barrier around the active center. Hence older active centers would demonstrate lower reactivity by nature of this shielding effect. When the irradiation is interrupted all active centers age and the overall reactivity is reduced. However, from the experimental data, Equation 5.5 can be empirically modified to account for the sudden decrease in the rate of reaction. The slope of the epoxy conversion before and after the light has been turned off can be used to account for the decrease given in Equation 5.7.

$$D = \frac{\dfrac{M_{t3} - M_{t4}}{t_3 - t_4}}{\dfrac{M_{t1} - M_{t2}}{t_1 - t_2}} = \frac{m_{after}}{m_{before}} \qquad (5.7)$$

M_{t1} and M_{t2} is the M/M_0 during irradiation, and M_{t3} and M_{t4} is after the light has been turned off. Therefore the Equation 5.5 can be modified by this diffusion limitation D shown in Equation 5.8.

$$\frac{M}{M_{ts}} = \exp\left[-k_p \cdot C_0 \cdot t \cdot \left(1 - \exp^{-k_i \cdot ts \cdot D}\right)\right] \qquad (5.8)$$

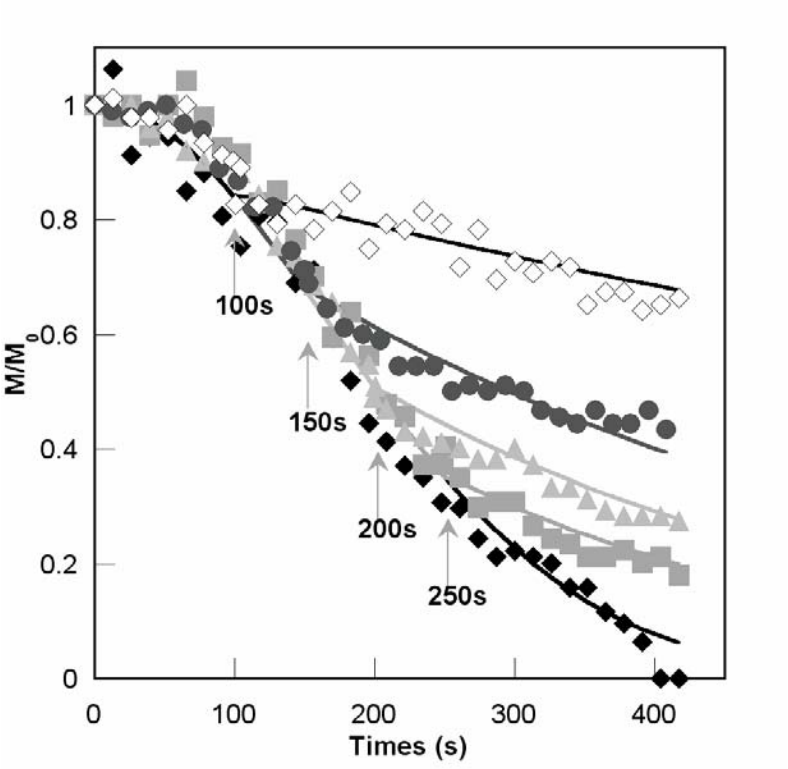

Figure 5.6. Model to fit experimental data using Equations 5.7 and 5.8: 100 s (◇),150 s (●), 200 s(▲), 250 s(■), and 500 s(◆) from top to bottom respectively.

D was calculated for the different irradiations times and the best-fit curves are shown in Figure 5.6 where *D* is 0.4 for the 250 s, 200 s, and 150 s exposure and 0.2 for the 100 s EB exposure. These results are consistent with the measured changes of reaction rate at the time the EB is shut off. Given the scatter in the NIR results the model appears to fit the data reasonably well. It should be possible to relate the parameter D to the change in overall reactivity.

5.4. Analysis of Dark Reactions

The long-term dark reaction data can be used to gain some insight into the deactivation behavior of the active centers. By analyzing dark reaction behavior in UV cured systems using similar photoinitiators, researchers have found the half-life of the active centers to be on the order of 40 minutes [5, 6].

We analyze our dark reaction data based on the assumption that active center concentration follows first order decay kinetics so that the concentration of active centers is given by Equation 5.9:

$$I = I_s \cdot \left(\exp^{-k_d \cdot t}\right) \qquad (5.9)$$

In this equation I_s is the concentration of active centers at time t_s, computed using Equation 5.9 and, k_d is the first order deactivation rate constant. The rate of propagation after t_s is therefore given by Equation 5.10.

$$\frac{dM}{dt} = R_p = -k_p \cdot M \cdot I_s \cdot \exp^{-k_d t} \qquad (5.10)$$

Rearranging Equation 5.10 and taking its logarithm yields Equation 5.11 which can be used to obtain k_d as represented by the slope of the equation.

$$\ln\left(\frac{R_p}{M}\right) = \ln k_p \cdot I_s - k_d \cdot t \qquad (5.11)$$

Equation 5.11 was used to analyze the dark reaction data given in Figure 5.6 with the exception of the 100 s data and the results are shown in Figure 5.7. The initial portion of these curves has a slight negative slope or a slope close to 0. The associated k_d values are reported in Table 5.2. The sharp increase in k_d as time increases is potentially a result of diffusional limitations and associated trapping of active centers. These data, however, show significant scatter suggesting that improvements in technique and additional experiments are needed in order to obtain reliable quantification of the deactivation rate constant. Nevertheless the results corroborate the contention that reactive sites exist having long half-lives.

In addition to the abovementioned experiments a secondary assessment of the deactivation rate constant for long-lived reactive centers was undertaken. Dried PGE was fully cured by UV using 3 pph photo-initiator in a vial. The resulting polymer left in the oven at 50°C. After two hours PGE was added to the vial at a 1:1 ratio and well mixed. The conversion of epoxy was monitored using NIR. After 100 minutes, a significant decrease in the epoxy peak corresponding to 14% conversion was observed. The data from the first 100 minutes was used to obtain k_d, which yielded a 233 min half life. This result further supports the notion of living cationic polymerization in these systems.

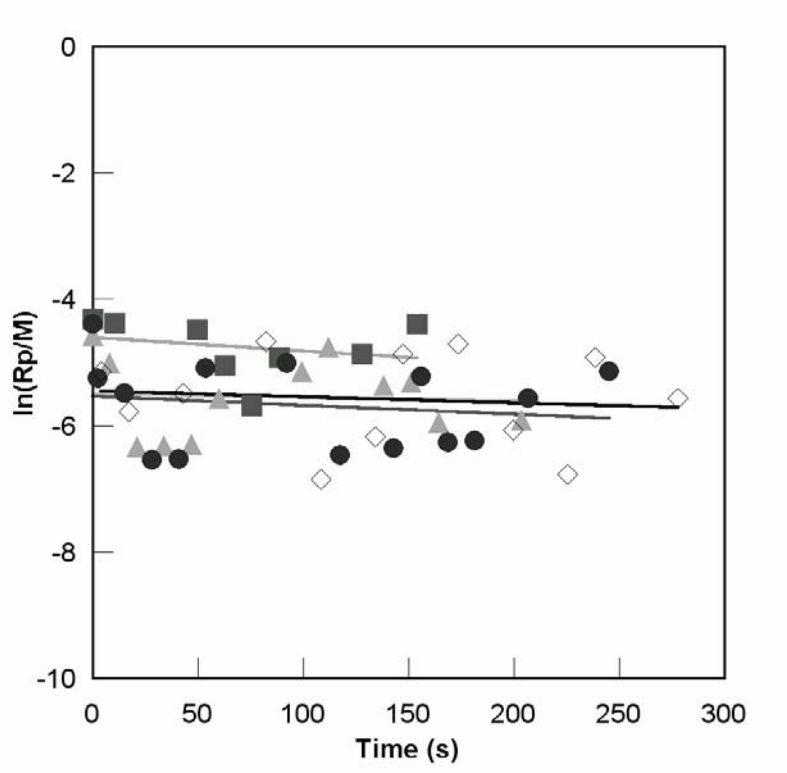

Figure 5.7. Natural log of the rate of polymerization divided by monomer concentration versus time used to obtain active center deactivation rate: 250 s (■), 200 s (▲), 150 s (●), and 100 s (◇).

Table 5.2. The kinetic constants for deactivation and its corresponding half-life show there may be long half lives of these active centers.

	150s EB exp	**200s EB exp**	**250s EB exp**
k_d **(s^{-1})**	0.00128	~0	0.00175
$t^{1/2}$**(s)**	540 s	–	396 s

5.5. Reassessment of Previous Calorimetry Experiments

The proposition that the dark reactions in EB cured epoxy systems can better be explained by the existence of two types of active centers – one short lived, and another with a significantly longer half-life, is further supported when reassessing results from the previously mentioned calorimetry experiments [9, 10].

Figure 5.8 shows the measured temperature and calculated dose from a calorimetry experiment in which approximately 4.5 kGy of irradiation was applied in 4 equal doses, between which irradiation was paused for about 300 s. During the test, specimen temperature increased gradually from about 20°C to a maximum of slightly more than 90°C, which occurred just after the fourth irradiation dose. Figure 5.9 shows a comparison between the calculated resin cure rates for this experiment and the predictions of a discretized version of the Mascioni model [9]. As with the other calorimeter measurements, although overall agreement was quite good, there also some evident discrepancies. As shown in the figure, the model failed to predict the "spikes" in cure rate observed each time the specimens were irradiated (each dose was applied over 40s). The model also did not predict the subsequent decay in cure rate, which in reality began immediately each time the irradiation was stopped. Analysis showed that the observed discrepancies can neither be accounted for by specimen temperature change during irradiation, since this is adequately dealt with by the model, nor by global diffusion effects on cure rate, since the version of the model used here includes a description for this phenomenon.

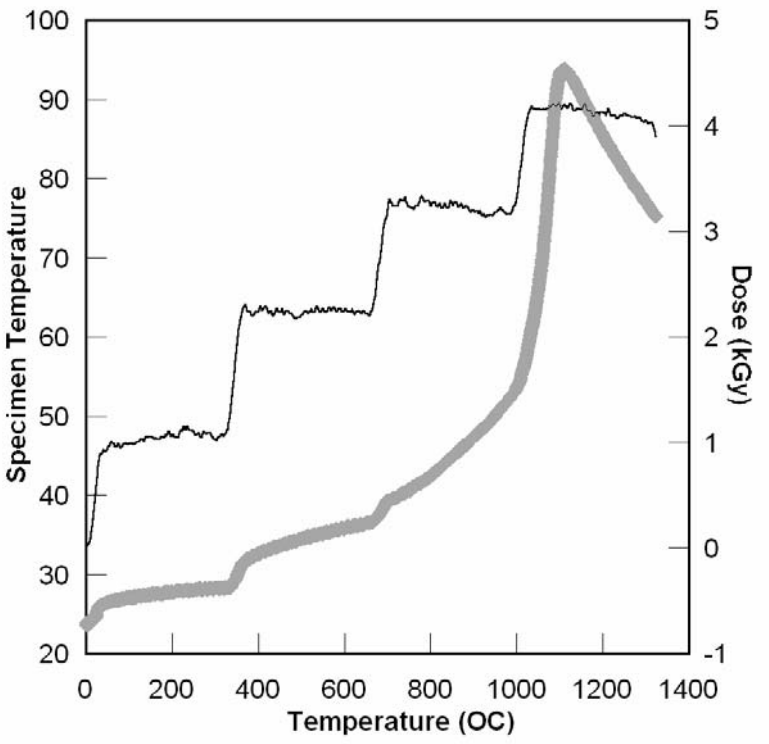

Figure 5.8. Measured temperature of the specimen (—) and calculated dose (◆) during a multi-step irradiation [1].

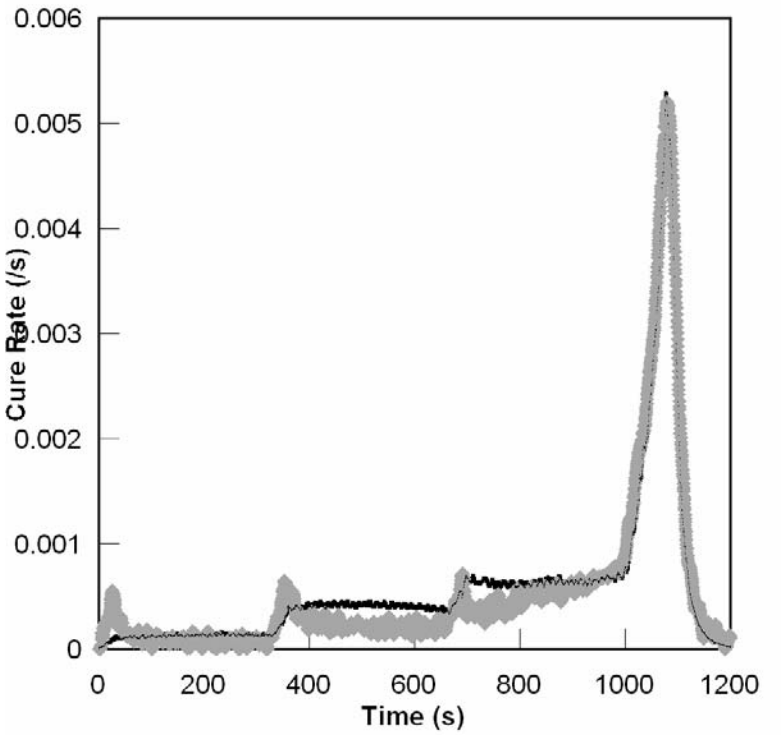

Figure 5.9. Measured (◆) and predicted (—) cure rates during a multi-step irradiation – single active center assumed (Masconi model) [1].

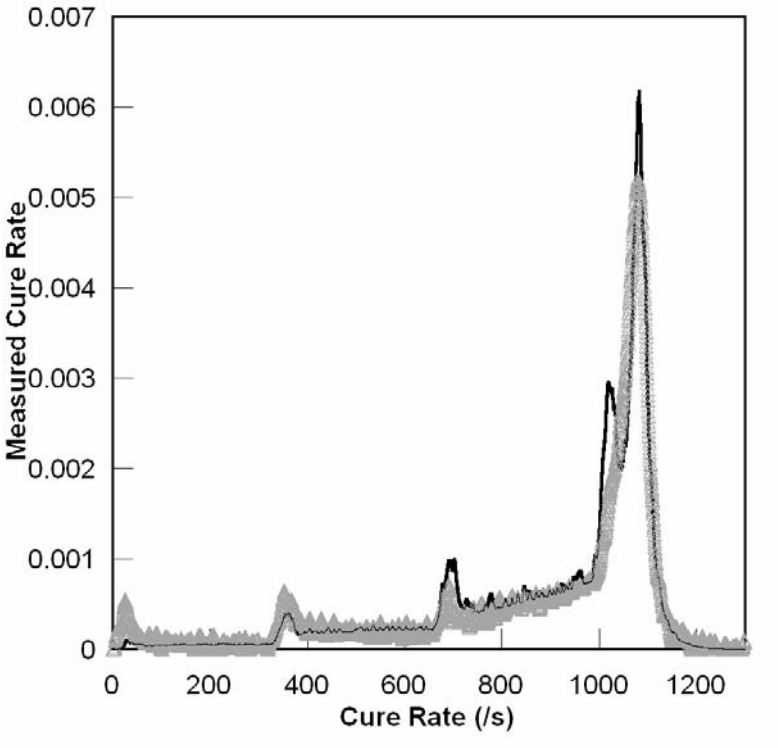

Figure 5.10. Measured (▲) and predicted (—) cure rates during a multi-step irradiation – dual active center [1].

To establish whether a better fit with experimental results could be obtained using a model assuming two active centers, one long-lived and one short-lived, a minor modification was made to the Mascioni cure model. In the revised model, *total* active center activation rate is kept the same as before, but two such centers are tracked; one with a long life (arbitrarily set to 5s) and one with an infinite life. During irradiation, both centers are assumed to contribute to the curing reaction, but upon halting irradiation, the short-lived version quickly decays and the cure rate drops by 60%. Applying this model to prediction of the calorimeter measurements (all other model parameters kept the same as previously), we see from Figure 5.10 that much better qualitative and quantitative agreement is obtained.

5.6. Conclusion

In this work, the light and dark reactions (i.e. those during and following irradiation) of radiation-cured cured cationic epoxy systems using an *in situ* NIR fiber optic technique to evaluate the kinetics of active center deactivation and potential impacts that this might have on typical cure processing of composite materials were investigated. Previous work focused on the cure behavior of such systems under continuous irradiation (light reactions only). A successful model had been developed that assumed the time scale for active center deactivation to be much greater than the characteristic time for complete reaction. This assumption was based on literature values of deactivation constants for similar systems and on the observation that polymerization continues to occur many hours after epoxy samples are exposed to EB irradiation. However, in practice, EB processing is usually not conducted in a continuous fashion but rather as a set of irradiation steps separated by variable length irradiation free periods. Although the

model worked well for continuous EB exposure experiments, it was found that it did not describe data from interrupted-dose experiments well. In particular, reaction rates during dark reaction periods were over predicted. In this work conversion data for PGE was obtained for the time period following EB irradiation for a number of exposure doses. The key observations were: first, that the reaction persists for a long time after the irradiation, and second, that there is a rapid decrease in the rate of reaction when the EB is turned off. The sudden reduction in the rate of reaction is roughly 60% for the conditions investigated at the time the EB is turned off. Long time dark polymerization experiments show that the active centers possess a half-life greater than 100 minutes. Using an empirical adjustment to a propagation model without initiation if was possible to fit both NIR and calorimetry data well.

5.7. Reference

1. Lee J, Johnston A, Palmese GR. SAMPE Int Symp, (2004).
2. Mascioni M, Sands JM, Palmese GR. SAMPE Int Symp, 47 ,93 (2002).
3. Mascioni M, Sands JM, Palmese GR. Nuc Inst and Meth in Phys Res B, 208, 353-357 (2003).
4. Palmese GR, Stein G. SAMPE Int Symp, 48, (2003).
5. Sipani V, Scranton AB. J Polym Sci Part A: Polym Chem, 41, 2064 (2003).
6. Sipani V, Scranton AB. J Photochem and Photobio A: Chem, 159, 189 (2003).
7. Lopata ES,.Riccitiello SR. J Applied Poly Sci, 21, 91 (1977).
8. Crivello JV, Ortiz RA. J Polym Sci Part A: Polym Chem, 39, 2385 (2001).
9. Johnston A, Palmese GR, Cole KC, Petrescue L, Chen JH, Lopata V. Society of Adv of Mat and Process Eng, (2003).
10. Lee J, Palmese GR, SAMPE Int Symp, (2005).
11. Chen JH, Johnston A, Petrescue L, Bordovsky L. Proceedings of 4th Canadian Int Conf on Comp Mat, (2003).
12. Chen JH, Johnston A, Petrescue L, Hojjati M. Rad Phys and Chem, 75, 336-349 (2006).
13. Rohr DF, Klein MT. Center for Comp Mats Rep, 87-44 (1987).

CHAPTER 6: PROPERTIES OF TRIGLYCIDYL ETHER OF TRISPHENOL-METHANE (TACTIX 742)

6.1. Introduction

In selecting a thermoset resin, one must consider properties such as tensile strength, modulus, and glass transition temperature, material availability, ease of processing, and cost. Epoxy resins such as DGEBA used throughout this work provides a unique balance of chemical and mechanical properties combined with extreme processing versatility. However, there are limitations in tailoring the network of DGEBA to satisfy particular requirements which will be discussed in a later chapter. Tactix 742 is a trifunctional epoxy that can provide improved properties. This chapter investigates the improvements Tactix 742 can provide to optimize mechanical properties in our DGEBA system.

6.2. Materials

The chemical structures of materials used in this investigation are given in Table 6.1. The difunctional epoxy used in this study was diglycidyl ether of bisphenol A (DGEBA) (Resolution Epon 825). Water was removed from DGEBA using 4Å molecular sieves (Aldrich Chemical Company, Inc) conditioned at 120°C for 12 hours prior to use. Such drying limits water concentration to below 0.1% in the DGEBA. The trifunctional epoxy used was triglycidyl ether of trisphenol-methane (Ciba Tactix 742). Unlike DGEBA, Tactix 742 is considered to be in a solid state in room temperature. However due to it's viscosity, it must be frozen to be transfered and then heated to be mixed into the system. Diphenyl iodonium hexafluoroantimonate (Applied Poleramics CD1012) was used as the photoinitiator.

Table 6.1. The chemical structures of the materials used in this experimental work.

Material	**Chemical Structure**
Diglycidyl ether of bisphenol A (DGEBA). EPON 825	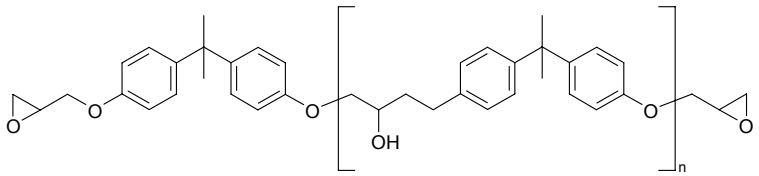
Triglycidyl Ether of Trisphenol-methane (Tactix 742)	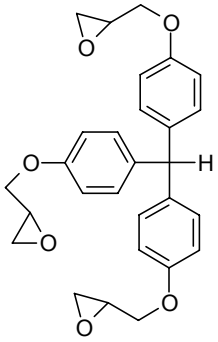
Diphenyl iodonium hexafluoroantimonate CD1012	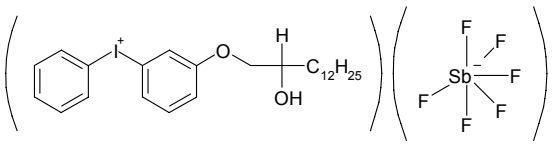

6.3. Procedure

6.3.1. Preparation of DGEBA and Tactix 742

Tactix 742 is a trifunctional epoxy that has higher T_g than of DGEBA. However the resin is extremely viscous and difficult to work with. Different ratios of Tactix 742 and DGEBA were studied to find an optimum combination to retain high T_g without causing the viscosity to reach unusable levels. Samples of DGEBA and various concentrations of Tactix 742 ranging from 10 wt% to 90 wt% were mixed with 1 pph photoinitiator. All samples were kept at a higher temperature of 80°C due to the viscosity of Tactix 742.

6.4. Results

6.4.1. Synthesis and Application of Tactix 742 and DGEBA

Tactix 742 is a trifunctional epoxy that has higher T_g than of DGEBA as previously mentioned. Different ratios ranging from 10 wt% to 90 wt% of Tactix 742 with DGEBA were studied to find an optimum combination to retain high T_g without causing the viscosity to reach unusable levels as shown in Figure 6.1 and 6.2. As the concentration of Tactix decreased in the system, the fracture toughness increased while the T_g decreased. For strength and modulus, as the concentration of Tactix increased the strength decreased as the modulus increased. In all cases one property would improve as another property decreased, thus another factor was accounted for. Tactix 742 is a highly viscous material; hence the Tactix 742 was kept to a minimum so that the resin could be applied to composites. It is also important to note that the relative values were taken due to the contamination of water in the system.

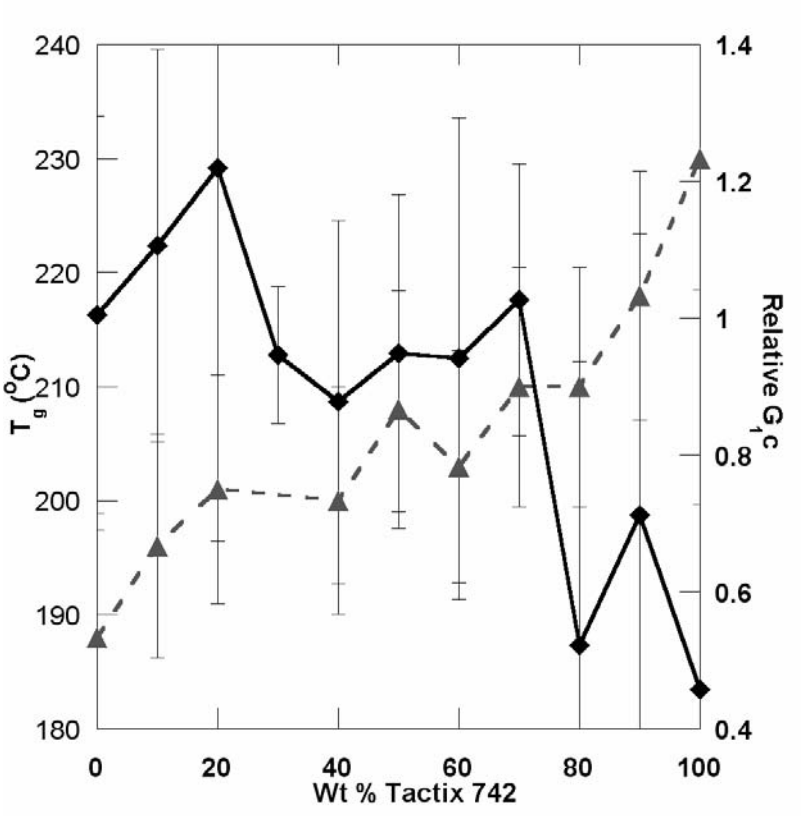

Figure 6.1. Various ratios of Tactix 742 and DGEBA were made and cured via EB and tested for fracture toughness (◆) and T_g (▲). With increasing amounts of Tactix 742 fracture toughness decreases, the glass transition temperature increases.

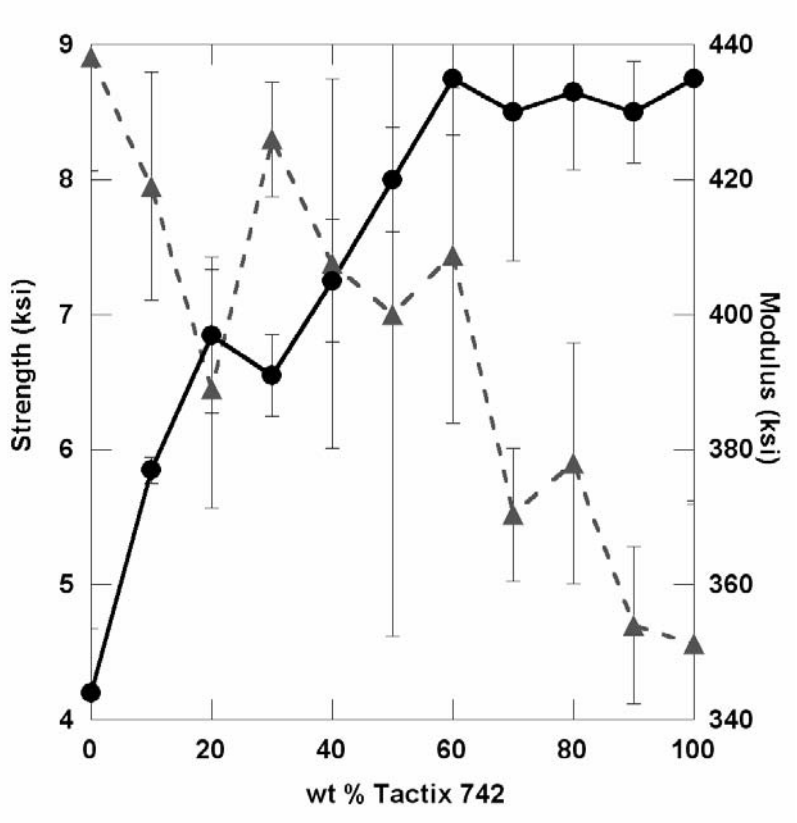

Figure 6.2. Various ratios of Tactix 742 and DGEBA were made and cured via EB and tested for strength (▲), modulus (•). With increasing amounts of Tactix 742 strength decreases, and modulus increases.

6.5. Conclusion

Various concentrations of Tactix 742 were mixed with DGEBA to find the optimum material properties. Between 20 wt% and 40 wt% of Tactix 742 in DGEBA seemed to result in the best balance of properties. However, due to the viscosity of Tactix 742, 40 wt% would be difficult to process into a composite.

6.6. Reference

1. Dabestani R, Ivanov I. SAMPE Int Symp, 46, 2075 (2001).

CHAPTER 7: IMPROVED EB CURED DGEBA SYSTEMS BY COPOLYMERIZATION WITH NOVEL TETRAHYDROFURAN FUNCTIONAL COMONOMERS

7.1. Introduction

As discussed in previous chapters, electron beam (EB) cured epoxy-matrix composites have significant processing advantages over their thermally cured counterparts, but suffer from low compressive strength and poor interlaminar shear strength [1-10]. One reason for this is that cationically cured DGEBA possesses poor fracture toughness when compared with amine or anhydride cured DGEBA systems. The focus of this chapter is to design improved EB cured DGEBA systems by modification with appropriate chain extenders designed to impart the appropriate level of network flexibility while maintaining glass transition temperature requirements. This is shown schematically in Figure 7.1 where tailoring the network is accomplished by copolymerization with other monomers that increase the molecular weight between crosslinks. This method also allows for varying chain flexibility to adjust material properties by changing the monomer type.

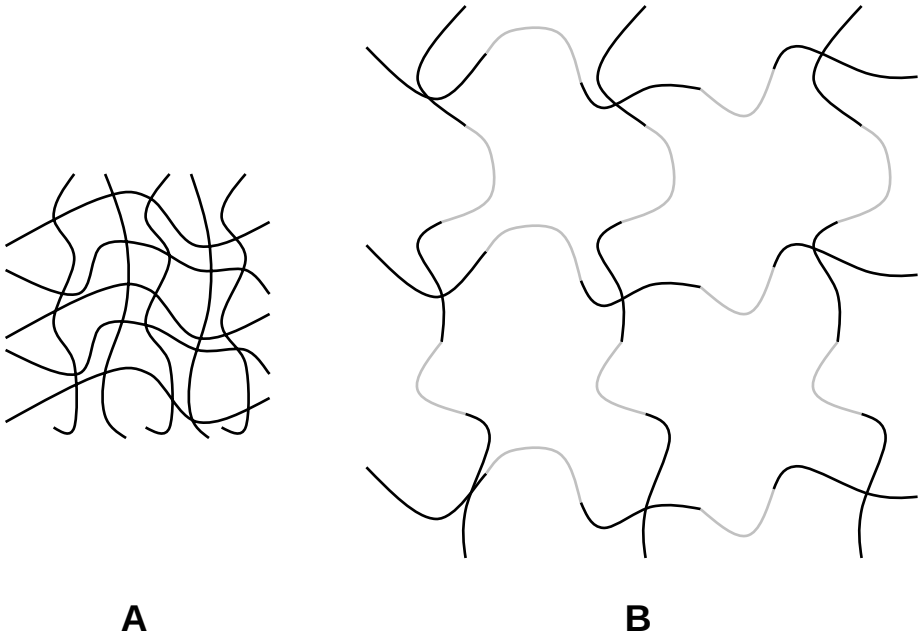

Figure 7.1. Schematic representation of a highly crosslinked network (A) and homogeneously modified by copolymerization with a chain extender (B).

In previous work, Ghosh et al. investigated factors influencing the polymerization of epoxy resins and found that hydroxyl groups, specifically alcohols, can play an important role in the polymerization of epoxies. Alcohols with –OH groups positioned on different carbon atoms of the chain (primary, secondary, and tertiary) were studied to determine their influence on the network formation of DGEBA via cationic polymerization. Ghosh et al. concluded that the intrinsic reactivity of alcoholic species with the active center relative to that of a glycidyl ether moiety with active centers changed the degree to which the network structure was disrupted. This showed that the potential exists to tailor epoxy network formation in such systems by introducing specifically designed comonomers with appropriate –OH functionality [10].

In Chapter 5, the influence of water on DGEBA cationic polymerization induced by EB and found that the addition of water affects the cure behavior of DGEBA and the formation of the network structure. In such cases an initial retardation period followed by acceleration in the epoxy conversion was observed. Increased concentrations of water caused longer delays and increased epoxy conversion. Consumption of water during the polymerization indicated that the resulting network structure was altered. The addition of water decreased the glass transition temperature significantly from ~190°C for "dry" epoxy to values as low as 170°C for systems modified with 1 wt% water. This decrease in T_g was accompanied by a modest increase of fracture toughness from a G_{1C} of 56 J/m^2 for the "dry" system to a G_{1C} ~140 J/m^2 for the material modified with water. These results suggest that the increase of G_{1C} resulted from the decrease of cross-link density associated with chain transfer reactions with water [19]. The objective of this Chapter is to discuss the design of improved EB cured epoxy systems based on diglycidyl ether of

bisphenol A (DGEBA) by the use of network modifiers.

7.2. Experimental

7.2.1. Materials

The chemical structures of materials used in this investigation are given in Table 7.1. These include the materials used to synthesize THF functional comonomers. Diglycidyl ether of bisphenol A (DGEBA) (Resolution Epon 825) was used in this investigation. Water was removed from this material using 4Å molecular sieves (Aldrich) conditioned at 120°C for 12 hours prior to use. Such drying limits water concentration to below 0.1% in the DGEBA. Diphenyl iodonium hexafluoroantimonate (Applied Poleramics CD1012) was used as the photoinitiator.

Phenyl glycidyl ether (PGE) obtained from Aldrich (99.0%) was treated the same as DGEBA. The chain extender tetrahydrofuran (THF) was obtained from Aldrich (≥99.0%, H_2O <0.05%; inhibited with 250 ppm butylated hydroxytoluene) and was also dried using molecular sieves. The other chain extenters were purchased from Aldrich, cyclohexene oxide (CHO) (98.0%), phthalan was (99.0%), 2,3-dihydrobenzofuran (Coumaran) (99.0%). Tetrahydro-2-furoic acid (Aldrich: 97%; inhibited with 250 ppm butylated hydroxytoluene) was used to synthesize difunctional and trifunctional chain extending comonomers based on the esterification reaction with DGEBA and triglycidyl ether of trisphenol-methane (Tactix 742) respectively. The esterification procedure is described in section 7.3.

Table 7.1. The chemical structures of the materials used in this experimental work.

Material	**Chemical Structure**
Diglycidyl ether of bisphenol A (DGEBA). EPON 825	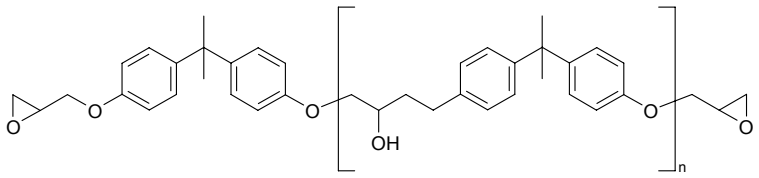
Triglycidyl Ether of Trisphenol-methane (Tactix 742)	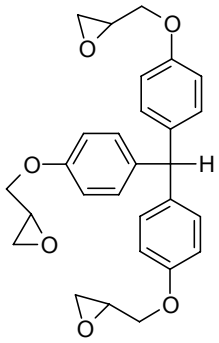
Diphenyl iodonium hexafluoroantimonate CD1012	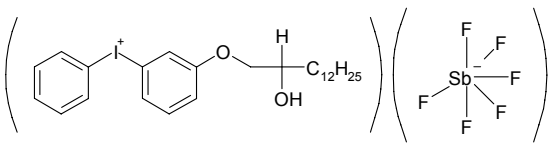
Phenyl Glycidyl Ether (PGE)	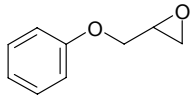
Cyclohexene oxide (CHO)	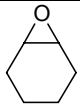
Tetrahydrofuran (THF)	
Tetrahydro-2-furoic acid	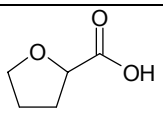
Tetrahydro-3-furoic acid	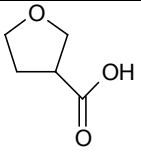
Phthalan	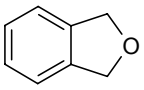
2,3-Dihydrobenzofuran (Coumaran)	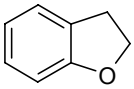

7.3. Procedure

7.3.1. Preparation of DGEBA and PGE or CHO Systems

DGEBA and various concentrations of the co-monomers ranging from 1 wt% to 10 wt% were premixed before adding the CD1012 photoinitiator. Samples were kept in a sealed dark container at 60°C until cured.

7.3.2. Preparation of DGEBA and THF Systems

Before preparing samples with DGEBA and THF, two tests were preformed to show that THF copolymerizes with epoxy systems. The first test was a weight loss test. 0 wt% to 90 wt% of THF was mixed with PGE with 1pph photoinitiator and weighed. All closed vials of THF and PGE were fully cured (NIR spectroscopy showed no signs of an epoxy peak) for 30 mins. Then the caps were opened and placed in the oven at 80°C overnight to allow the unreacted THF to be released. Placing the sample at 80°C allows the THF to be at gaseous phase allowing the unreacted solvent to escape. Then the specimens were weighed again to calculate the weight loss. Table 7.2 shows the theoretical amount of THF that were initially put into the vials (%THF (theo calc)) and the actually amount that reacted into the epoxy system (%THF (act calc)). The difference between the theoretical amount and the actual amount are negligible up 20 wt% of THF, however with increasing amounts above that the difference becomes considerable as shown in Figure 7.2. The second test was to run GPCs to ensure the copolymerization of PGE and THF. Figure 7.3 shows the change in MW with increased amounts of THF into the PGE system. As the amount of THF increases in the system, it was observed that the side hump at around 15 min decreased.

Table 7.2. Calculation of the amount of THF placed into the epoxy system and the actual amount that reacted.

%THF (theo)	g of PGE	g of THF (initial)	g of THF (final)	g of weight loss	%THF (theo calc)	%THF (act calc)
0	2.01141	0	-0.00238	0.00238	0	-0.11847
1	1.98015	0.02546	0.019596	0.005864	1.26944	0.97992
5	1.90297	0.10183	0.09799	0.00384	5.07931	4.89715
10	1.80552	0.20509	0.19923	0.00586	10.20039	9.93790
20	1.60061	0.40008	0.36957	0.03051	19.99710	18.75818
30	1.40077	0.60049	0.47132	0.12917	30.00560	25.17614
40	1.2051	0.80186	0.63687	0.16499	39.95396	34.57548
50	1.007	1.00266	0.52606	0.4766	49.89202	34.31438
60	0.80022	1.2169	0.53553	0.68137	60.32859	40.09208
70	0.60928	1.4006	0.59057	0.81003	69.68575	49.22032
80	0.40047	1.60316	0.6379	0.96526	80.01278	61.43282
90	0.21021	1.80918	0.57923	1.22995	89.59042	73.372268

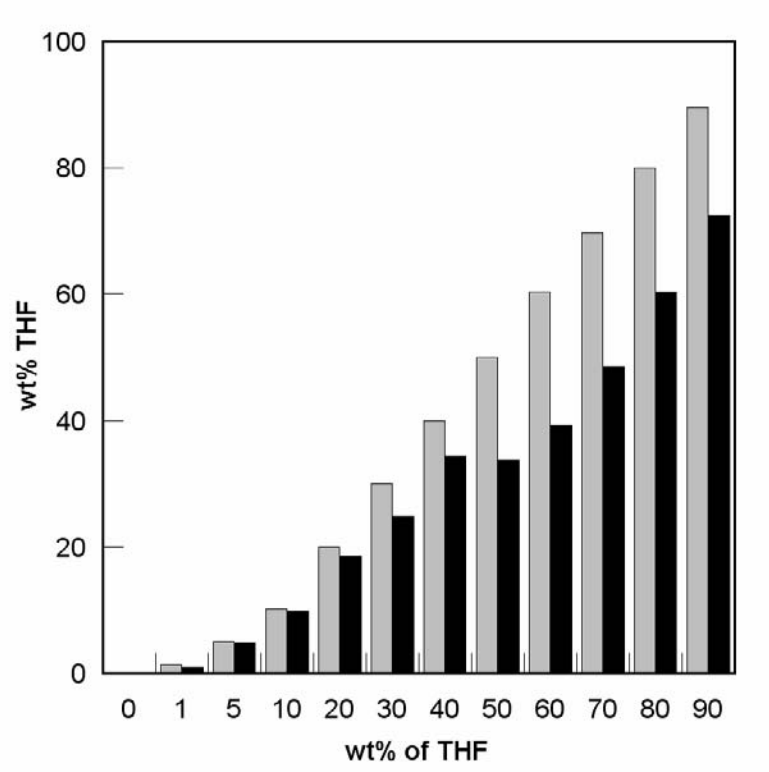

Figure 7.2. The theoretical % of THF (gray) versus the actual % of THF (black) was reacted into the epoxy system.

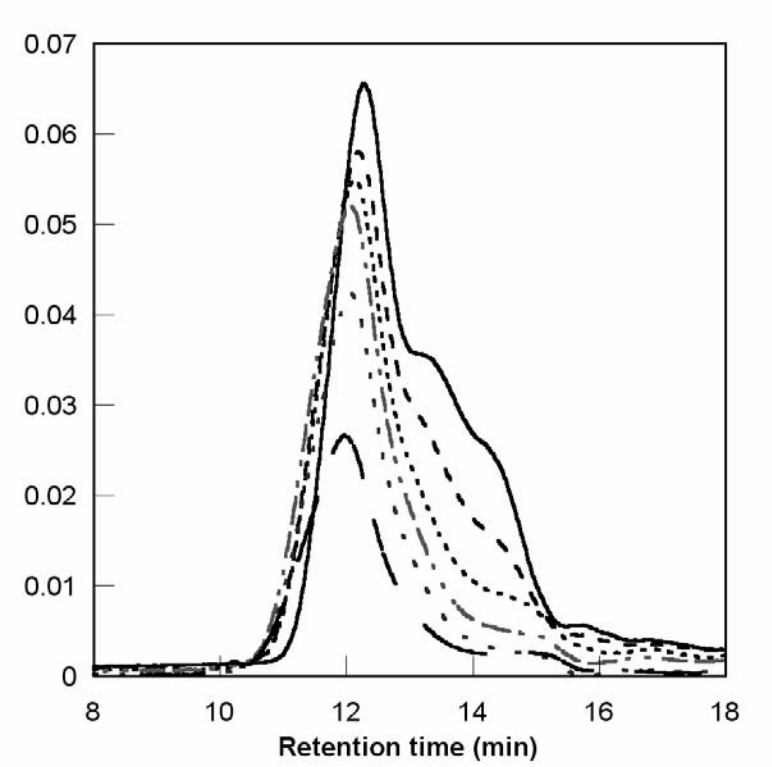

Figure 7.3. GPC of 0wt% to 90 wt% of THF in PGE cured via UV light, where pure PGE (—), 10 wt% THF (- - -), 30 wt% THF (····), 50 wt% THF (·· — —), 70 wt% THF (· · ·), and 90 wt% THF (— —).

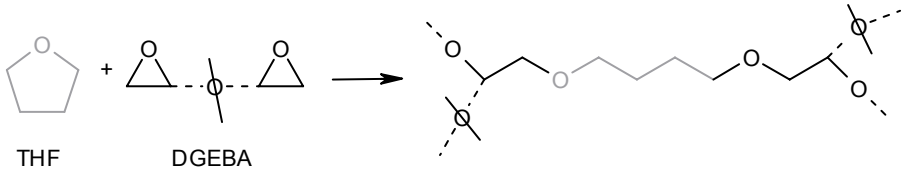

Figure 7.4. Proposed ring opening reaction of DGEBA and THF resulting in the insertion of a flexible chain.

Samples of DGEBA and various concentrations of THF ranging from 1 wt% to 20wt% were premixed. With the appropriate photoinitiator THF copolymerizes readily with DGEBA epoxies. The use of ring-opening comonomers based on five member ether rings like tetrahydrofuran are shown schematically in Figure 7.4. Such copolymerization leads to the insertion of 4 methylene linkages in the crosslinked DGEBA structure. After samples were mixed with 1 pph photoinitiator, they were kept in a sealed dark container at 60°C until cured.

7.3.3. Preparation of DGEBA and Tetrahydro-2-furoic Acid Systems

DGEBA systems with pure THF have disadvantages that will be discussed in the next section. Thus new monomers containing the THF functional groups were tested. The linear equivalent was first tested to show that the new monomers copolymerized. PGE and tetrahydro-2-furoic acid (THF2) in stoichiometric quantities (1:1 molar ratio) were mixed and reacted at 60°C using 1 wt% AMC-2 catalyst (Aeroiet Fine Chemicals). THF functional monomers were synthesized by the esterification reaction shown in Figure 7.5. The esterfication reaction was monitored on the NIR to ensure all the epoxy was reacted. Then a sample with 20 wt% of the new monomer THF2PGE was mixed with pure PGE and 1pph photoinitator and irradiated by UV light. At every minute time interval, a small quantity of the sample was taken out to run GPC as shown in Figure 7.6.

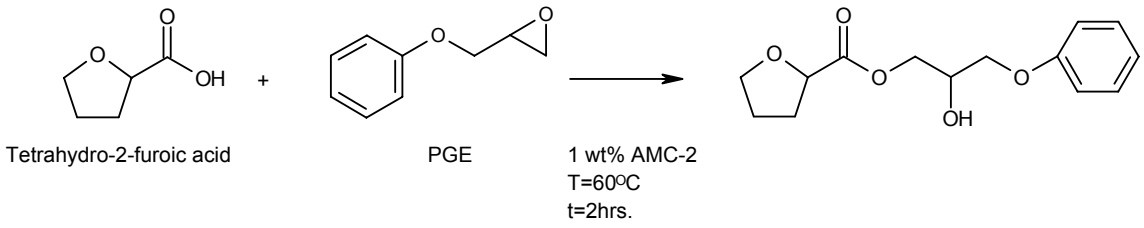

Figure 7.5. The chain extender was synthesized using an esterfication reaction of tetrahydro-2-furoic acid and PGE with AMC-2 catalyst.

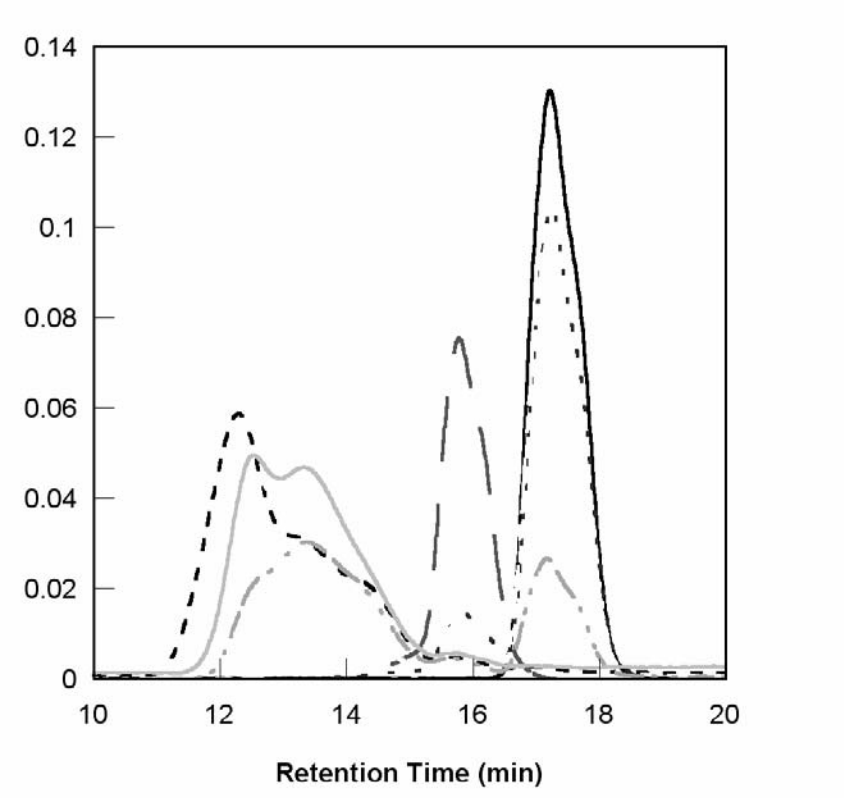

Figure 7.6. GPC of 20 wt% THF2PGE in PGE cured via UV light were taken at various cure times to show the reaction progression where uncured PGE (—), cured PGE (- - -), uncured THF2PGE (− −), 2 min (· · ·), 4 min (·· – –), 6 min (—).

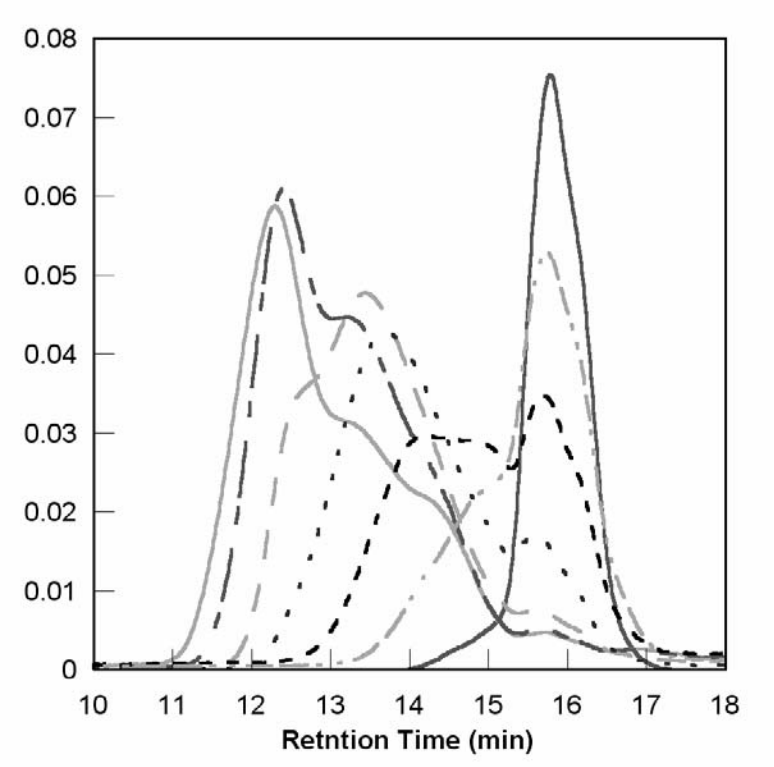

Figure 7.7. GPC of 0wt% to 90 wt% of THF2PGE in PGE cured via UV light where uncured THF2PGE (—), cured PGE (—), 10 wt% (- —), 30 wt% (— —), 50 wt% (· · ·), 70 wt% (- - -), 90wt % (·· — —).

The GPC shows that full cure was reached around 6 minutes of UV exposure. The uncured THF2PGE comes out around 16.5 min and uncured PGE is at 18 min. After full cure, the 20 wt% THF2PGE peak comes out slightly later at 11.5 min than that of cured pure PGE at 11 min. Then various concentrations of THF2PGE were mixed with pure PGE to observe the different increasing resulting molecular weight. Figure 7.7 shows the GPC of 10 wt% to 90 wt% of THF2PGE mixed with PGE. As the concentration of THF2PGE increases, the MW decreases.

The PGE was then replaced by DGEBA to design new resins. New difunctional monomer (GP3) with THF functional end groups was synthesized by the esterification reaction shown in Figure 7.8. DGEBA and tetrahydro-2-furoic acid in stoichiometric quantities (1:2 molar ratio) were mixed and reacted at 60°C using 1 wt% AMC-2 catalyst. Samples were kept in a sealed dark container at 60°C for two hours and stirred at half hour intervals. Various concentrations of the new monomers were mixed with DGEBA and 1 pph photo-initator and kept in a sealed dark container until cured. GP2 (DGEBA and tetrahydor-3-furoic acid) was made similarly to GP3, where the chemistry is shown in Figure 7.9.

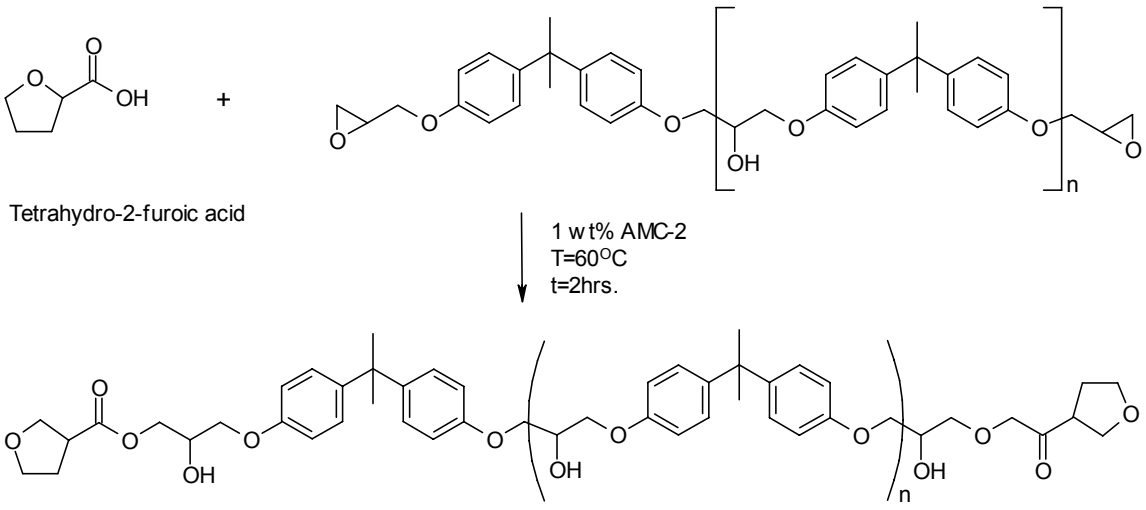

Figure 7.8. The chain extender was synthesized using an esterification of tetrahydro-2-furoic acid and DGEBA using AMC-2 catalyst (GP3).

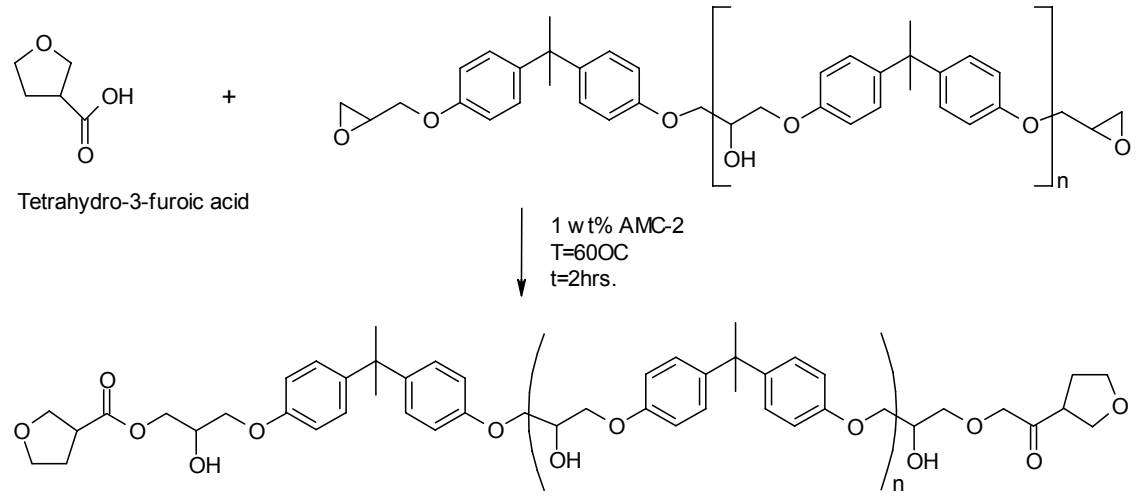

Figure 7.9. The chain extender was synthesized using an esterification of tetrahydro-2-furoic acid and DGEBA using AMC-2 catalyst (GP2).

7.3.4. Preparation of DGEBA and Coumaran Systems

Samples of DGEBA and various concentrations of Coumaran from 1 wt% to 10 wt% were premixed. The use of ring-opening comonomers based on five member ether rings similar to the tetrahydrofuran polymerization is shown schematically in Figure 7.10. Such copolymerization leads to the insertion of 4 methylene linkages along with the ridigity of the aromatic ring in the crosslinked DGEBA structure. After samples (JL1) were mixed with 1 pph photo-initiator and DGEBA, they were kept in a sealed dark container at 60°C until cured.

7.3.5. Preparation of DGEBA and Phthalan Systems

Phthalan samples were similarly prepared to those of DGEBA and Coumaran as shown in Figure 7.11. The linear equivalent was first tested to show that the new monomers copolymerized. PGE and phthalan in stoichiometric quantities (1:1 molar ratio) were mixed. Various concentrations of phthalan were mixed with pure PGE to observe the different MW of polymers following photo-polymerization. Figure 7.12 shows the GPC of 10 wt% to 90 wt% of phthalan mixed with PGE. As the concentration of phthalan increase, the MW decreases.

The PGE was then replaced by DGEBA to design new resins. Various concentrations of the new monomer JL2 were mixed with DGEBA and 1 pph photo-initator and kept in a sealed dark container until cured.

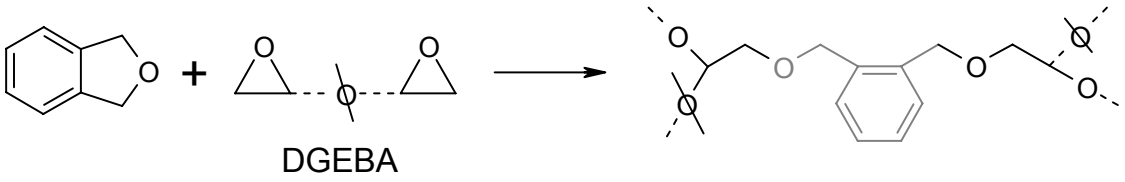

Figure 7.10. Ring opening reaction of DGEBA and Coumaran (JL1).

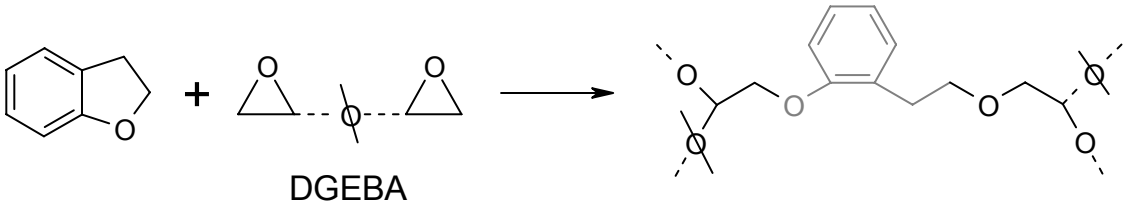

Figure 7.11. Ring opening reaction of DGEBA and Phthalan (JL2).

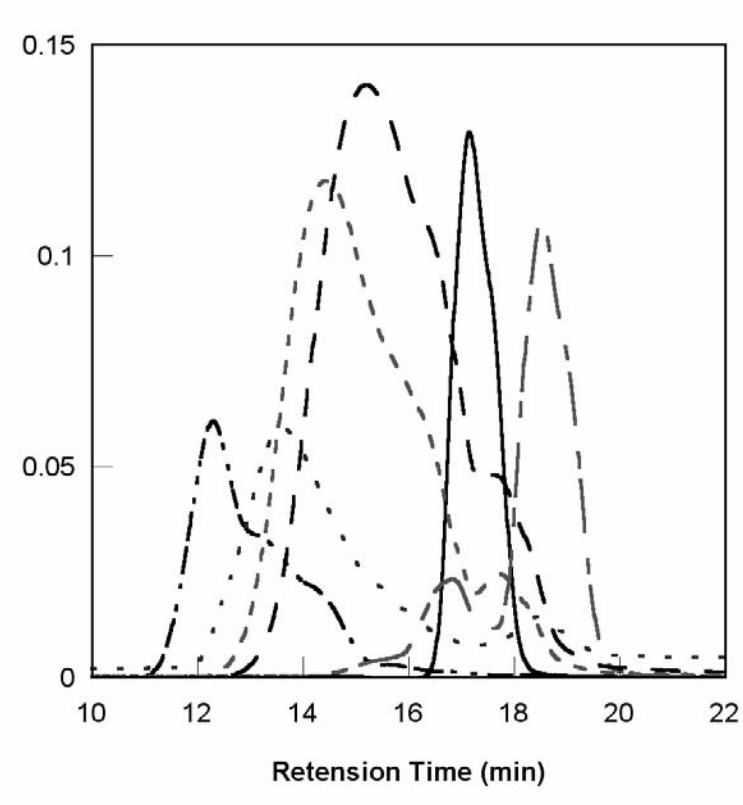

Figure 7.12. GPC of 0wt% to 90 wt% of phthalan in PGE cured via UV light where uncured PGE (—), cured PGE (··– –), uncured phthalan (– —), cured phthalan (— —), 50 wt% phthalan (· · ·), 90wt % phthalan (- -).

7.3.6. Preparation of Tactix 742 and Tetrahydro-2-furoic Acid Systems

A new trifunctional monomer (GP5 shown in Figure 7.13) with THF functional end groups was synthesized from the esterification reaction similar to GP3 synthesis. Tactix 742 and tetrahydro-2-furoic acid in stoichiometric quantities (1:3 molar ratio) were mixed and reacted at 60°C using 1 wt% AMC-2 catalyst. Samples were kept in a sealed dark container at 60°C for two hours. Various concentrations of the new monomers were mixed with DGEBA and 1 pph photo-initator and kept in a sealed dark container until cured. GP4 (DGEBA and tetrahydor-3-furoic acid) was made similarly to GP5, where the chemistry is shown in Figure 7.14.

7.3.7. Composites Processing

A wet hand lay-up technique was used to fabricate composite plaques. In this method 5HS 12k tow AS4 carbon fabric with G' sizing was used for reinforcement. In the experiments, eight layers of carbon fiber fabric were used to prepare the composites and all fabric layers were aligned in the same direction. After lay-up the system was bagged and a vacuum was applied with a hot air blower keeping the system at 60°C. Cured composite fiber volume fraction was ~ 55%.

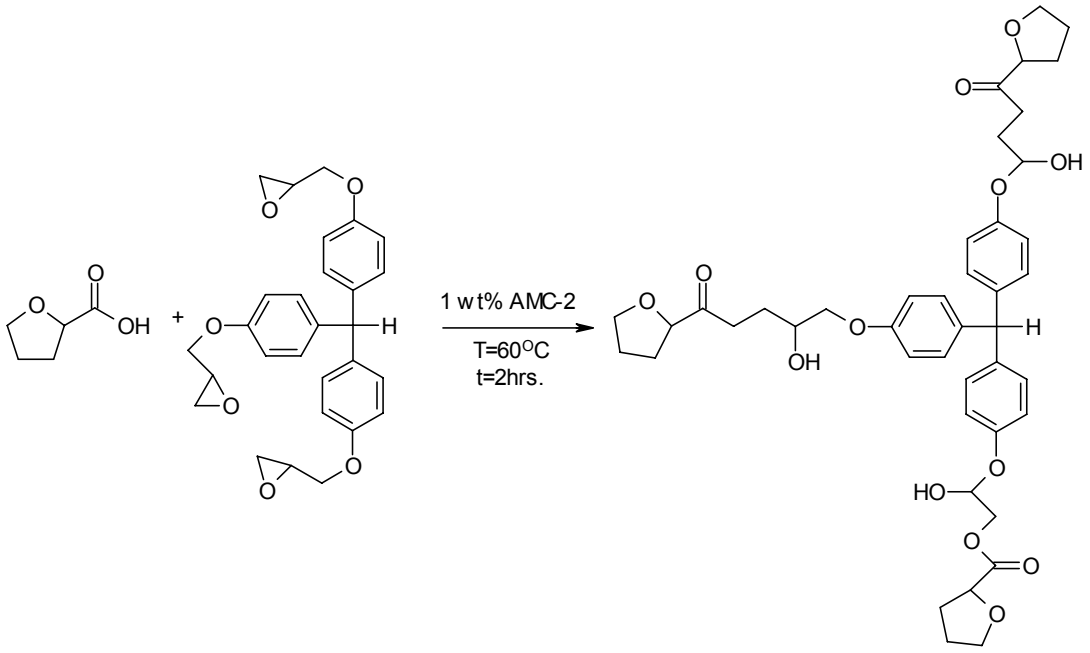

Figure 7.13. The chain extender was synthesized using an esterification of tetrahydro-2-furoic acid and Tactix 742 with AMC-2 catalyst to produce chain extender (GP5).

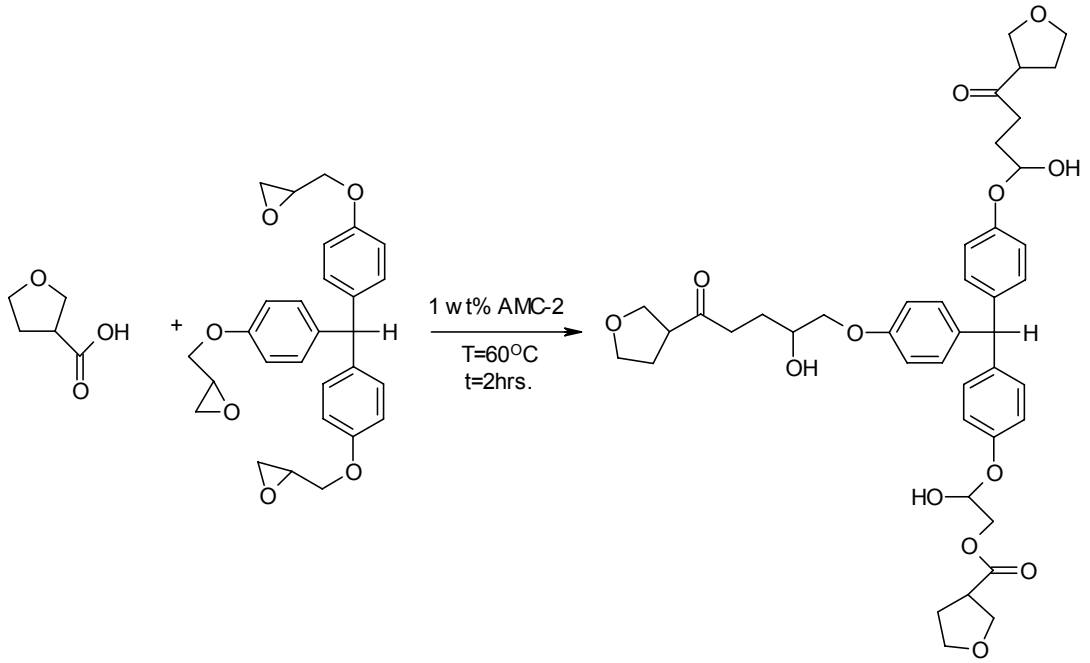

Figure 7.14. The chain extender was synthesized using an esterification of tetrahydro-3-furoic acid and Tactix 742 with AMC-2 catalyst to produce chain extender (GP4).

7.3.8. Sample Irradiation

Neat resin samples were prepared using DGEBA with various concentrations of the comonomers mentioned above. The resin mixtures were transferred to a mold and then covered with a clear plastic film to prevent water absorption. EB cure was performed at the University of Dayton Research Institute Laboratory for Research on Electron Beam Curing of Composites. The EB machine is a 3.5 MeV EB accelerator specifically designed for irradiating samples in a controlled manner. The samples were irradiated as follows: 25 pulses/second, 60% scan width, 150 mA/pulse, and 3 kGy/pass for a total dose of 54 kGy. Resin plaques were post-cured up to a temperature of 150°C. Composites were cured by EB using the same irradiation schedule and were post-cured up to a temperature of 200°C.

7.4. Results

This work addresses the influence of comonomers on the performance of DGEBA systems by tailoring properties of network polymers using chain extension. The first part of this section reports results of the investigation regarding the copolymerization of DGEBA with monofunctional chain extenders with particular emphasis on mechanical properties. The second part explores using THF based functional monomers to provide extension while maintaining higher T_g. The third part uses trifunctional THF monomers to further improve properties based on the results from the previous chapter on Tactix 742. The fourth part integrates the use of trifunctional epoxy with with chain extenders containing a cyclic backbone. The final part of this work summarizes preliminary data concerning composite behavior.

7.4.1. Monofunctional chain extenders

Epoxy systems cured via EB result in poor properties as previously mentioned. However in Chapter 4, it was observed that the presence of water changed the final properties of the resulting polymer. Water lowered the T_g of the final polymer while providing a higher fracture toughness. This lead to the idea that the by using chain extenders, one can tailor properties of network polymers. First mononofunctional chain extenders were explored to improve the final properties of the polymer.

7.4.1.1. Chain Extension with Phenyl Glycidyl Ethers (PGE)

Initially, phenyl glycidyl ether was used to tailor the network structure due to its availability and to use a monomer containing an epoxy group. Since polyPGE is a linear polymer, the addition of the chain extender would decrease the crosslink density. However with initial DMA tests, the results showed that the T_g decreased significantly as shown in Table 7.3. There is a double peak in the DMAs, where one T_g was below 100°C and the other peak was closer to that of the T_g of pure DGEBA as shown in Figure 7.15. Thus, due to the formation of two distinct peaks, the DGEBA and PGE system required no further testing.

7.4.1.2. Chain Extension with Cyclohexene Oxide (CHO)

Due to the versatility of the systems and availability, CHO was the next monomer used to copolymerize with DGEBA to improved mechanical properties. The T_g results obtained by DMA loss modulus peaks are given in Table 7.4. Similar to the PGE system, CHO at 5 wt% CHO resulted in a double peak as shown in Figure 7.16. Also when the resin was polymerized, it resulted in a cloudy opaque plaque. Thus further testing was not conducted for DGEBA and CHO.

Table 7.3. DMA results of the co-polymerization of DGEBA and PGE as the chain extender.

PGE concentration	T_g (°C) 2nd run
1 wt %	124
	183
5 wt %	119
	170
10 wt %	103
	147

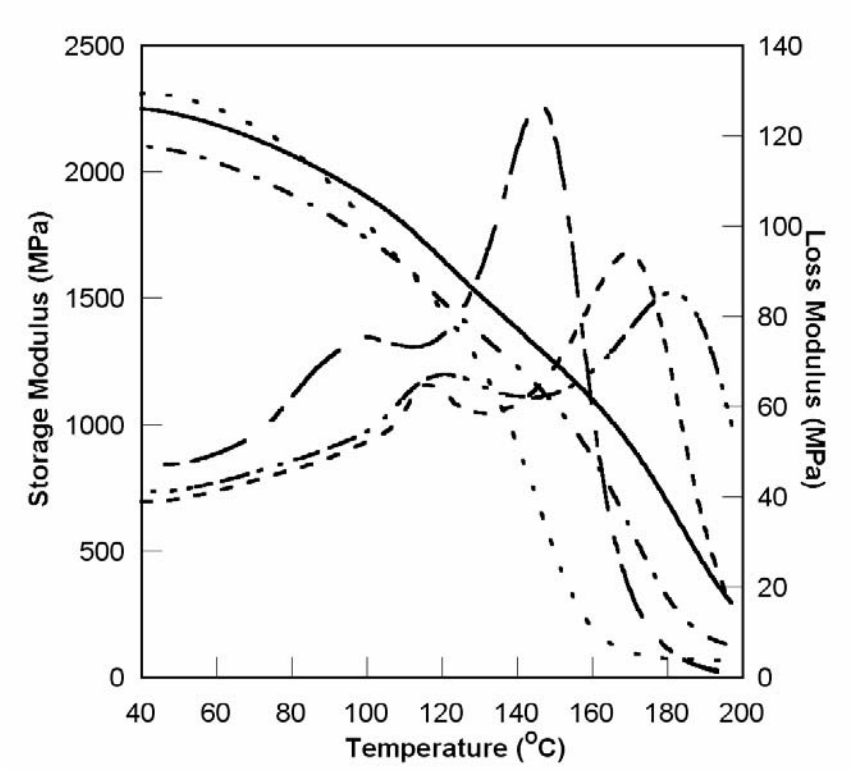

Figure 7.15. DMA (2nd run) of DGEBA with PGE as a chain extender, where 1 wt% PGE storage modulus (—),1 wt% PGE loss modulus (···– –), 5 wt% PGE storage modulus (· – · –), and 5 wt% PGE loss modulus (- - -), and 10 wt% PGE storage modulus (····),10 wt% PGE loss modulus (– —) are shown.

Table 7.4. DMA results of the co-polymerization of DGEBA and CHO as the chain extender.

CHO concentration	T_g (°C) 2nd run
1 wt%	170
5 wt%	125
	176
10 wt%	165

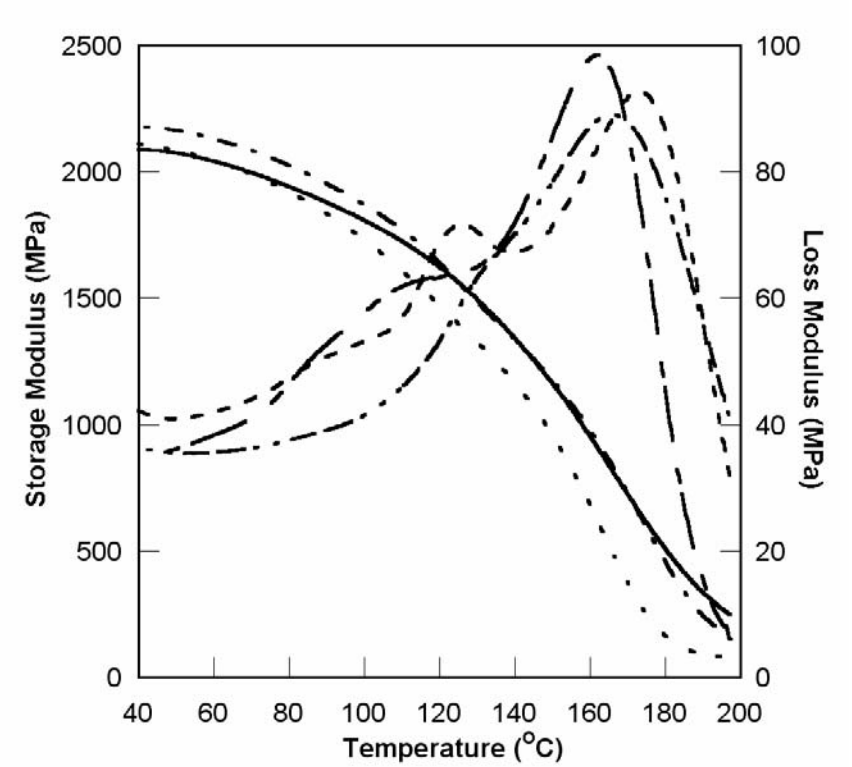

Figure 7.16. DMA (2nd run) of DGEBA with CHO as a chain extender, where 1 wt% CHO storage modulus (—),1 wt% CHO loss modulus (··· −), 5 wt% CHO storage modulus (· − · −), and 5 wt% CHO loss modulus (- - -), and 10 wt% CHO storage modulus (····),10 wt% CHO loss modulus (− —) are shown.

7.4.1.3. Chain Extension with Tetrahydrofuran (THF)

Other chain extending strategies needed to be explored to tailor the network structure and improve mechanical properties. The most interesting of these was the use of ring-opening comonomers based on five member ether THF rings as shown schematically in Figure 7.4. It is presumed that a tetramethylene ether grouping is added to the crosslinked network comprised primarily of DGEBA via ring opening of the THF molecule. This would necessarily result in a decreased crosslink density and potentially higher fracture toughness. In fact, our results show improved mechanical properties. At 10 wt% THF in DGEBA, the G_{1C} value increased almost by a factor of four: from 56 J/m^2 for neat dry DGEBA to 217 J/m^2 for the modified system. However, the T_g of these systems suffered a very significant loss of T_g from 190°C for neat DGEBA to 129°C as shown in Table 7.5.

Some of the loss could be a result of plasticization due to unreacted THF remaining in the system. However, after postcuring it is expected that unreacted THF will have been removed and no appreciable weight loss was observed. The high volatility of THF presents a practical problem in its use and application to commercial processes. And, while the decrease in T_g can be somewhat curtailed by reducing the concentration of THF used, the dangers associated with THF evolution cannot. It was hypothesized that using THF as reactive endgroup on monomers possessing similar chain structure to DGEBA would result in toughened systems with higher T_g. The next section explores the possibility using such difunctional monomers.

Table 7.5. DMA results of the co-polymerization of DGEBA and THF as the chain extender.

THF concentration	T_g (°C) 2nd run
1 wt%	175
5 wt%	159
10 wt%	129

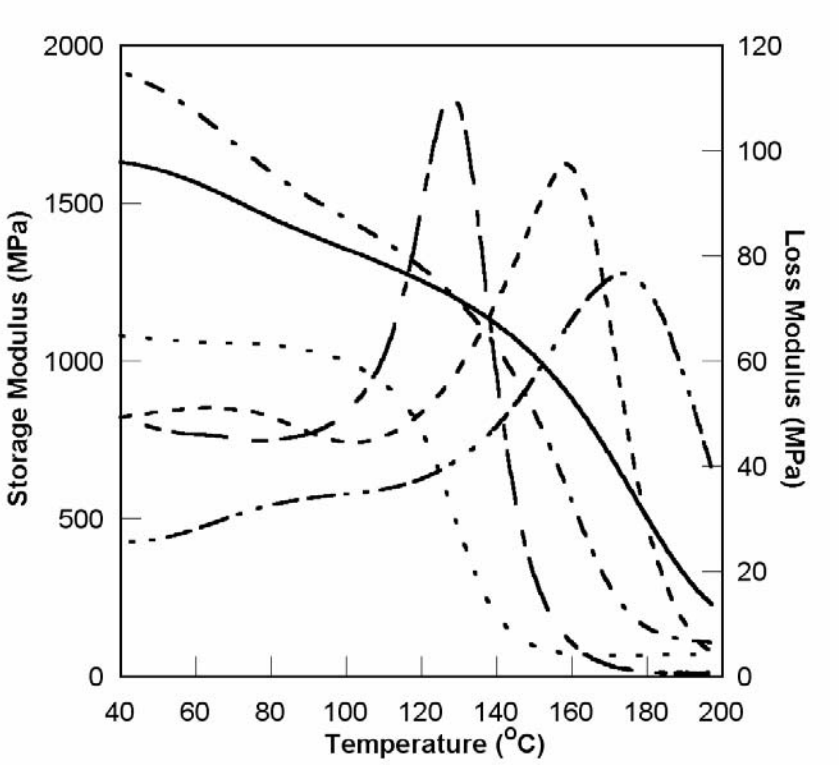

Figure 7.17. DMA (2nd run) of DGEBA with THF as a chain extender, where 1 wt% THF storage modulus (—),1 wt% THF loss modulus (···−−), 5 wt% THF storage modulus (· − · −), and 5 wt% THF loss modulus (- - -), and 10 wt% THF storage modulus (····),10 wt% THF loss modulus (− —) are shown.

7.4.2. Difunctional chain extenders

The previous section showed the potential of using THF as a chain extender in tailoring the epoxy system. However due to the drawbacks of THF such as high volatility, other monomers containing the THF functionality were explored. THF in DGEBA also resulted in a lower T_g, this factor also had to be accounted for in tailoring the properties. Thus using THF difunctional monomers were made to provide chain extension while maintaining higher T_g.

7.4.2.1. Synthesis and Application of Chain Extenders by Esterification of DGEBA and Tetrahydro-2-furoic acid

A new monomer, GP3, was synthesized by the esterification of DGEBA with tetrahydro-2-furoic acid as described in the experimental section and shown in Figure 7.8. This reaction adds THF functionality to the ends of DGEBA. DGEBA was mixed with GP3 at 20 wt% and 35 wt% loading and cured according to the procedures described earlier. The properties of the resulting polymers as obtained by DMA analysis and fracture toughness measurements in comparison to neat DGEBA polymers are given in Table 7.6. In both cases fracture toughness increased substantially with a concomitant decrease in T_g. The drop in T_g is significantly less than that observed for pure the THF modification. In fact, 35 wt% GP3 corresponds roughly to the molar concentration of THF moieties found in 10 wt% THF modified DGEBA systems. Thus the comparison of 35 wt% GP3 with 10 wt% THF shows a significant increase in T_g as well as slightly improved fracture toughness value. A likely explanation for this behavior is that the use of difunctional GP3 places a crosslink between two tetramethylene ether groupings in the resulting network structure.

Table 7.6. Fracture toughness and T_g values for neat DGEBA and GP3 modified DGEBA.

	T_g (°C) 2nd run	**G_{1C} (J/m^2)**
Epoxy	190	56±7
20wt% GP3	169	146±19
35wt% GP3	131	275±33

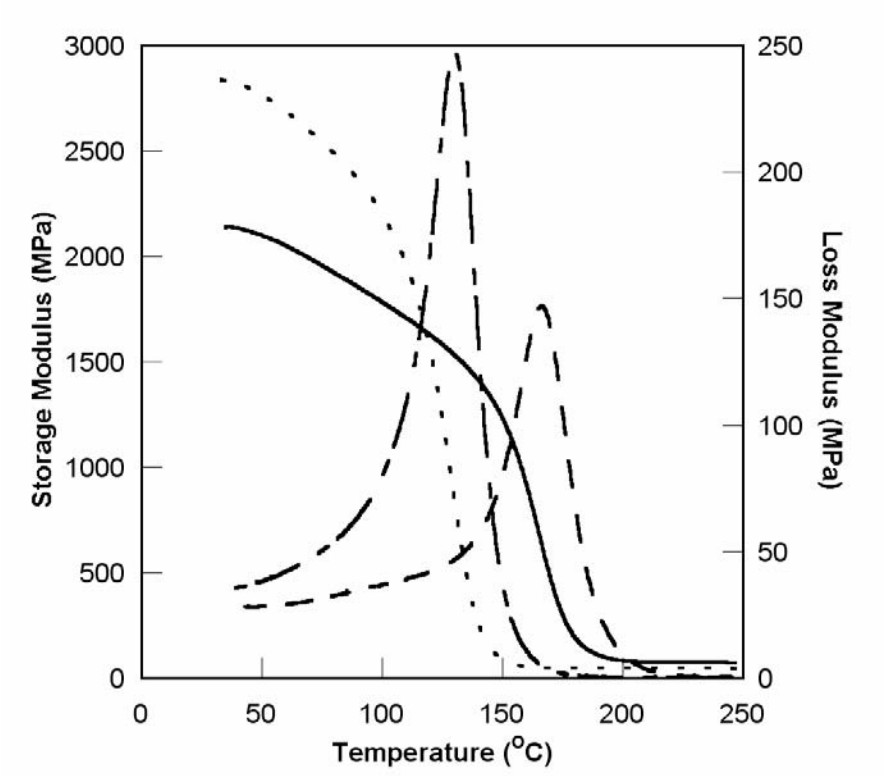

Figure 7.18. DMA (2nd run) of DGEBA with GP3 as a chain extender, where 20 wt% GP3 storage modulus (—), 20 wt% GP3 loss modulus (− −), 35% wt % GP3 storage modulus (····), and 35% wt % GP3 loss modulus (− ─) are shown.

A second interesting observation is that the 20 wt% GP3 system possesses a T_g similar to that of DGEBA modified with 1 wt% water and a similar fracture toughness to that system. These results indicate the potential for improving the mechanical properties of EB cured DGEBA systems. The challenge remains to improve fracture toughness with minimal or no loss in other properties, particularly T_g.

7.4.2.2. Synthesis and Application of Chain Extenders by Esterification of DGEBA and Tetrahydro-3-furoic acid

A new monomer, GP2, was synthesized by the esterification of DGEBA with tetrahydro-3-furoic acid as described in the experimental section and shown in Figure 7.9. This reaction adds THF functionality to the ends of DGEBA similarly to GP3. DGEBA was mixed with GP2 at 20 wt% and 35 wt% loading and cured according to the procedures described earlier. The properties of the resulting polymers as obtained by DMA analysis and fracture toughness measurements in comparison to neat DGEBA polymers are given in Table 7.7. In both cases fracture toughness increased substantially with a concomitant decrease in T_g. The drop in T_g is significantly less than that observed for the pure THF modification. The fracture toughness of the system was greatly improved compared to that of pure DGEBA; however the concern for the T_g must be acknowledged, thus the next section explores trifunctional epoxies.

Table 7.7. Fracture toughness and T_g values for neat DGEBA and GP2 modified DGEBA

	T_g (°C) 2nd run	**G_{1C} (J/m^2)**
Epoxy	190	56±7
20wt% GP2	174	173±36
35wt% GP2	151	221±59

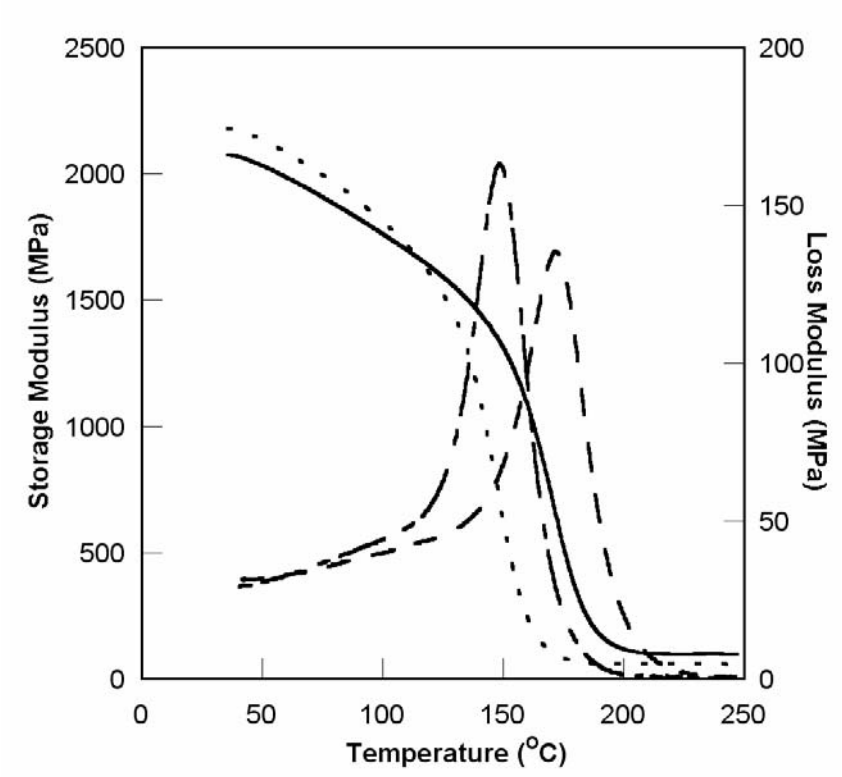

Figure 7.19. DMA (2nd run) of DGEBA with GP2 as a chain extender, where 20 wt% GP2 storage modulus (—), 20 wt% GP2 loss modulus (− −), 35% wt % GP2 storage modulus (····), and 35% wt % GP2 loss modulus (− ─) are shown.

7.4.3. Trifunctional chain extenders

In Chapter 6, the initial goal was to use Tactix 742 to see if this could increase the T_g of the epoxy system. Various concentrations of Tactix 742 in DGEBA resulted in an increase in one property while another property suffered. An optimum combination for these properties was found to be 20 to 40 wt% of Tactix 742 in DGEBA. The viscosity also had to be factored into choosing the quantity of the trifunctional epoxy used for future use in composites. However, the use of this trifunctional epoxy increased the final T_g of the polymer. Thus this section explores the use of this trifunctional epoxy in order to increase the T_g while maintaining the high mechanical properties resulted from the THF functional monomers.

7.4.3.1. Synthesis and Application of Chain Extenders by Esterification of Trifunctional Epoxies (Tactix 742) with Tetrahydro-2-furoic acid

Based on the results obtained for the difunctional THF endcapped system described in the previous section, analogous trifunctional systems were considered with the notion that these should result in higher T_g materials when used as modifiers for DGEBA. Tactix 742 is a well known trifunctional epoxy that is commonly used for higher T_g applications compared to DGEBA. A new monomer, GP5, was synthesized via the esterification of Tactix 742 with tetrahydro-2-furoic acid as described in the experimental section and shown in Figure 7.10. This reaction adds THF functionality to the ends of the trifunctional epoxy resulting in a modifier with three THF functional groups. DGEBA was mixed with GP5 at 1, 5 and 10 wt% loading and cured via EB according to the procedures described earlier. The properties of the resulting polymers as obtained by DMA analysis, flexural testing and fracture toughness measurements in

comparison to the neat DGEBA polymer are given in Table 7.8.

The T_g of the modified DGEBA systems was found to be only slightly influenced by GP5 loading. Moreover the loss behavior observed by DMA and given in Figure 7.20 for the series of GP5 modified samples shows not only a nearly unchanged T_g but also a sharper transition indicating the existence of a more homogeneous network for systems containing higher concentrations of GP5. The results of flexural testing show that the modifier has no influence on the flexural modulus of the material but that a significant increase in the flexural strength was obtained for all GP5 modified materials. A large, almost five-fold, improvement in fracture toughness was observed for the DGEBA modified with only 10 wt% GP5. This is a striking result given that there was not an accompanying significant loss in T_g. Moreover it suggests that it is possible to improve the properties of cationically EB cured DGEBA based epoxy systems without the loss of other important material properties.

Table 7.8. Mechanical properties of DGEBA modified using GP5 at various concentrations.

	T_g (°C) 2nd run	G_{1C} (J/m^2)	Flexural Properties	
			Strength (ksi)	Modulus (ksi)
Neat Epoxy	190	56±7	8.9±0.8	344±10
1% GP5	180	167±29	10.0±0.9	334 ±14
5% GP5	187	186±18	10.1±1.0	336 ±18
10% GP5	180	250±42	10.7±1.0	334 ±13

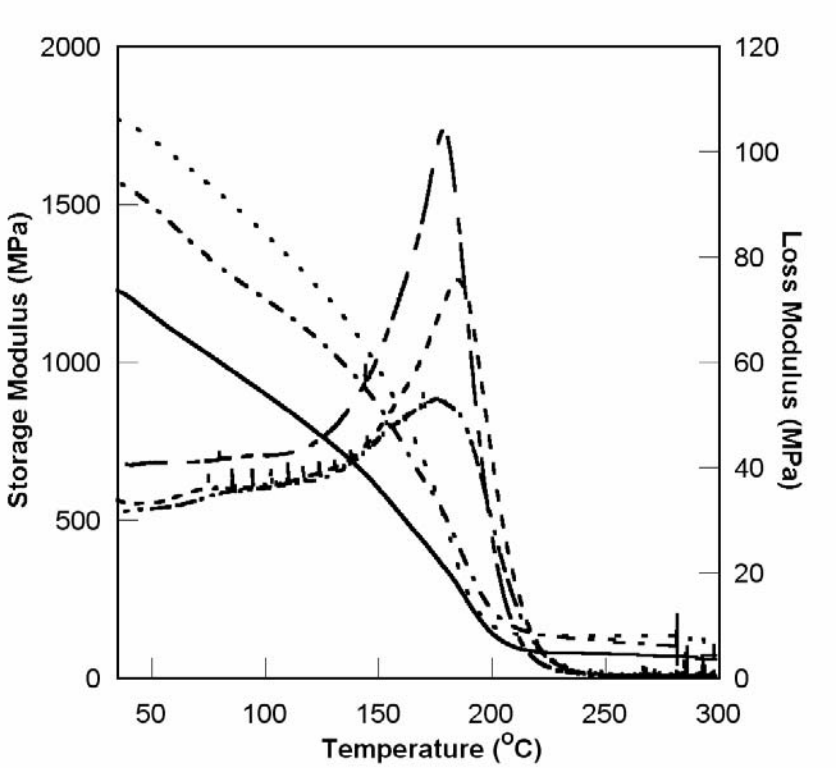

Figure 7.20. DMA (2nd run) of DGEBA with GP5 as a chain extender, where 1 wt% GP5 storage modulus (—),1 wt% GP5 loss modulus (··− −), 5 wt% GP5 storage modulus (· − · −), and 5 wt% GP5 loss modulus (- - -), and 10 wt% GP5 storage modulus (····),10 wt% GP5 loss modulus (− —) are shown.

7.4.3.2. Synthesis and Application of Chain Extenders by Esterification of Trifunctional Epoxies (Tactix 742) with Tetrahydro-3-furoic acid

A new monomer, GP4, was synthesized via the esterification of Tactix 742 with tetrahydro-3-furoic acid as described in the experimental section and shown in Figure 7.11. Similar to the GP5, this reaction adds THF functionality to the ends of the trifunctional epoxy resulting in a modifier with three THF functional groups. DGEBA was mixed with GP4 at 1, 5 and 10 wt% loading and cured via EB according to the procedures described earlier. The properties of the resulting polymers as obtained by DMA analysis, flexural testing and fracture toughness measurements in comparison to the neat DGEBA polymer are given in Table 7.9.

The T_g of the modified DGEBA systems was found to be only slightly influenced by GP4 loading. Moreover the loss behavior observed by DMA and given in Figure 7.21 for the series of GP4 modified samples shows not only a nearly unchanged T_g but also a sharper transition indicating the existence of a more homogeneous network for systems containing higher concentrations of GP4. GP4 showed similar results to GP5.

Table 7.9. Mechanical properties of DGEBA modified using GP4 at various concentrations.

	T_g (°C) 2nd run	G_{1C} (J/m^2)	Flexural Properties	
			Strength (ksi)	Modulus (ksi)
Neat Epoxy	190	56±7	8.9±0.8	344±10
1% GP4	186	182±11	8.9±1.5	336 ±15
5% GP4	189	213±53	10.9±1.5	309 ±17
10% GP4	186	202±23	9.6±0.6	337 ±9

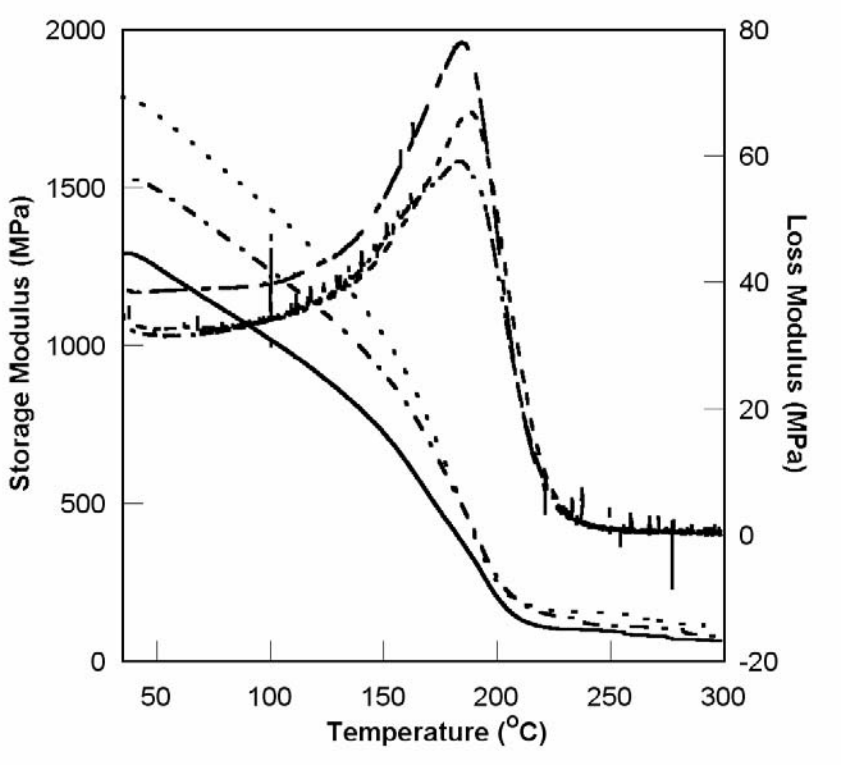

Figure 7.21. DMA (2nd run) of DGEBA with GP4 as a chain extender, where 1 wt% GP4 storage modulus (—),1 wt% GP4 loss modulus (···– –), 5 wt% GP4 storage modulus (· – · –), and 5 wt% GP4 loss modulus (- - -), and 10 wt% GP4 storage modulus (····),10 wt% GP4 loss modulus (– —) are shown.

7.4.4. Cyclic chain extenders

The use of trifunctional epoxy to synthesize new monomers with THF functionality showed improvement with the mechanical properties while maintaining the T_g. However further improvement was desired to increase the T_g of the epoxy system. The T_g can be improved by increasing the stiffness of the of the network by adding monomers with cyclic backbones. This section explores the use of cyclic monomers containing the THF functionality to further improve the final polymer.

7.4.4.1. Synthesis and Application of Chain Extenders of DGEBA and Coumaran

JL1 was synthesized by mixing of DGEBA with 2,3-dihydrobenzofuran as described in the experimental section. DGEBA was mixed with JL1 at 1, 5 and 10 wt% loading and cured via EB according to the procedures described earlier. The properties of the resulting polymers as obtained by DMA analysis, flexural testing and fracture toughness measurements in comparison to the neat DGEBA polymer are given in Table 7.10.

The T_g of the modified DGEBA systems was found to cause a double peak by JL1 loading as shown in Figure 7.22. This indicated two different polymers forming in the system. The first T_g peak is extremely low and continues to suffer with increasing amounts of JL1. The second T_g peak is similar to that of regular DGEBA, but decreased significantly with higher concentrations of JL1. However all the other mechanical properties increase with increase amounts of the comonomer. However due to the T_g behavior, this comonomer JL1 was not tested futher.

Table 7.10. Mechanical properties of DGEBA modified using JL1 at various concentrations.

	T_g (°C) 2nd run		G_{1C} (J/m^2)	Flex	
				Strength (ksi)	Modulus (ksi)
Neat Epoxy	190		56±7	8.9±0.8	344±10
1wt% JL1	83	180	160±23	12.6 ±1.0	319 ±13
5wt% JL1	75	157	223 ±38	14.3 ±1.5	340 ±8
10wt% JL1	67	136	263 ±46	15.1 ±1.9	380 ±37

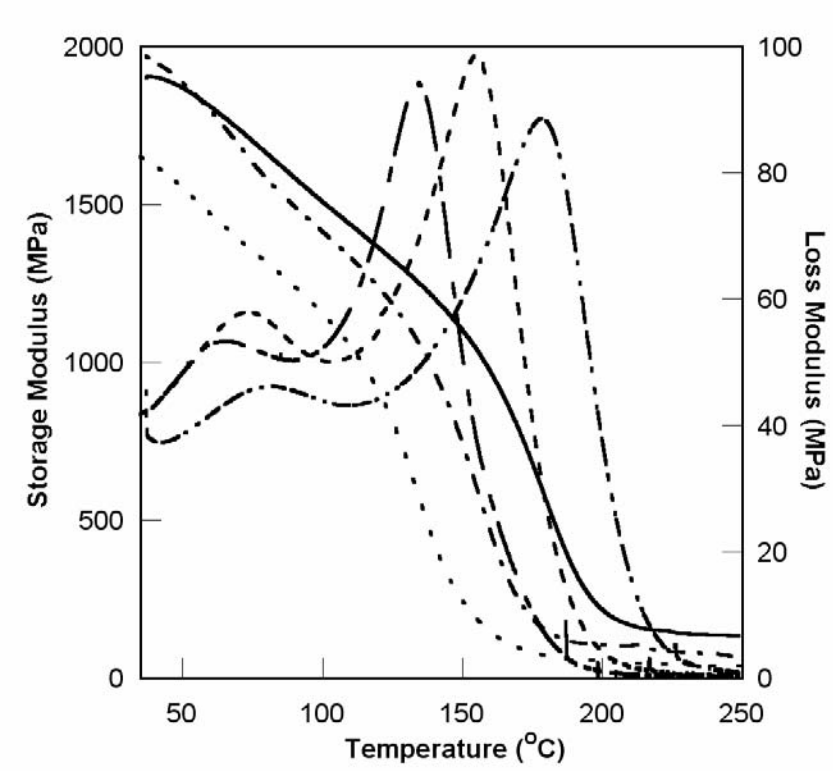

Figure 7.22. DMA (2nd run) of DGEBA with JL1 as a chain extender, where 1 wt% JL1 storage modulus (—),1 wt% JL1 loss modulus (···– –), 5 wt% JL1 storage modulus (· – · –), and 5 wt% JL1 loss modulus (- - -), and 10 wt% JL1 storage modulus (····),10 wt% JL1 loss modulus (– —) are shown.

Table 7.11. Mechanical properties of DGEBA modified using JL2 at various concentrations.

	T_g (°C) 2nd run	G_{1C} (J/m^2)	Flex	
			Strength (ksi)	Modulus (ksi)
Neat Epoxy	190	56±7	8.9±0.8	344±10
1% JL2	181	159±43	8.6 ±1.0	355 ±17
5% JL2	167	187 ±43	10.5 ±1.5	345 ±14
10% JL2	154	180 ±23	10.5 ±1.9	374 ±20

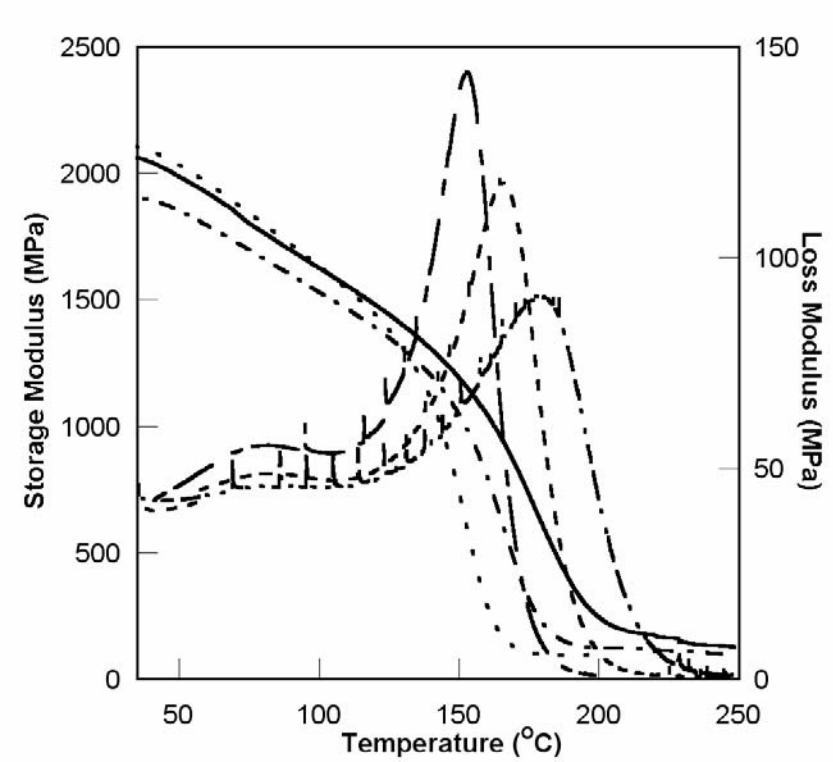

Figure 7.23. DMA (2nd run) of DGEBA with JL2 as a chain extender, where 1 wt% JL2 storage modulus (—),1 wt% JL2 loss modulus (···– –), 5 wt% JL2 storage modulus (· – · –), and 5 wt% JL2 loss modulus (- - -), and 10 wt% JL2 storage modulus (····),10 wt% JL2 loss modulus (– ─) are shown.

7.4.4.2. Synthesis and Application of Chain Extenders of Epoxies and Phthalan

JL2 was synthesized by mixing of DGEBA with phthalan as described in the experimental section. DGEBA was mixed with JL2 at 1, 5 and 10 wt% loading and cured via EB according to the procedures described earlier. The properties of the resulting polymers as obtained by DMA analysis shown in Figure 7.23, flexural testing and fracture toughness measurements in comparison to the neat DGEBA polymer are given in Table 8.11.

The T_g of the modified DGEBA system decreased similarly to the other difunctional epoxy systems. However at 10 wt% loading of JL2, the fracture toughness increased over three fold. The strength increased to an optimum of 10.5 ksi, but the modulus remained relatively constant despite the addition of JL2. Also in comparison to the tetrahydro-2-furioc and tetrahydro-3-furioc acid, the base cost is significantly less. Thus the next logical step was to synthesize a comonomer using a trifunctional epoxy system.

To improve T_g, JL2 and Tactix 742 (3:1) was mixed then 10 wt% of this was then mixed with DGEBA. The T_g of the resulting polymer was the same as that of GP5 at 180°C. The fracture toughness was almost four fold that of pure epoxy at 193±53 J/m^2. The flexural testing resulted with a modulus of 348±26 ksi and a strength of 11.6±1.4 ksi.

Table 7.12. Material properties of modified DGEBA systems with THF functional monomers, such as SBS strength and flexural strength and modulus.

	SBS (ksi)	Flex	
		Strength (ksi)	Modulus (ksi)
Neat Epoxy	6.0±0.4	109±7.8	7,619±189
35% GP3	7.5±0.2	103±6.6	7,710±947
10% JL2	4.6±0.2	69±7.2	5,697±254
10% GP5	6.3±0.3	103±6.6	7,603±816

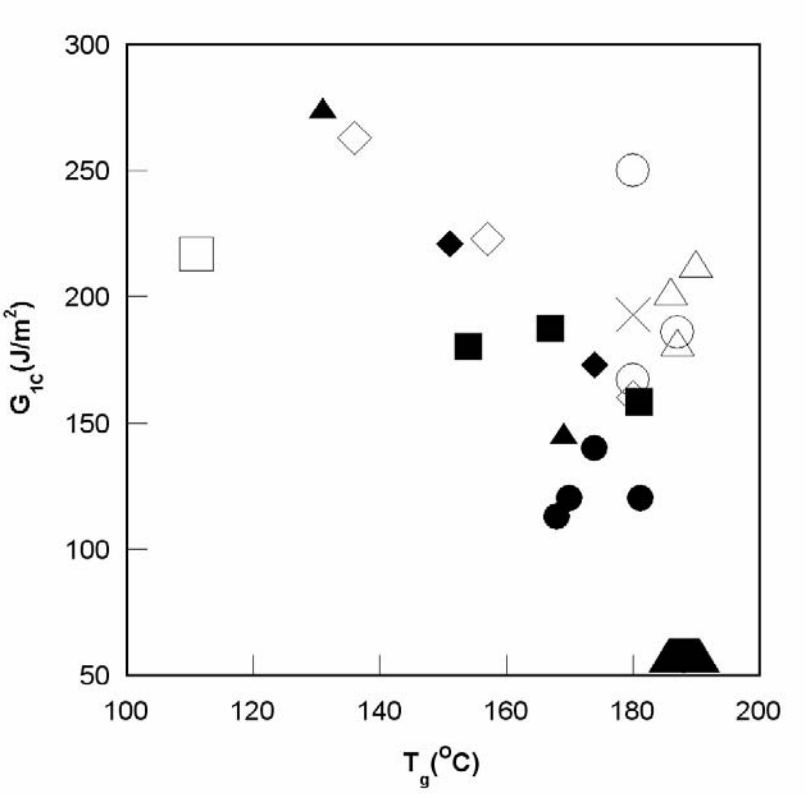

Figure 7.24. Improving the fracture toughness while maintaining a high T_g, where neat DGEBA (▲), water (●), THF (□), GP2 (◆), GP3 (▲), GP4 (Δ), GP5 (○), JL1 (◇), JL2 (■), JL3 (x).

7.4.5. Composite Properties

Carbon fiber composites were fabricated using a wet layup technique and cured by EB as describe in the experimental section. Modification of DGEBA resin with the THF functional monomers GP3, GP5, and JL2 may improve interlaminar shear behavior as measured by SBS tests shown in Table 7.12. The SBS strength of neat DGEBA – carbon fiber composites using G' sized 5HS AS4 fabric was 6.0±0.4 ksi. This is a typical result for EB cured epoxy systems and is one of the principal shortcomings associated with such materials. A similarly fabricated composite using DGEBA modified with 35 wt% GP3 as a matrix was found to have SBS strength of 7.5±0.2 ksi which is a considerable improvement that further illustrates the potential of THF functional modifiers. JL2 matrix was found to have SBS strength of 4.6±0.2 ksi. In the case of the modified DGEBA with the trifunctional monomer, for 10 wt% GP5 the SBS strength was found to be 6.3±0.3 ksi. The improvement was slight in this situation, however with higher loads can result in increased interlaminar shear behavior. However there were difficulties in the manufacture of these composites. The curing process must be applied immediately after the fabrication of the composite; unfortunately the turn around time for this was not ideal. Time is a huge factor in manufacturing the composites due to the system being under vacuum and when sent over for the curing process some vacuum is lost over time. When vacuum is reapplied with heat the resin in the composite has the potential of being sucked out. In fact, when the composites were cut, there were voids in many of the samples. Most importantly these systems are sensitive to light and water as described in the previous chapters. The exposure to daylight could initiate the cure process and the water could plasticize the system. The flexural tests resulted in the

following, where the strength of pure epoxy was 109±7.8 ksi and the modulus was 7,619±189 ksi. For JL2, the strength was 69±7.2 ksi and the modulus was 5,697±254 ksi. For GP5 modified system the strength was 103±6.6 ksi and the modulus was 7,603±816 ksi. Despite the manufacturing difficulties, the initial composites clearly show a significant increase in interlaminar shear with the copolymerization of epoxies and THF functional monomers.

7.5. Conclusions

One of the major drawbacks associated with EB curing of DGEBA based systems is the poor fracture toughness obtained for such materials. In this chapter new chain extending modifiers were explored to tailor the network structure and improve mechanical properties of DGEBA epoxies cured cationically via EB. Initial tests with CHO, PGE, and THF lead to the discovery that THF copolymerizes readily with DGEBA under EB irradiation and in the presence of a photoinitiator such as diphenyl iodonium hexafluoroantimonate. It is presumed that via the ring opening of the THF molecule, a tetramethylene ether grouping is added to the crosslinked network comprised primarily of DGEBA. This results in lower crosslink density (lower T_g) and higher fracture toughness. In order to maintain T_g while improving fracture toughness a number of novel difunctional and trifunctional monomers were developed based on endcaping difunctional and trifunctional epoxies with THF moieties via appropriate synthetic procedures. These monomers were used as modifiers of DGEBA in the range of 1-35 wt%. All combinations increased fracture toughness considerably and in the case of the trifunctional system at 10 wt% loading, fracture toughness was improved almost five-fold with little effect on T_g resulting in a material with G_{1c} of 250±42 J/m^2 and a T_g of 180°C.

The results of DGEBA resin modification conducted in this investigation are summarized in Figure 7.24 as a plot of G_{1C} vs T_g. It is clear that fracture toughness can be improved while maintaining T_g. Moreover, preliminary results suggest that the resin improvements also translate into improved composite properties.

7.6. References

1. Beziers D, Capdepuy B. SAMPE Int Symp, 35 1220 (1990).
2. Saunders CB, Lopata VJ, Kremers W, McDougall TE, Tateishi M, Singh A. SAMPE Int Symp, 38, 1682 (1993).
3. Saunders CB, Lopata VJ, Kremers W, Chung M, Barnard JW. SAMPE Int Symp, 40, 112 (1995).
4. Janke CJ, Havens SJ, Dorsey GF, Lopata VJ. SAMPE Int Tech Conf, 41, 196 (1996).
5. Janke CJ, Havens SJ, Dorsey GF, Lopata VJ. SAMPE Int Tech Conf, 28, 901 (1996).
6. Janke CJ, Havens SJ, Lopata VJ, Chung M. SAMPE Int Tech Conf, 28, 901 (1996).
7. Goodman DL, Brix DL, Palmese GR, Chen A. SAMPE Int Symp, 41, 207 (1996).
8. Janke CJ, Norris RE, Yarborough K, Havens SJ, Lopata VJ. SAMPE Int Symp, 42, 477 (1997).
9. Dabestani R, Ivanov I. SAMPE Int Symp, 46, 2075 (2001).
10. Palmese GR, Ghosh NN, McKnight SH. SAMPE Int Symp, 45 (2000).
11. Chabanne P, Tighzert L, Pascault J. J. Appl. Polym. Sci., 53, 769(1994).
12. Chabanne P, Tighzert L, Pascault J. J. Appl. Polym. Sci., 53, 787 (1994).

13. Chabanne P, Tighzert L, Pascault J, Bonnetot**.** J. Appl. Polym. Sci., 49, 685 (1993).

14. Bouillon N, Pascault J, Tighzert L. Makromol Chem, 191, 1403 (1990).

15. Bouillon N, Pascault J, Tighzert L. Makromol Chem, 191, 1417 (1990).

16. Bouillon N, Pascault J, Tighzert L. Makromol Chem, 191, 1435 (1990).

17. Lunak S, Krejcar E. Die Angew Makol Chem, 10, 109 (1970).

18. Lee J, Johnston A, Palmese G.R. SAMPE Int Symp, (2004).

19. Lee J, Palmese GR. SAMPE Int Symp, (2005).

CHAPTER 8: CONCLUSIONS

8.1. Summary

This work developed a fundamental understanding of the physical and chemical processes underlying EB polymerization of epoxy systems in order to design improved systems. This investigation included (i) developing a cure kinetics model that accounts for active center deactivation and the effects of water (ii) developing an understanding of the relationships among cure process/variables with network structure/morphology and properties and (iii) designing new systems with improved properties based on the science base developed in i and ii. This was accomplished by investigating the influence of process variables such as temperature, time, dose/dose rate, initiator concentration, and impurities. NIR spectroscopy was also further developed and used to investigate the EB induced polymerization of epoxy cured systems.

8.2. Water Reactions

The purpose of this investigation was to gain further understanding of the influence of water on phenyl glycidyl ether (PGE) and diglycidyl ether of bispehnol A (DGEBA). A near infrared (NIR) spectroscopy technique reported earlier was further developed to perform real-time *in-situ* kinetic analysis of radiation induced, electron beam (EB) and ultraviolet (UV), cationic polymerization of epoxy systems with water. Experiments were conducted with four purposes: (1) to quantify the concentration of water in PGE and DGEBA prior to cure via near infrared spectroscopy (NIR); (2) to determine the reaction kinetics of the mono-epoxy system PGE and water cured via UV and EB (3) to determine the reaction kinetics of di-epoxy system DGEBA and water cured via UV and EB; and (4) and to investigate the effect of water on the network

formation of a DGEBA epoxy-matrix composite. The chemical kinetics results indicated that the presence of water affects the polymerization of the epoxy systems by (a) the appearance of a pronounced retardation period, (b) an accelerated reaction following the retardation period when compared to "dry" systems, and (c) higher conversion at shorter times. A kinetic mechanism was proposed to explain this behavior and a model based on this mechanism was found to be in good qualitative agreement with experimental results. It was also shown that the presence of water influences the behavioral characteristics of cationically cured epoxies by reducing glass transition temperature (T_g) and increasing fracture toughness.

8.3. Dark Reactions

Process variables, such as dose, dose rate, initiator concentration, temperature, time, and impurities, influence the generation of active centers and subsequent polymerization of epoxies induced by ultraviolet (UV) and electron beam (EB) radiation by cationic mechanisms. Longer exposure to radiation produces higher concentration of active centers that has previously been modeled by a simple first order kinetic model that assumes infinite life for the generated centers. However, it appears that such a model is not suitable for predicting the behavior of interrupted EB exposure experiments. NIR spectroscopy was used to monitor the epoxy concentration throughout the polymerization of glycidyl ethers for experiments in which the EB is turned off before complete conversion is achieved and dark reactions are monitored thereafter. This investigation is based on the continued development of a near infrared (NIR) spectroscopic technique for performing real-time *in situ* kinetic measurements of EB induced cationic polymerization of epoxy systems. The results of these experiments indicate that a significant reduction

in reactivity occurs when radiation is curtailed and that the active centers possess very long half-lives.

8.4. Co-monomers for Chain Extension

The overall objective of this work was the design of improved EB cured epoxy systems based on diglycidyl ether of bisphenol A (DGEBA). One method for designing such systems is the use of network modifiers. This work developed a new class of chain extenders based on the ring opening copolymerization of tetrahydrofuran (THF) with DGEBA. Copolymerization of THF with DGEBA can be induced by EB in the presence of an appropriate photoinitiator. THF was found to increase fracture toughness with a concomitant decrease in glass transition temperature. THF presents practical processing difficulties associated with its high volatility. Thus a series of novel THF functional comonomers were designed to mitigate the aforementioned drawbacks associated with THF. These include difunctional and trifunctional monomers possessing THF functionality. The system was further modified by introducing cyclic backbone to add stiffness to the network in order to increase the T_g. Methods of synthesis and the properties of DGEBA systems modified with these novel monomers were presented. It was found that the fracture toughness of EB cured DGEBA systems can be improved almost five fold without loss of T_g. Moreover preliminary results indicate that composite properties can also be improved using these comonomers.